EPA/600/2-89/048
September 1989

EXPERIMENTAL INVESTIGATION OF CRITICAL FUNDAMENTAL ISSUES IN HAZARDOUS WASTE INCINERATION

Prepared By:

John C. Kramlich
Elizabeth M. Poncelet
Robyn E. Charles
Wm. Randall Seeker
Gary S. Samuelsen
Jerald A. Cole

Energy and Environmental Research Corporation
18 Mason
Irvine, CA 92718-2798

EPA Contract 68-02-3633

EPA Project Officer: W. Steven Lanier

Combustion Research Branch
Air and Energy Engineering Research Laboratory
U.S. Environmental Protection Agency
Research Triangle Park, NC 27711

AIR AND ENERGY ENGINEERING RESEARCH LABORATORY
OFFICE OF RESEARCH AND DEVELOPMENT
U.S. ENVIRONMENTAL PROTECTION AGENCY
RESEARCH TRIANGLE PARK, NC 27711

EPA-600/2-89-048
(AEERL-509)
Fig. 3-7 (pg 3-15)

COPYRIGHT RELEASE

The Combustion Institute hereby grants permission for the use of Figure 5 from Kramlich et al., [20th Symp. (Int.) Combust., p. 1995, The Combustion Institute (1984)] in an Environmental Protection Agency report. It is understood that the National Technical Information Service will reproduce the report, and offer it to the public for sale. It is further understood that the figure caption accompanying said figure will identify the original source of the figure.

THE COMBUSTION INSTITUTE

By _____

Title President

Dated 24 June 1989

TECHNICAL REPORT DATA
(Please read Instructions on the reverse before completing)

1. REPORT NO.	2.	3. RECIPIENT'S ACCESSION NO.
EPA/600/2-89/048		PB90 108507/AS

4. TITLE AND SUBTITLE	5. REPORT DATE
Experimental Investigation of Critical Fundamental Issues in Hazardous Waste Incineration	September 1989
	6. PERFORMING ORGANIZATION CODE

7. AUTHOR(S)	8. PERFORMING ORGANIZATION REPORT NO.
J. C. Kramlich, E. M. Poncelet, R. E. Charles, W. R. Seeker, G. S. Samuelsen, and J. A. Cole	

9. PERFORMING ORGANIZATION NAME AND ADDRESS	10. PROGRAM ELEMENT NO.
Energy and Environmental Research Corporation 18 Mason Irvine, California 92718-2798	11. CONTRACT/GRANT NO. 68-02-3633

12. SPONSORING AGENCY NAME AND ADDRESS	13. TYPE OF REPORT AND PERIOD COVERED
EPA, Office of Research and Development Air and Energy Engineering Research Laboratory **Research Triangle Park, NC 27711**	Task Final; 1/84 - 4/85 14. SPONSORING AGENCY CODE **EPA/600/13**

15. SUPPLEMENTARY NOTES AEERL project officer W. S. Lanier is no longer with the Agency. For details, contact William P. Linak, Mail Drop 65, 919/541-5792.

16. ABSTRACT The report gives results of a laboratory-scale program investigating several fundamental issues involved in hazardous waste incineration. The key experiment for each study was the measurement of waste destruction behavior in a subscale turbulent spray flame. (1) Atomization Quality: The performance of subscale nozzles was directly measured in terms of droplet size by lazer diffraction. The large increase in time required to evaporate the substantially increased number of very large droplets resulted in penetration of unevaporated waste through the flame and to the wall. (2) Secondary Atomization. Test results showed that, when atomization quality was the limiting process, secondary atomization markedly improved both waste destruction efficiency and overall combustion efficiency, as measured by CO and total hydrocarbon emissions. (3) Compound Concentration. Test results support the hypothesis that varying secondary atomization intensity with compound concentration in the feed explains most of the variation in laboratory-scale studies. A mechanism involving mixing limited equilibrium chemistry is proposed to explain the field data. (4) Formation of Products of Incomplete Combustion. The broad spectrum of volatile organic compounds from a simplified flame were measured. Test results show that most of the organic compounds present were from the fuel.

17. KEY WORDS AND DOCUMENT ANALYSIS

a. DESCRIPTORS		b. IDENTIFIERS/OPEN ENDED TERMS	c. COSATI Field/Group	
Pollution	Atomizing	Pollution Control	13B	13H, 07A
Incinerators	Concentration	Stationary Sources		07D
Waste Disposal		Hazardous Waste	15E	
Wastes		Incomplete Combustion	14G	
Toxicity			06T	
Combustion			21B	

18. DISTRIBUTION STATEMENT	19. SECURITY CLASS *(This Report)*	21. NO. OF PAGES
Release to Public	**Unclassified**	128
	20. SECURITY CLASS *(This page)* **Unclassified**	22. PRICE

EPA Form 2220-1 (9-73)

NOTICE

This document has been reviewed in accordance with U.S. Environmental Protection Agency policy and approved for publication. Mention of trade names or commercial products does not constitute endorsement or recommendation for use.

ABSTRACT

The results of a laboratory-scale program investigating various fundamental issues in hazardous waste incineration are presented. The key experiment for each study was the measurement of waste destruction behavior in a subscale turbulent spray flame.

Atomization Quality: Previous work has shown that poor atomization of liquids containing wastes can lead to poor waste destruction efficiency. In the present program the nozzle performance of subscale nozzles was directly measured in terms of droplet size by laser diffraction. The principal attribute of nozzle degradation that caused poor waste destruction efficiency was the substantial increase in the number of very large droplets. The large increase in time required for the evaporation of the droplets resulted in penetration of unevaporated waste through the flame and to the wall.

Secondary Atomization: Because some wastes can be highly viscous or contain solids, atomization quality can be a limiting factor, even for correctly operating nozzles. One approach that has been investigated for heavy fuel oils is the use of emulsions or volatile doping agents to induce disruptive combustive or secondary atomization in the flame. (Secondary atomization is a phenomenon in which a volatile component is introduced into the fuel; during heating this volatile component leads to internal vaporization which fractures the droplet, thereby improving atomization quality.) The destruction efficiency of waste compounds which induced secondary atomization in No. 2 fuel oil was compared with the efficiency for compounds that did not cause disruptive combustion. The results showed that when atomization quality was the limiting process, secondary atomization markedly improved both waste destruction efficiency and overall combustion efficiency, as measured by CO and total hydrocarbon emissions.

Compound Concentration: Even in the absence of secondary atomization an influence of compound concentration in the feed stream has been noted in field data. The question of the mechanism that gives rise to this correlation was addressed by measurements in the turbulent flame reactor. The

results support the hypothesis that varying secondary atomization intensity with compound concentration in the feed explains most of the variation in the lab-scale studies. This mechanism does not fully explain the field correlation. A mechanism involving mixing limited equilibrium chemistry is proposed to explain the field data.

PIC Formation: In field testing a large number of Appendix VIII compounds that are apparently unrelated to the original waste compounds are observed. Potential sources of these compounds are from undetected contaminants in the waste, true PICs from the waste compounds, or contaminants from the combustion air or scrubber water. These options are difficult to differentiate in the field data because of the complexity of the feed streams and the difficulty in obtaining a comprehensive characterization of the feed materials. In the present study the broad spectrum of volatile organic compounds from a simplified flame were measured. The laboratory scale flame was fired on No. 2 fuel oil doped with a single waste compound, 2-chlorophenol. The results indicate that the bulk of the organic compounds present were from decomposition or incomplete reaction of the auxiliary fuel.

CONTENTS

CONTENTS (Concluded)

FIGURES

FIGURES (CONTINUED)

FIGURES (CONCLUDED)

TABLES

1.0 INTRODUCTION

Incineration is an attractive alternative for the disposal of organic hazardous wastes. As opposed to landfilling or deep well injection, it effects a permanent solution. However, incineration is attractive only if the waste is destroyed to an acceptable efficiency and if harmful emissions of hazardous by-products are avoided. The Federal government has recognized that the public welfare requires government regulation of waste disposal through the Resources Conservation and Recovery Act (RCRA) [1]. Through RCRA Congress has charged the Environmental Protection Agency (EPA) with the development of regulations and the enforcement of these regulations. The EPA has identified over 300 compounds as hazardous [2,3] and has established licensing and operating regulations for devices destroying these compounds [4]. These regulations recognize the fact that thermal destruction devices cannot operate to 100 percent efficiency. Therefore, some emission level must be defined as a minimum standard for safety. Presently, 99.99 percent destruction and removal efficiency (DRE) of the principal organic hazardous constituents (POHCs) is the standard.

Field testing of full-scale waste destruction facilities [5] and testing of subscale flames [6] has shown that well designed systems have little trouble meeting the performance standard. Indeed, the evidence suggests that a substantial perturbation of design or operational parameters are necessary for substantial emissions to occur [6]. These perturbations have been termed "failure modes" because the perturbation has caused some fundamental rate limiting step to fail to completely destroy the waste [7]. Thus, the key questions with respect to DRE are:

1. What are the mechanisms that permit the small amounts of waste to escape during high efficiency operation?

2. What different mechanisms are responsible for waste release during a failure mode?

The present study addresses these and other questions through fundamental research.

There are presently three issues of regulatory and environmental interest with respect to incineration:

1. Ease of Incineration Rankings: The problem of applying the ease of incineration criteria to the selection of POHCs has motivated most of the research into fundamental mechanisms. The approach has been to hypothesize various escape mechanisms. The influence of each of the escape mechanisms on the various waste compounds is evaluated to yield a hypothetical ease of incineration ranking. Examples include:

- Post-Flame Thermal Destruction: This approach assumes that the rate limiting step is the destruction of waste in the bulk of the post-flame or afterburner. This destruction is assumed to take place under equilibrated radical concentrations and under dilute waste levels. The kinetics of waste destruction under these conditions has been developed at laboratory scale in isothermal plug-flow reactors [8-11]. These kinetics have been used to develop ease of incineration rankings. Researchers at Union Carbide have attempted to correlate post-flame ease of destruction with compound properties to yield a predictive relationship [12,13].

- Flame-Zone Kinetics: This approach, proposed by the National Bureau of Standards, assumes that the compound most resistant to radical attack will be the most difficult to remove [14]. Waste compounds are ranked by the strength of their weakest bond.

- Vaporization Parameters: Under this approach, compounds with high normal boiling points or high values of latent heat of vaporization are assumed to dominate the waste emissions. The mechanism assumes that the delay in vaporizing these compounds leads to a significant reduction in the time available for reaction.

- Heat of Combustion: The ease of destruction is assumed to be controlled by the energy released as the compound is oxidized [15]. The more energy released (i.e., the higher the heat of combustion) the more easily the compound is destroyed.

- Miscellaneous Approaches: These include ease of incineration rankings based on various compound properties [15]. These include heat of formation, Gibbs free energy, ionization potential, thermal decomposition activation energy, and heat of ionization.

Earlier work at Energy and Environmental Research Corporation was directed toward defining whether any of the proposed rankings could predict the data obtained from laboratory scale flames [6,7]. These results indicated that no single ranking was appropriate for all the flame conditions examined. Rather the rankings, and their escape mechanism, was dependent on the specific experimental operating conditions.

In summary, the problem of selecting POHCs and the question of rankings are directly coupled to the question of fundamental escape phenomena and mechanisms.

2. Compliance Monitoring: The present licensing regulations are directed toward proving initial compliance with the regulations and ensuring continued compliance through restrictions on operating conditions. The limitation with this approach is that DRE performance can degrade due to changes in waste composition or facility degradation, while constant operating conditions are maintained. The alternative of directly monitoring DRE performance during day-to-day operation is not practical due to the complexity of these analytical techniques and the delay between sampling and the availability of results. The viable alternative is to develop an indirect monitoring technique in which some property directly related to incinerator performance is monitored continuously and in real time.

EPA has conducted several studies to evaluate potentially reasonable monitoring approaches. At EER the use of total hydrocarbon measurement as a

means of monitoring pre-license incinerator performance was conceptually evaluated and then experimentally evaluated [16]. The experimental work utilized a laboratory-scale turbulent spray flame and demonstrated the nature of the flame zone correlation between CO, total hydrocarbons, and DRE:

- Total hydrocarbons and waste emissions were linearly correlated as the reactor was perturbed from a high to a low efficiency condition.

- Carbon monoxide emissions increased markedly before increases in waste emissions were noted.

These results suggest a monitoring strategy in which CO is used to indicate the approach of a problem and total hydrocarbons are used as a direct indicator of waste emissions.

These results were extended through theoretical evaluation [17] to show that the just-described CO/total hydrocarbon/DRE correlation is characteristic of flame zones. However, the correlation may be modified by post-flame processes. Thus, additional experimentation was recommended to evaluate the utility of CO and total hydrocarbons as indicators of DRE under combined flame and post-flame conditions.

The problem of defining DRE in terms of indirect monitors is strongly coupled to the nature of the fundamental waste release mechanisms. This can be reduced to two statements:

1. What are the rate limiting steps, processes or phenomena that limit waste destruction to less than 100 percent?

2. How do the variety of proposed continuous monitoring strategies respond to the processes that limit waste destruction?

Thus, a knowledge of fundamental waste escape mechanisms is critical to the systematic selection and use of indirect monitoring strategies.

PIC Formation

One drawback to the application of incineration technology is the potential that the hazard associated with a waste stream may be increased through the formation of extremely hazardous byproducts. Of particular, though not exclusive, concern are polychlorinated dibenzo-p-dioxins (PCDDs) and polychlorinated dibenzofurans (PCDFs).

In an incinerator the majority of gas streamlines provide an environment sufficient to completely destroy any organic compound [18]. At the same time these high-efficiency pathways will also quantitatively destroy hazardous products of incomplete destruction (PICs). Thus, the pathways of interest are the marginal paths in which wastes and PICs are only partially destroyed. To develop experiments which simulate PIC formation and emission, as it occurs in incinerators, a fundamental understanding of how low-efficiency environments arise must be obtained.

Objectives

The objectives of the present study are to define and address experimentally a series of issues fundamental to hazardous waste incineration. These issues were selected because they represent practical problems or approaches to practical problems that can be addressed through fundamental research. These issues include:

- Effect of Waste Concentration on DRE: Field data have indicated a correlation between waste concentration and DRE. Identification of the mechanism responsible for this behavior would be an important step toward defining the fundamental release mechanism.

- Effect of Waste Atomization on DRE: It is known that combustion efficiency can be degraded in industrial flames by poor fuel atomization (i.e., large droplets). The key question is the definition of the mechanism by which DRE is influenced by waste atomization.

- Effect of Secondary Atomization on DRE: This addresses the question whether fragmentation of waste droplets by internal boiling can improve DRE.

- PIC Formation: Considerable work has been done identifying PICs in idealized plug flow experiments [8-11, 19]. Here we address the appearance of PICs in turbulent spray flames.

In addition to providing specific information on these issues, one goal of this work is to provide insight into the critical, rate-limiting processes that govern waste release from practical devices.

Quality Assurance/Quality Control requirements are applicable to this project. The data contained in this report are NOT supported by QA/QC documentation as required by the United States Environmental Protection Agency's Quality Assurance Policy.

2.0 EXPERIMENTAL

The broad range of activities identified in the previous discussion required an equally broad range of experimental equipment. Because some apparatus were used in more than one experiment, all facilities are described here rather than duplicated under the major experimental headings.

2.1 Slip Flow Reactor

The slip-flow reactor was originally designed to study the thermal decomposition characteristics of synthetic fuel oils; it has proven useful for the examination of physical processes accompanying the thermal decomposition and combustion of all liquid fuels. The reactor consists of a 5 x 28 cm flat-flame burner downfired into a chimney of similar dimensions. The flat flame is supported on a water-cooled sintered stainless steel plate. The chimney is fitted with four 156 x 28 cm Vycor windows for optical access. The two narrow sides and the bottom provide access ports for droplet injection and sample probing. As illustrated in Figure 2-1, fuel droplets are injected ballistically normal to the hot gas flow. This results in an isothermal droplet environment, and more importantly, the physical separation of soot from the droplets and droplet formed cenospheres. For the present experiment, the most important attribute of the reactor is the ease of optical access for visualization and probing during the relatively long time (order of 100 milliseconds) the droplet is in an isothermal environment. During the present study the reactor was used to screen the mixtures for secondary atomization intensity.

For the present experiment droplets were generated by forcing the fuel through a small orifice (100 micrometer diameter). The liquid jet is unstable and breaks into a polydisperse spray whose initial mean diameter is approximately twice the orifice diameter [20]. The design of the orifice head is shown in Figure 2-2. The fuel samples were supplied to the orifice by the manifold shown in Figure 2-3. Nitrogen was used to pressurize the samples, and the ball value arrangement was designed to allow a quick screening of five mixtures.

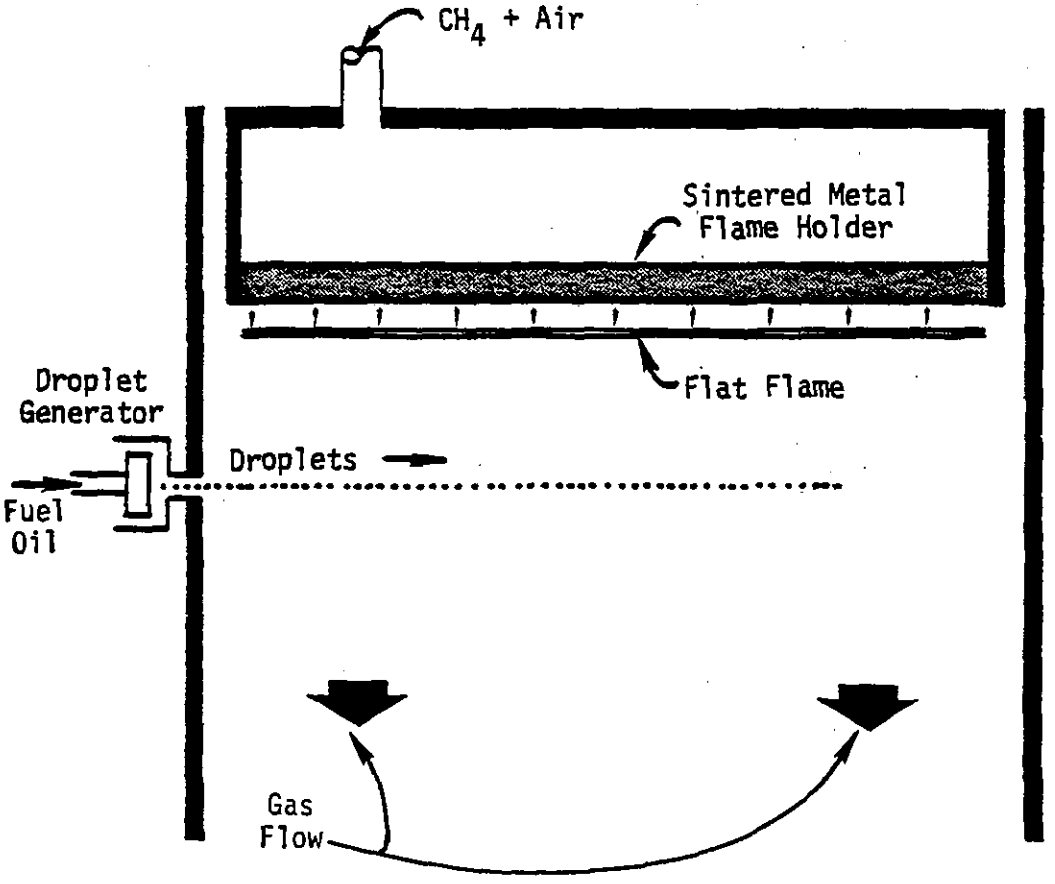

Figure 2-1. Slip-flow reactor.

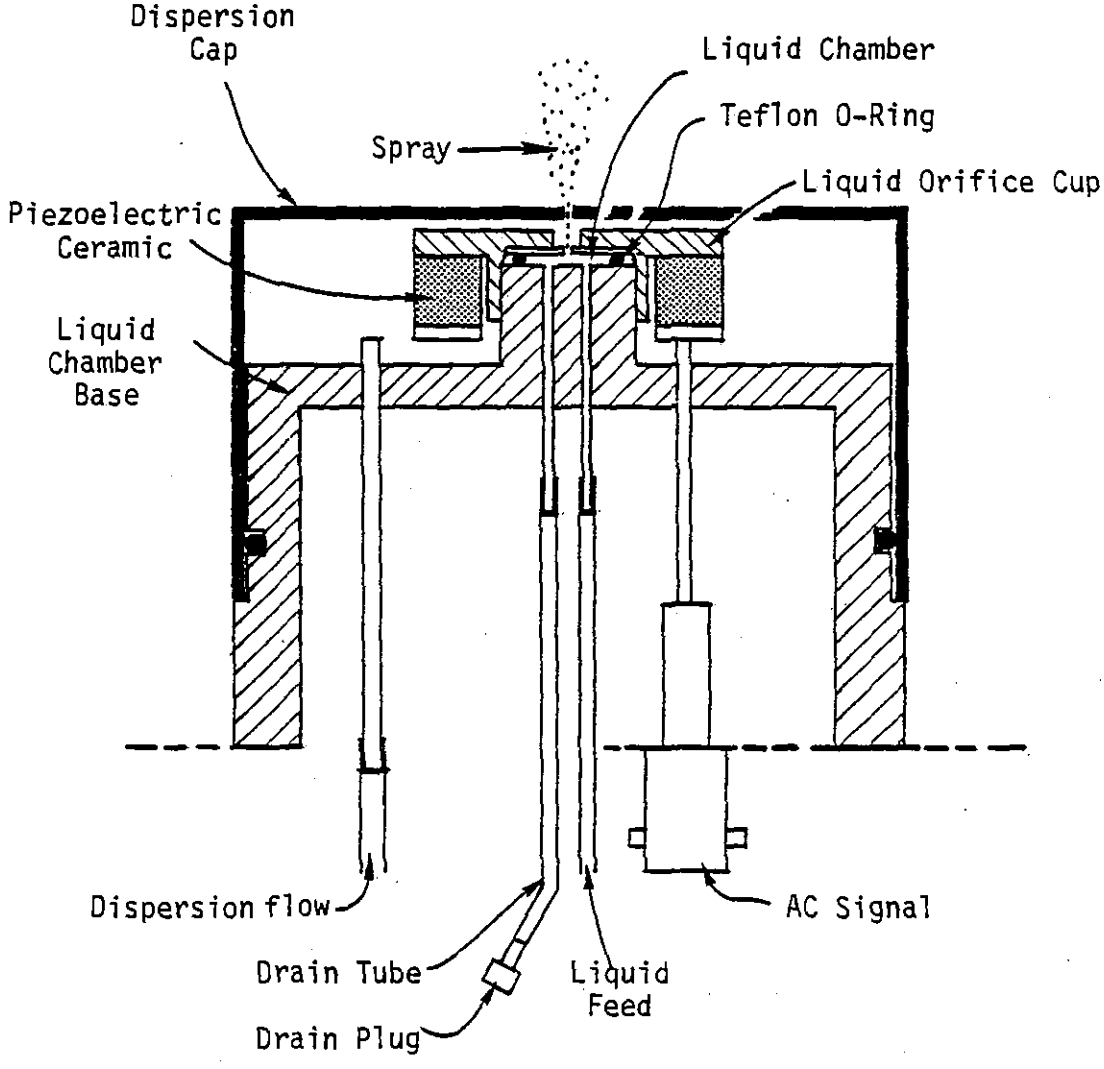

Figure 2-2. Schematic diagram of the droplet generator.

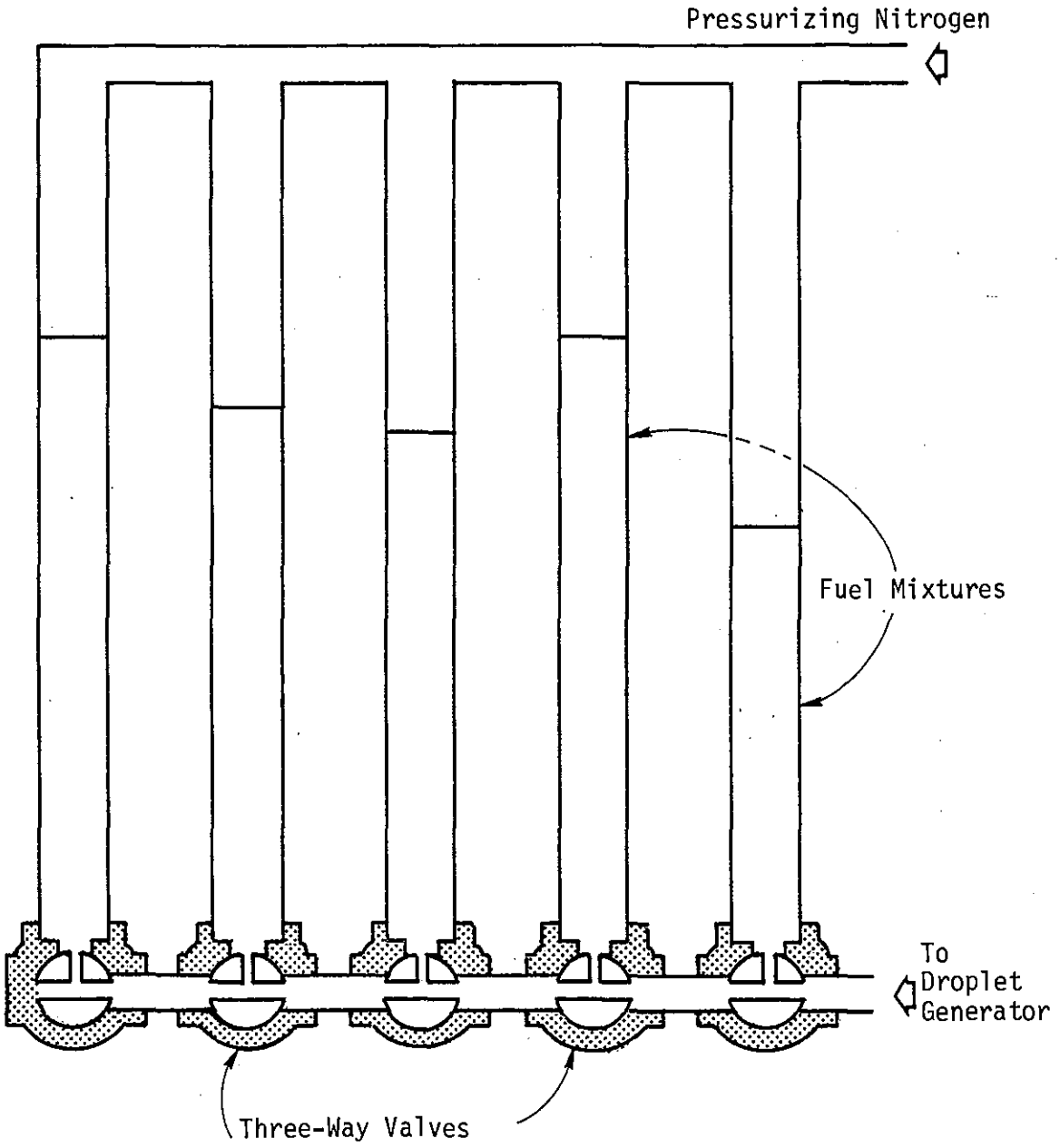

Figure 2-3. Fuel selection and delivery system.

2.2 Turbulent Flame Reactor

The turbulent flame reactor (TFR) is used to provide a turbulent liquid spray flame, including swirl, recirculation, broad drop-size distribution, and high variation in droplet number density. It is particularly important that the reactor be capable of simulating the compound escape mechanisms that can occur for flame zones of liquid injection incinerators. Very high heat removal rates are utilized to quench post-flame reactions. Thus, the destruction which occurs in the turbulent diffusion flame is emphasized over nonflame decomposition which occurs in the post-flame region. The reactor design is based on a configuration for which aerodynamic field data are available [21].

The reactor consists of a swirling air/liquid spray burner firing into a 30.5 cm diameter by 91.5 cm long water-cooled cylindrical enclosure shown in Figure 2-4. The water-cooled cylinder is made of 304 stainless steel and is formed into three interchangeable segments which are joined by flanges and gasketing. The lowest segment has four sight glass ports, one of which is used for flame ignition. The reactor top plate contains an exhaust fitting which includes the sampling ports, and a Vycor plate/mirror arrangement for obtaining an axial view of the flame.

The burner consists of a pressure-atomized nozzle (Delavan WDA series) located level with the bottom plate of the reactor as shown in Figure 2-4. The nozzle forms a 60^{o} angle hollow-coned spray pattern. The main burner air is introduced through the annular space around the nozzle. A research-type variable swirl block burner is used to introduce the burner air. As illustrated in Figure 2-5 this burner provides for tangential introduction of the air through swirl blocks into the burner throat. To provide a smooth entry of air into the burner and to prevent corner recirculation, a castable refractory quarl is placed in the lower water-cooled segment. As shown in the figure, this has the form of a 45-degree cone.

Liquid fuel was provided from a pressurized storage tank, through a rotameter and a control value, and into the burner nozzle. The burner air

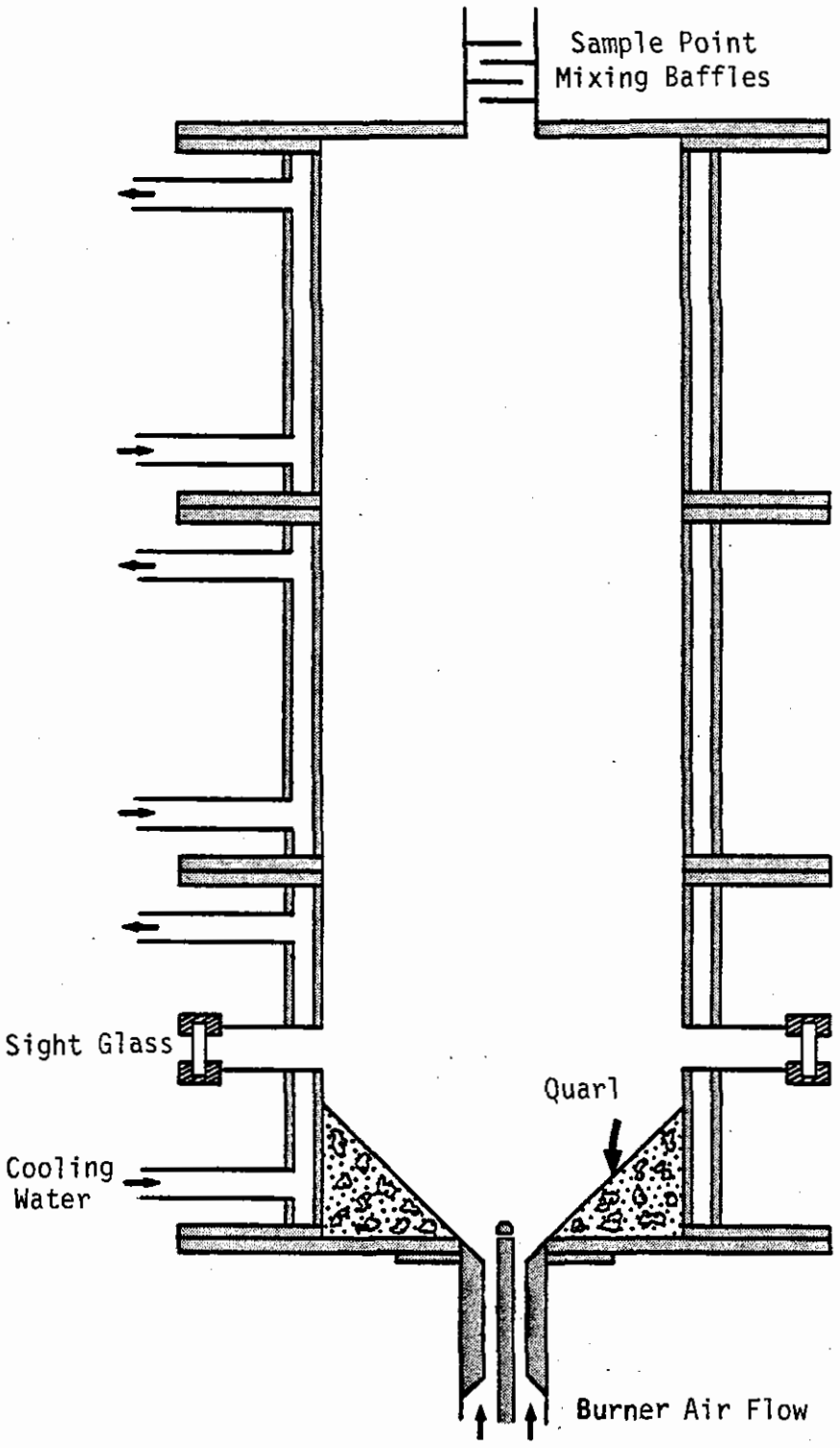

Figure 2-4. The turbulent flame reactor.

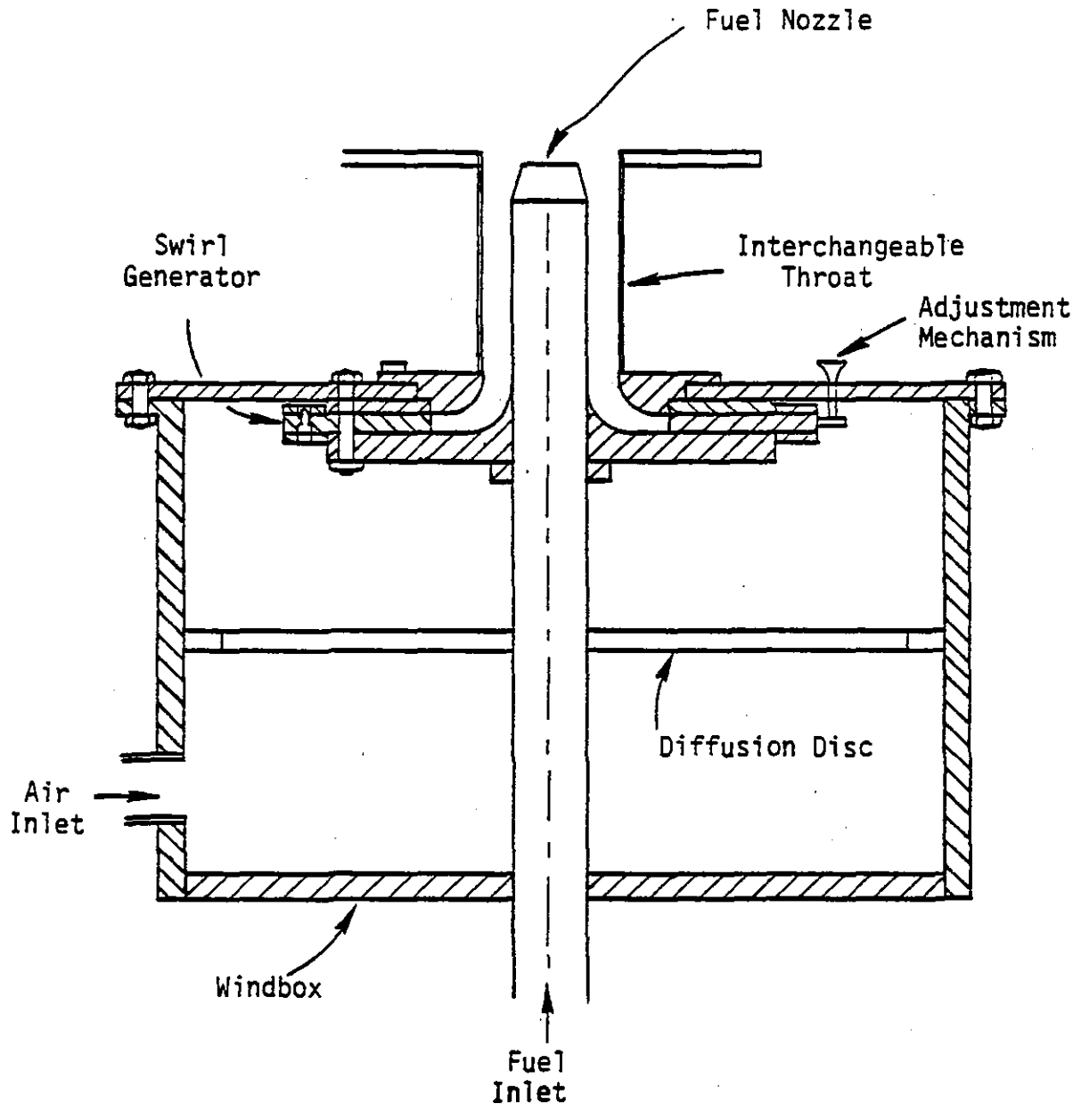

Figure 2-5. Schematic diagram of burner and windbox.

flow is supplied from the compressed air system and is metered by a venturi flow meter. Gas samples are withdrawn from the exhaust duct following a series of mixing baffles.

2.3 Atomizer Characterization Rig

The atomizer characterization rig was developed under a previous EPA-sponsored program for the testing and comparison of spray measurement techniques. The chamber is shown in Figure 2-6. It consists of a plexiglass cylinder in which the nozzle is mounted on centerline downfired. One air blower provides the primary air, which is introduced around the nozzle to simulate the air/droplet interaction that occur in a real burner. A second blower provides the screen air which is introduced uniformly through the top of the cylinder and whose purpose is to prevent droplets from recirculating into the measurement field.

Two ports at opposite sides of the chamber provide access for the Malvern 2600 HSD particle size analyzer. The Malvern measures dropsize distribution by measuring the diffraction of a laser beam as it passes through the spray field. The diffraction pattern is collected by a Fourier transform lens and is focused onto a detector array. A microcomputer reduces the detector signal to a droplet size distribution. This droplet size distribution can be expressed in terms of a two parameter model (e.g. Rosin-Rammler or log-normal) or in terms of a model independent fit which is capable of reproducing multimodal distributions.

The fuel supply system consists of two stainless steel cylinders in which the fuel is pressurized by nitrogen, a rotameter, and a flow control valve. The system was constructed to operate at pressures to 200 psig. The fuel droplets are collected at the bottom of the spray chamber and the air passes through a demister prior to venting.

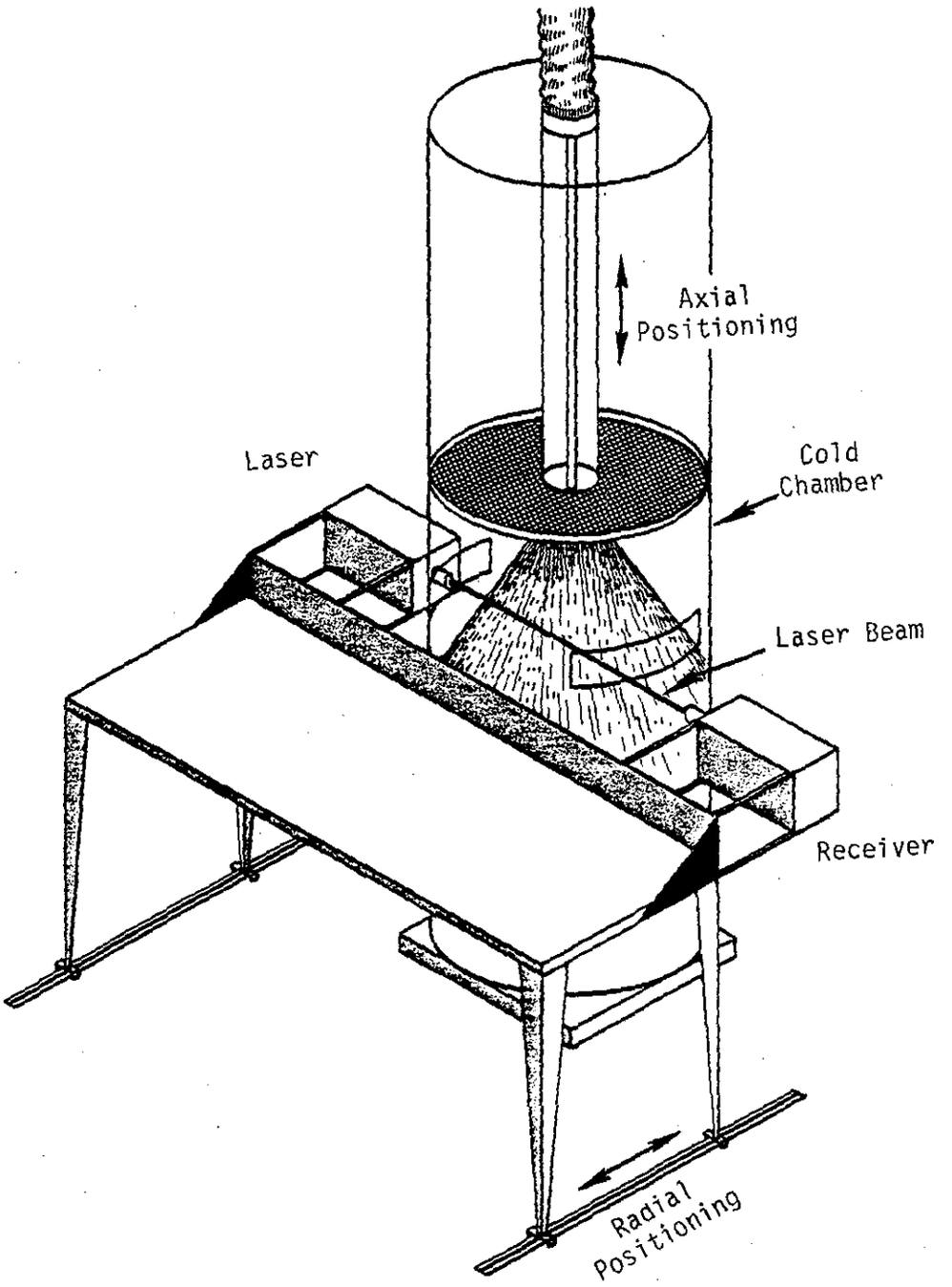

Figure 2-6. Laser diffraction system.

2.4 Conventional Analysis

Gas samples from the various experiments were analyzed for CO, CO_2, O_2, and total hydrocarbons. The sampling system is shown in Figure 2-7. The samples are withdrawn from the flue gas ducts by uncooled stainless steel probes and transferred via a heated stainless line to the filter oven. The filter oven is maintained at 200°C and it contains a 47 mm stainless steel filter holder. The sample gas is filtered by a glass fiber filter and passes through a condensate knockout. From the condensate trap the sample is pumped in series through an Anarad Model AR500R nondispersive infrared CO analyzer, a Horiba Mexa 300 CO_2 analyzer and a Beckman O_2 analyzer. Total unburned hydrocarbon measurements were performed with a Beckman Model 402 total hydrocarbon analyzer. The sample stream for this analyzer was withdrawn from the main sample line immediately behind the filter.

2.5 Volatile Organic Analysis

Volatile organic compounds are measured in the exhaust stream by use of a Nutech Volatile Organic Sampling Train (VOST). This instrument, shown in Figure 2-8 (adapted from Junglaus et al. [22]), preconcentrates the organic compounds present in a large volume of gas for gas chromatograph analysis.

Gas samples are drawn from the flue gas through a heated line to an ice water chiller/condenser. The majority of the organic compounds are stripped from the gas and condensate in the first cartridge filled with Tenax-GC. A second condenser and trap are provided to complete the stripping process and a final charcoal trap is used to capture very volatile organics that might break through both Tenax traps. A sampling rate of 1.0 l/min was maintained for 10 to 20 min. At the conclusion of sampling the traps were removed, sealed, and refrigerated until analyzed.

The contents of the Tenax cartridges were thermally desorbed for gas chromatographic analysis. Figure 2-9 shows the system used. Nitrogen flows through the two cartridges in series in the reverse direction of the original sampling. The released material is recollected on the Analytical Trap.

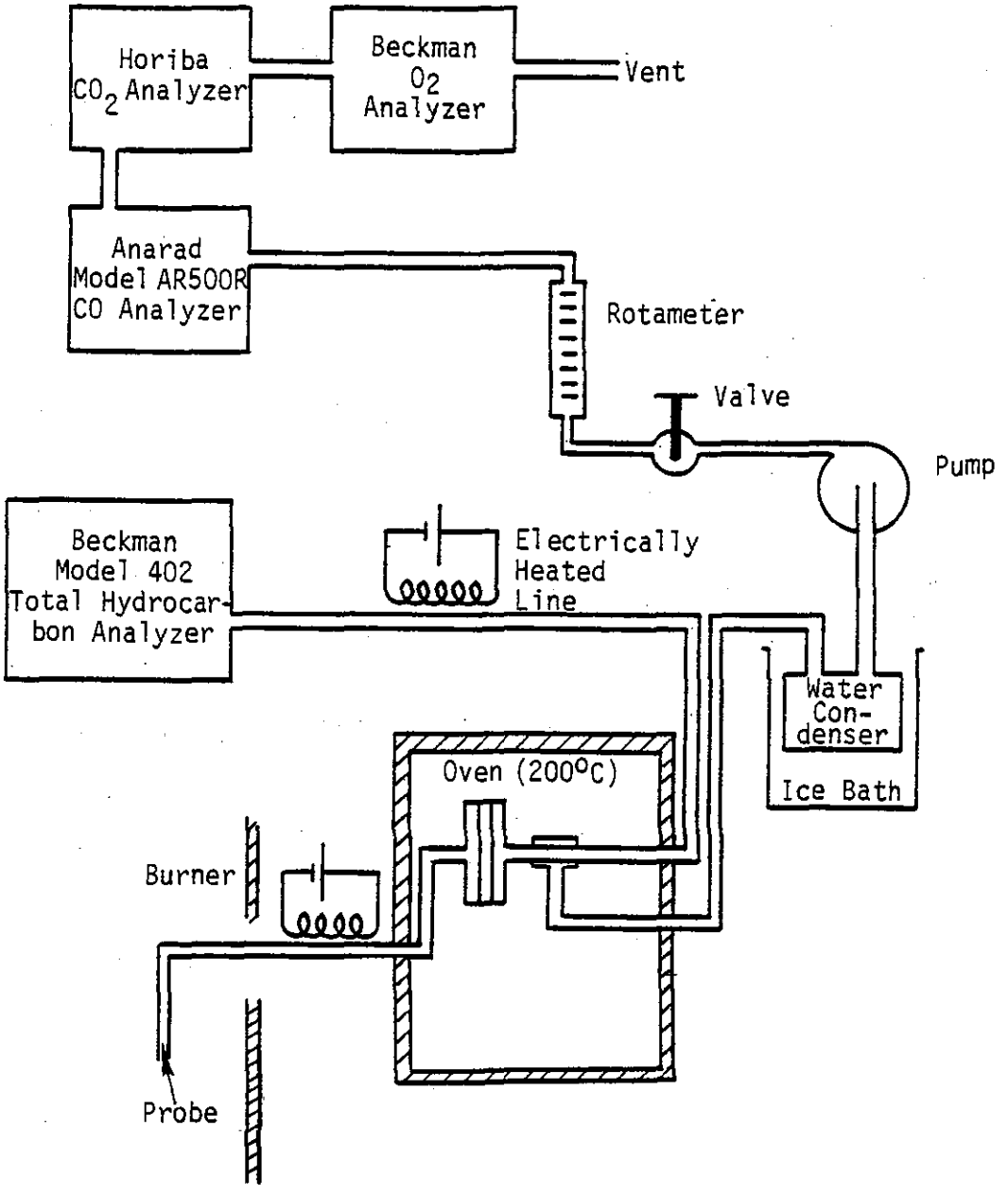

Figure 2-7. Sample train for conventional analysis.

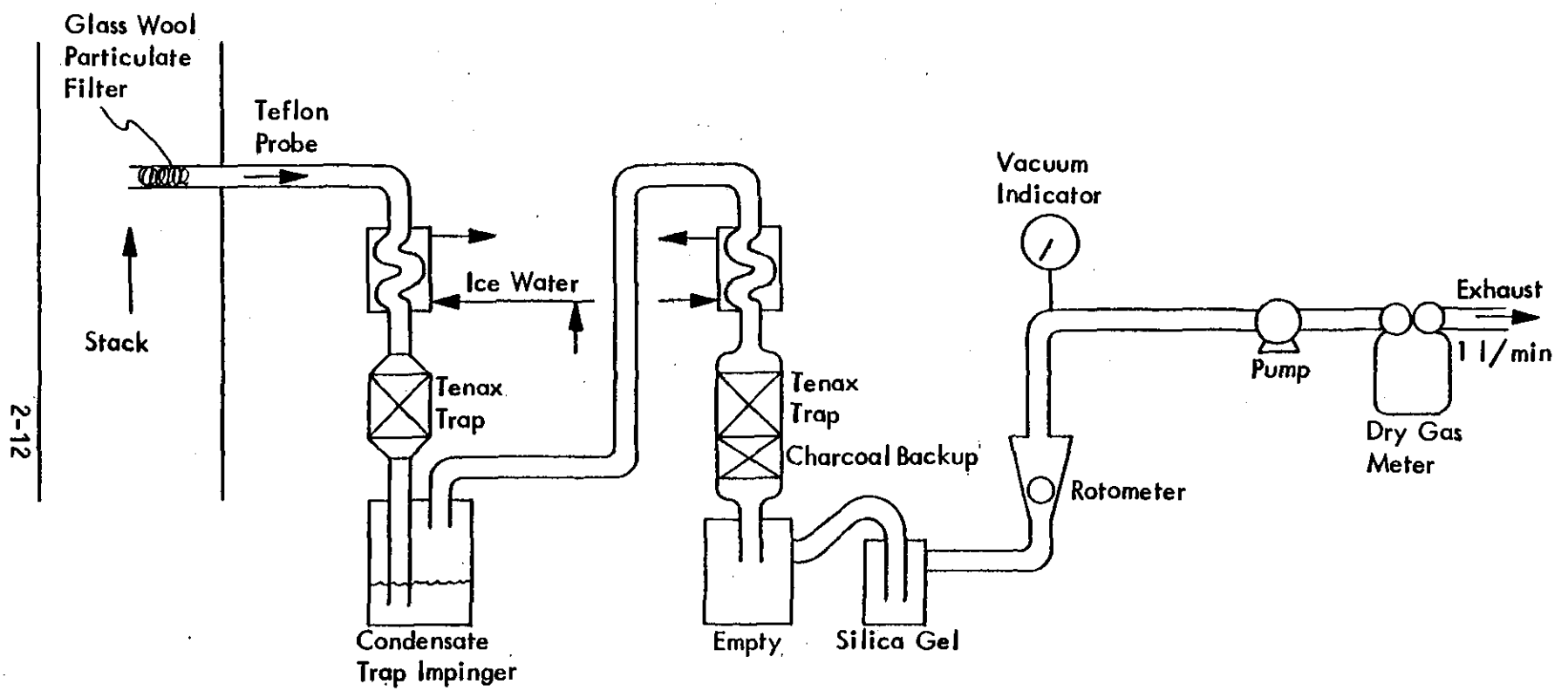

Figure 2-8. Volatile organic sampling train (VOST) [22].

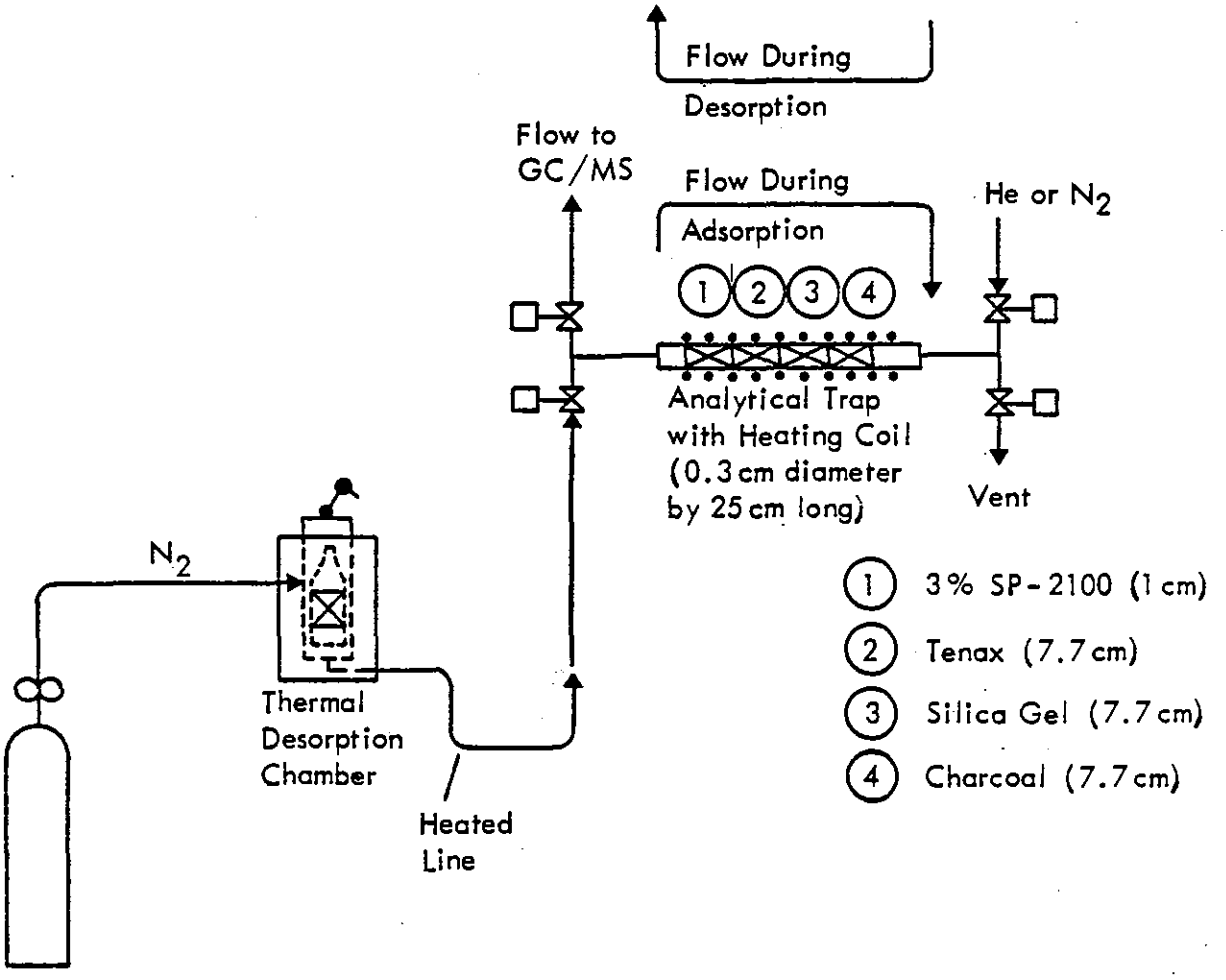

Figure 2-9. Schematic diagram of trap desorption/analysis system [22].

Following desorption the Analytical Trap is rapidly heated to force a rapid, quantitative release of sample onto the gas chromatograph column. The long, narrow design of the Analytical Trap lends itself to the purpose of providing a narrow, high-resolution injection peak. The injection spike was analyzed by a Perkin-Elmer Sigma-2 gas chromatograph equipped with a flame ionization detector. The carrier flow was 30 cc/min through a temperature programmed 3.0 m long by 3.2 mm diameter Porapak-N column (70°C for 2 min, 35°C/min to 180°C, hold at 180°C). The sampling and analysis system was characterized by:

- Comparison of direct compound response factors with those measured for the entire adsorption/desorption system to estimate compound recovery factors.

- Direct calibration of the VOST system through the use of highly dilute laboratory standards.

- Optimization of capture with sampling rate and time (i.e., avoiding breakthrough).

These quality assurance procedures are detailed in Appendix A.

3.0 HAZARDOUS WASTE ATOMIZATION

3.1 Background and Objectives

Work directed toward characterizing the effect of atomization quality on the combustion efficiency of liquid fuels suggests two ways in which atomization influences efficiency [23]. First, the spray must be sufficiently fine to allow complete evaporation within the flame. Secondly, the spray must be injected into the correct portion of the flow field to ensure stability. Organic hazardous waste can be viewed as simply an additional fuel constituent. A high DRE of the hazardous component can be viewed as its high "combustion" efficiency. Thus, the same atomization factors that influence fuel consumption efficiency would also be expected to influence waste DRE.

In practical units, atomization failure can be associated with worn or plugged nozzles. Incinerators are particularly susceptible to these problems because the fuels can be corrosive or may contain solids. Since design dimensions can be critical to nozzle performance, any changes in these result in degraded operation.

The decrease in combustion efficiency associated with a degradation in atomization quality can be attributed to one or a combination of two mechanisms [25]:

- Droplet Breakthrough. Off-design operation of nozzles results in an increased drop size and reduced droplet momentum [24]. Large droplets can penetrate the flame before completely evaporating and thereby preclude total consumption of the fuel.

- Nozzle Spray/Aerodynamic Mismatch. Ideally, a nozzle will inject a liquid into an aerodynamic field with a spatial distribution that will ensure sufficient fuel/air mixing, residence time, and thermal excursion to preclude the penetration of unoxidized material. The injection, for example, of fuel into the shear layer of a well

established recirculation zone will generally maximize the processing of the liquid. Any irregularity that could upset this balance (an improper spray angle, fuel collapse onto the centerline, distorted spray symmetry) can lead to inefficient combustion.

These same processes maybe expected to influence the DRE of wastes.

Previous results in our laboratory [6,7] have indicated that reduction in atomization quality can lead to increased waste emissions from subscale turbulent spray flames. The present nozzle characterization study was established to more fully address the effect of nozzle performance on waste destruction efficiency with emphasis on the acquisition of data on the atomization performance of the nozzles used in the previous lab-scale studies. Emphasis was placed on the behavior of the spray pattern with respect to operating parameters, and on the influence of spray pattern on DRE in the turbulent flame reactor.

3.2 Approach

The approach used to characterize the nozzles was to measure the droplet size distribution in a cold flow spray chamber using a Malvern 2600 HSD laser diffraction particle size analyzer, both of which are described in Section 2.0. The nozzles selected for testing were the four Delavan pressure atomized (WDA series-60^{o} spray angle) hollow coned models used in the previous flame tests. The four nozzles encompass nominal capacities of 1.9, 2.8, 3.8, to 5.7 liters/hour (0.5, 0.75, 1.0, to 1.5 gallons/hr). Testing concentrated on the fuels used during the flame testing: No. 2 fuel oil and heptane. Using this testing, the overall approach was as follows:

1. Characterize Pressure Jet Nozzles: The cold flow characteristics of the pressure jet nozzles were characterized with respect to mean droplet diameter and droplet size distribution. The key parameters were fuel properties, fuel pressure, nozzle scales axial distance

from the nozzle, and radial dropsize distribution. These tests addressed the questions:

- How are nozzle operating parameters linked to droplet size distributions.

- Where within the spray field do the large droplets appear.

2. Relate Size Distribution to DRE: The previous work [6,7] has shown that waste emissions increased when atomization quality was degraded in the TFR. The key questions are:

   - What is the relationship between droplet size distribution and DRE.

   - What is the droplet behavior that brought about insipient DRE failure in the turbulent flame reactor.

The development of the exact mechanism by which waste escapes the reactor under an atomization failure will help in predicting minimum standards for atomizer performance. This information will also be useful for characterizing PIC formation environments.

3.3 Results and Discussion

The discussion will be divided into three sections: Atomizer characterization, influence of atomization on DRE, and mechanisms of waste escape.

3.3.1 Atomizer Characterization

Axial Variation. The Sauter Mean Diameter (SMD) is presented in Figure 3-1 for three nozzles operating on water pressurized to 200 psig. The variation in SMD is shown, in this case, as a function of axial distance from the front face. A dip on the SMD occurs for all three nozzles close to the face. One explanation for the dip is that the smaller droplets take longer

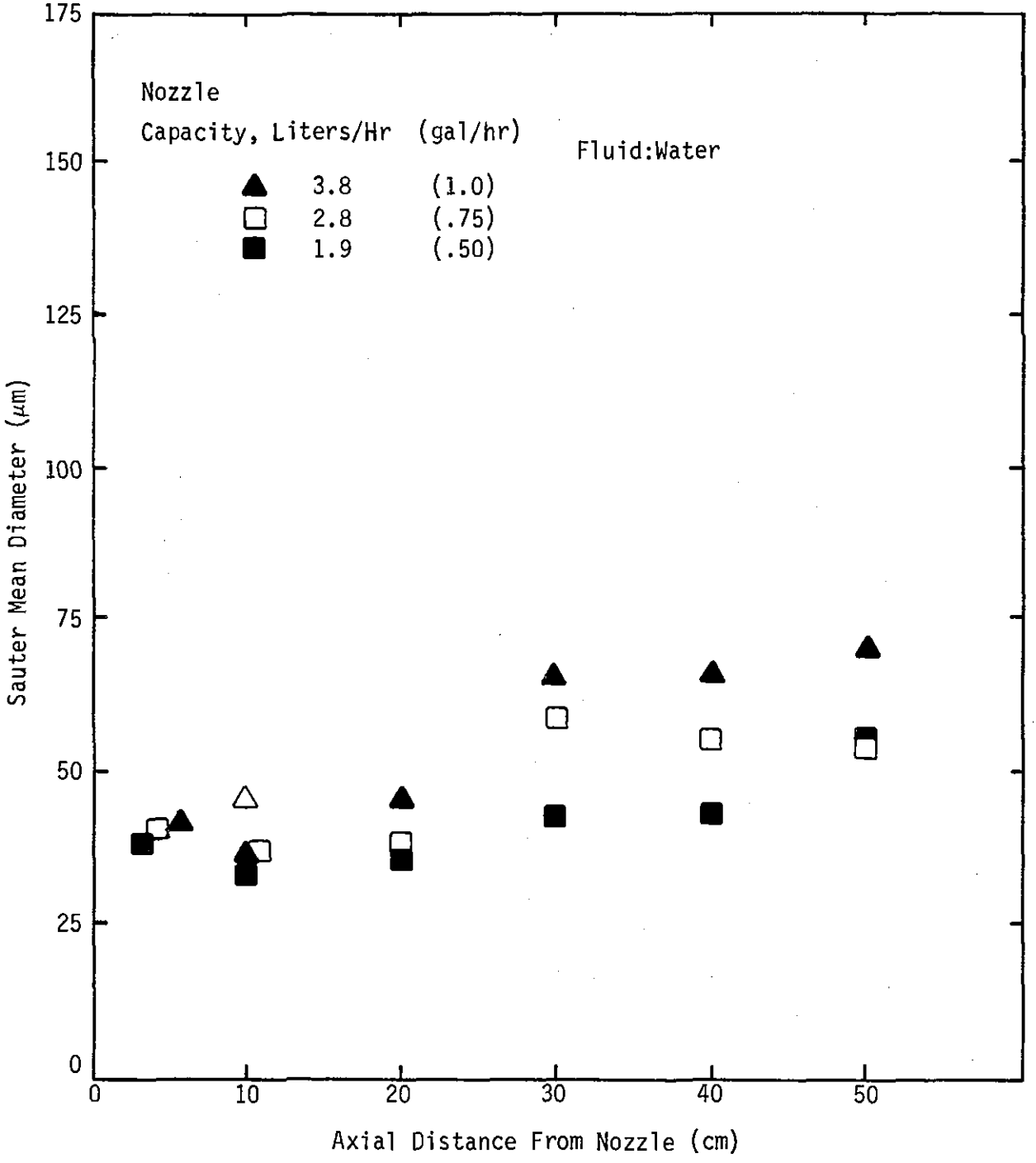

Figure 3-1. Droplet diameter as a function of centerline location, p = 200 psig.

to reach a terminal velocity than larger droplets. Hence, close to the nozzle, smaller droplets will be more heavily weighted due to a higher relative velocity. These data also suggest that the smaller capacity nozzles produce a smaller SMD in the case of water.

Radial Variation. The variation in SMD with radial departure from the spray centerline is illustrated in Figure 3-2, again as a function of axial distance from the nozzle. The data were obtained at each axial location by first projecting the Malvern transmitter beam through the centerline of the spray to obtain the bulk SMD that is conventionally measured in sprays. The spray was then moved radially until the transmitter beam projected through the edge of the spray to measure the aggregate SMD at the outer boundary. The data clearly show that, at the edge of the spray, droplets are substantially larger than within the bulk of the spray.

Pressure Dependence. The Sauter mean diameter for heptane sprays as a function of heptane pressure at the nozzle is presented in Figure 3-3a. The atomization depends only on liquid pressure for the four nozzles tested. Thus, different nozzles among the four-nozzle set will yield the same atomization quality if operated with heptane at identical pressures. The figure also indicates that the mean droplet size at the design pressure for those nozzles (150-200 psi) is about 30 microns. The same data as provided in Figure 3-3b for No. 2 fuel oil. These results show a few features that differ from the heptane data. At high pressure, the mean diameter has not yet reached an asymptotic value as did the heptane data. Also, a variation between the various nozzles is shown, although a systematic variation that would lead to a correlation with nozzle scale is not apparent.

Influence of Fuel Properties. The data presented in Figures 3-1, 3-2, and 3-3 show a strong relationship between SMD and atomizing pressure as well as fuel type. A theoretical analysis of the atomizer characterization results was undertaken to (1) define the limits of the predictive capability for the nozzles used in the TFR, (2) establish the minimum number of tests needed to characterize a nozzle, (3) define the limits to which the data can

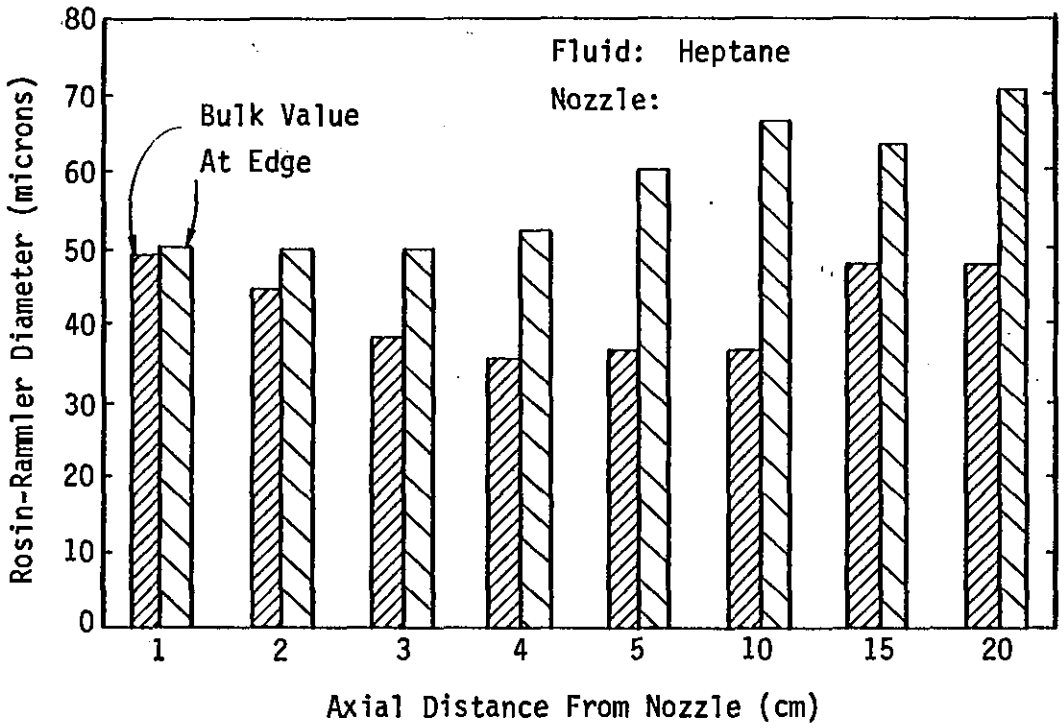

Figure 3-2. Droplet diameter as a function of radial location, p = 200 psig.

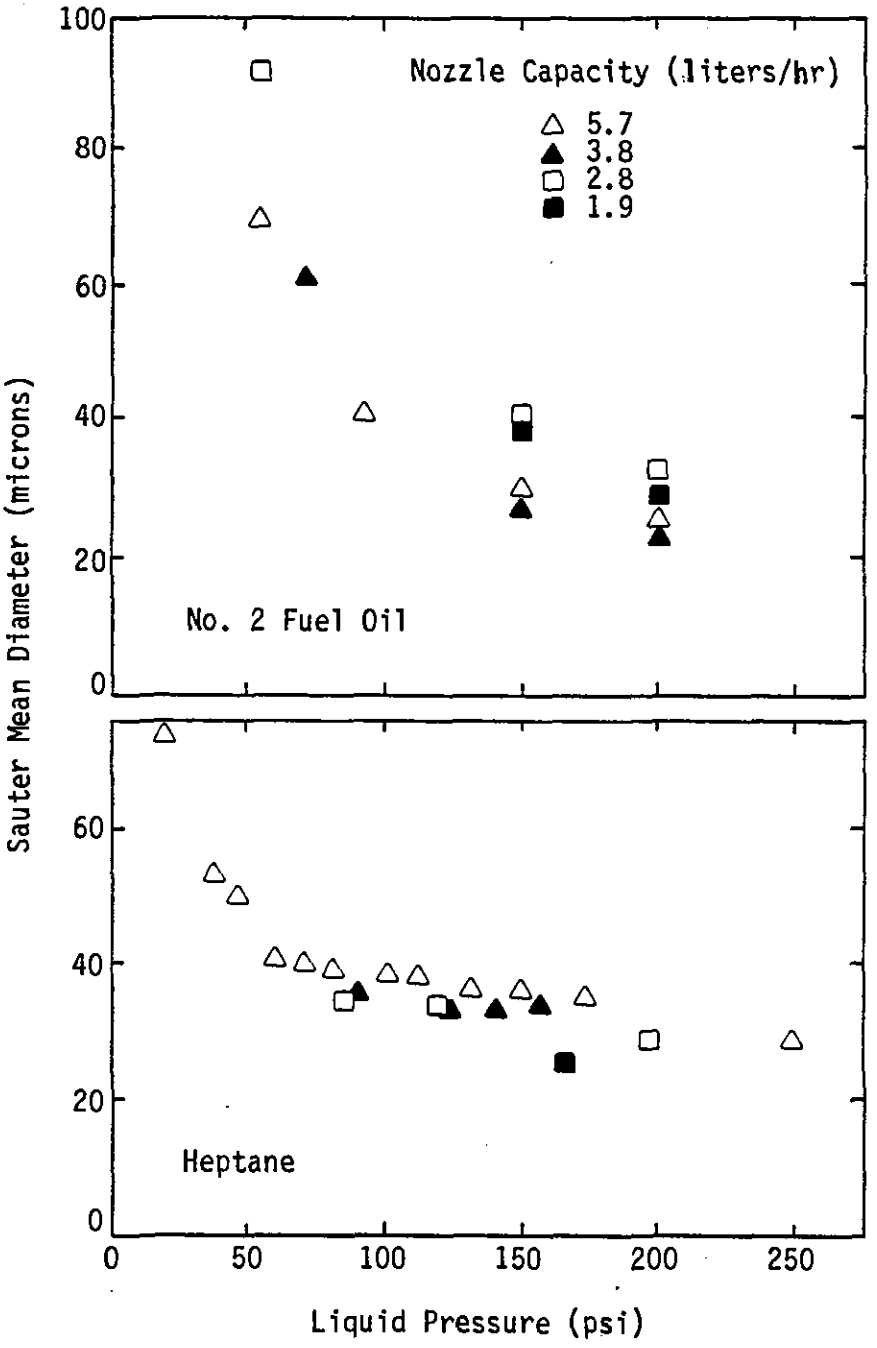

Figure 3-3. Droplet diameter as a function of liquid pressure.

be accurately extrapolated, and (4) upgrade the analytical capabilities for hazardous waste.

The nozzles used in the TFR were Delavan WDA series hollow-coned pressure-jet swirl atomizers. Figure 3-4 shows a cross-sectional schematic of the Delavan nozzle. The liquid is forced through the four tangential slots into the swirl chamber. The liquid vortex increases in tangential velocity as it approaches the exit where the spray exits with radial and axial velocity components that produce a characteristic spray cone angle. The dimensions shown are the critical values needed for the performance correlations.

Considerable research has been devoted to developing predictive relationships for the performance of this class of atomizers. The resulting relationships are empirical and, as such, can be used outside of their original range of variables only with great caution. We have selected a model developed from large-scale data [25]. This model is particularly interesting because the effect of both fuel properties and atomizer geometry were systematically varied. The performance correlation is:

$$D = 2.47\, M^{0.315}\, p^{-0.47}\, n_L^{0.16}\, n_A^{-0.04}\, \left(0.25\right)_L^{-0.22}\, (L_o/D_o)^{0.03} \qquad (1)$$

$$(L_s/D_s)^{0.07}\, (A_i/D_o D_s)^{-0.13}\, (D_s/D_o)^{0.21}$$

Table 3-1 defines the various terms, in conjunction with Figure 3-4.

The direct application of the model to the present atomizers leads to a substantial overprediction of droplet diameter.

The large error was not surprising since the correlation was derived for larger nozzles than the Delavan atomizers. However, the present use of the relationship is to:

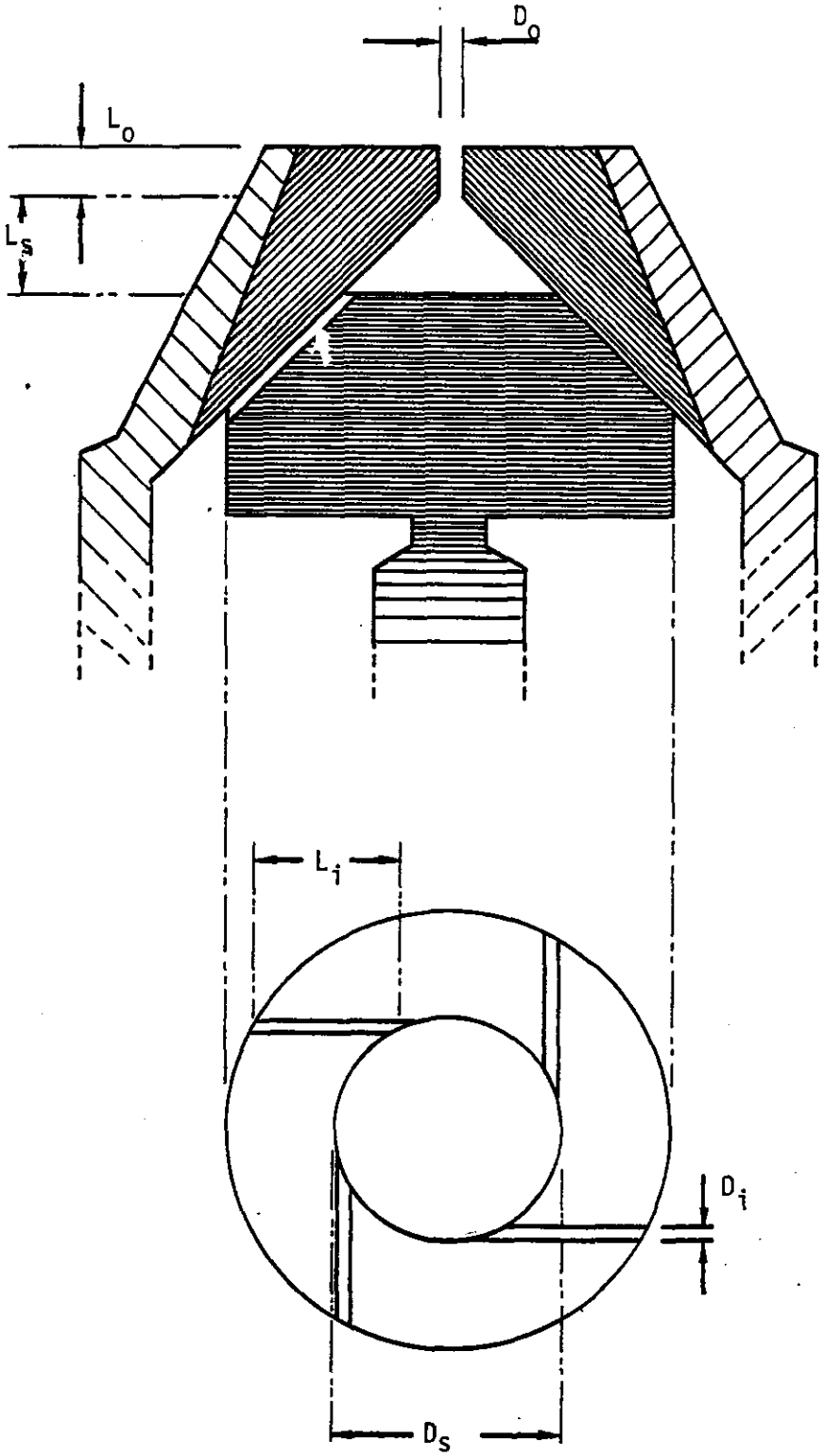

Figure 3-4. Definition of geometrical parameters for the Delavan WDA series swirl pressure-jet nozzle.

TABLE 3-1. PARAMETERS IN ATOMIZER PERFORMANCE CORRELATION

Parameter	Units	Definition
D	cm	Mean droplet diameter.
M	gm/sec	Fuel flowrate.
P	dynes/cm^2	Fuel pressure.
n_L, n_A	gm/cm/sec	Viscosity, fuel and air.
σ	dynes/cm	Fuel surface tension.
ρ_L	gm/cm^3	Fuel density.
L_o, D_o, L_s, D_s	cm	See Figure 3-4
A_i	cm^2	Total cross-sectional area of the four fuel slots (see Figure 3-4).

- Extrapolate data for one fuel and one nozzle to other operating conditions.

- Extrapolate data for a particular fuel and nozzle to other fuels.

If a single nozzle and fuel are in use, then Eq. 1 simplifies to

$$D \sim M^{0.315}\, p^{-0.47} \qquad (2)$$

Our previous data have shown that M and P are related by Bernoulli's equation for these nozzles. If Bernoulli's equation is used to eliminate either M or P from Eq. 2, the following are obtained:

$$D \sim M^{-0.63} \quad \text{or} \quad D \sim p^{-0.31} \qquad (3)$$

The first question is whether these are the appropriate exponents to describe the variation of mean diameter with flow and pressure. Figure 3-5 shows the comparison between the data for the 1.5 gal/hr nozzle (heptane) and Eq. 3 with the proportionality constant selected to provide the best fit. The close agreement indicates that the exponent shown in Eq. 3 provides a good fit for extrapolating mean droplet size data to various flow rates.

The fit for the pressure exponent is shown in Figure 3-6. This also indicates good extrapolating capability for the pressure relationship.

Atomization quality data obtained for the same nozzle with No. 2 fuel oil provided an opportunity to evaluate the correlation's capability to accommodate changes in fuel properties for an identical nozzle. Equation 1 was simplified to remove all of the nozzle-dependent parameters, but preserve the fuel-dependent terms. Using this simplified relation, the heptane results were used to predict the No. 2 fuel oil behavior. The results are shown in Figure 3-6. The model overpredicts the data at high pressures by approximately 50 percent. The change in predicted mean diameter is almost entirely due to the difference in viscosity. This sensitivity to viscosity may be an artifact of the large nozzles from which the correlation was derived.

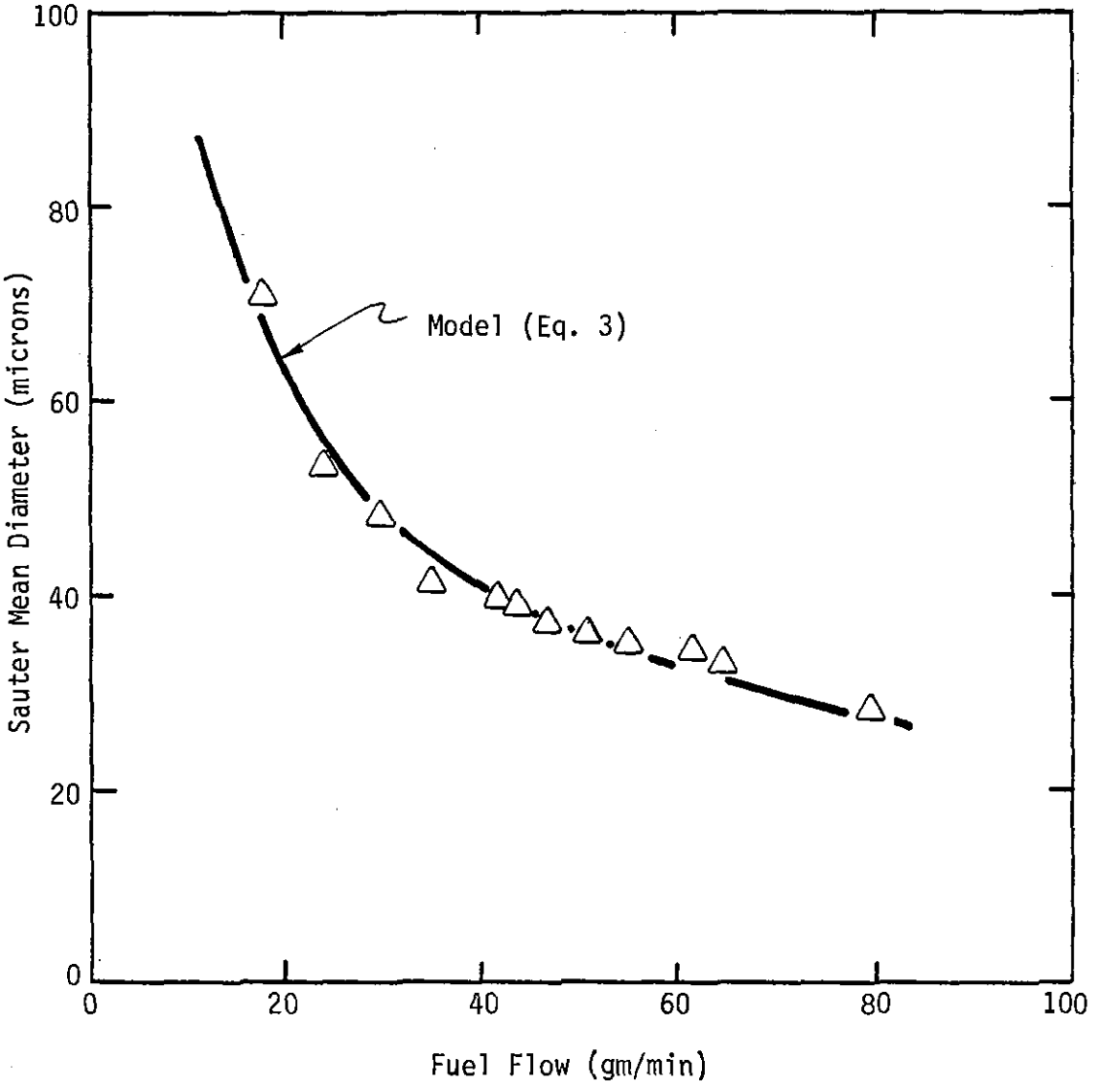

Figure 3-5. Variation of mean droplet diameter with fuel flow for heptane and the 1.5 gal/hr nozzle.

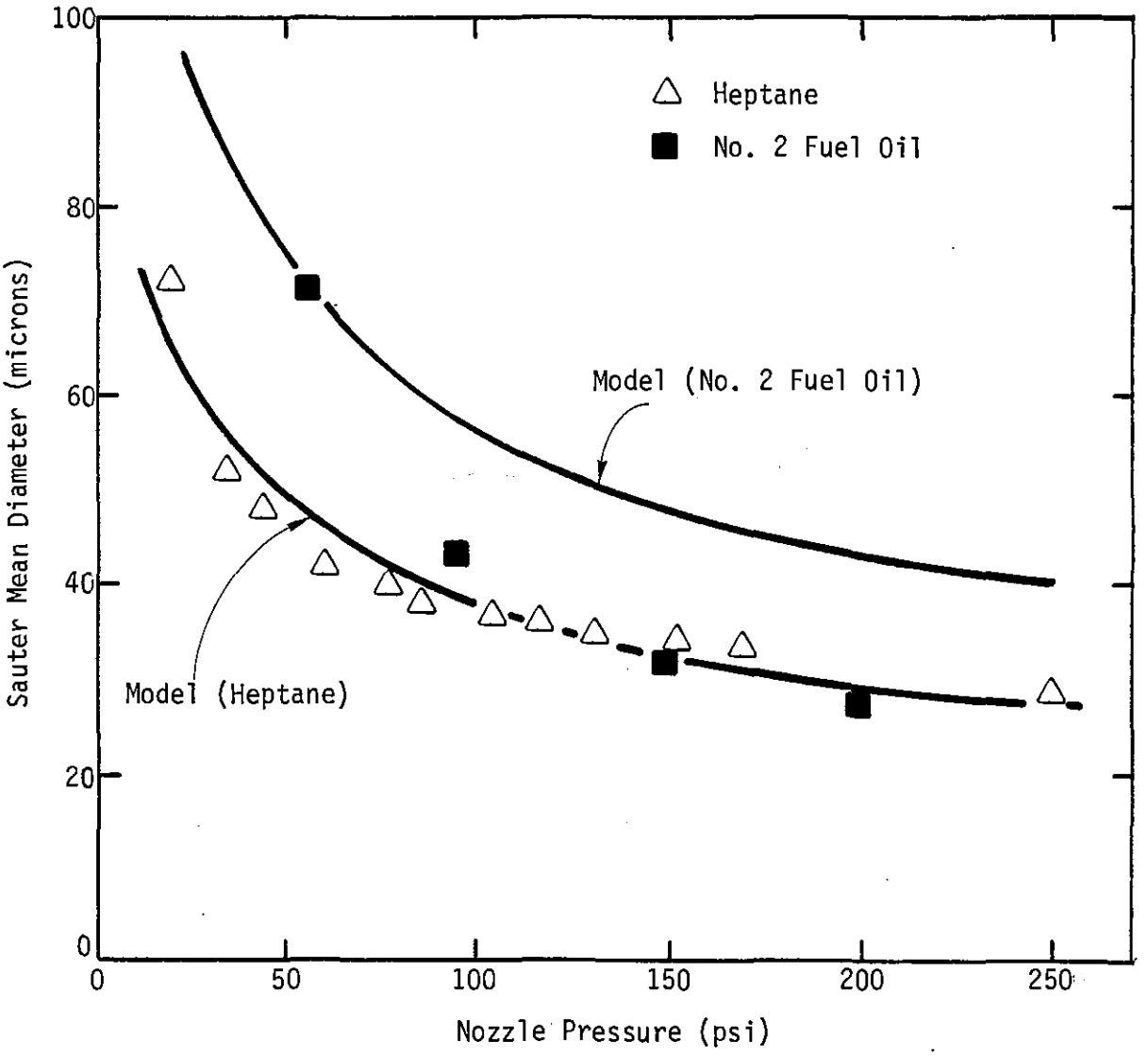

Figure 3-6. Variation of mean droplet diameter with fuel pressure for heptane and No. 2 fuel oil using the 1.5 gal/hr nozzle.

The conclusions are that, for a given nozzle and fuel, (1) atomization is principally a function of atomizing pressure and fuel flow, and (2) a limited number of measurements are sufficient to approximately characterize the variation of mean diameter with flow and fuel pressure.

3.3.2 Relation of DRE to Atomization Performance

In the previous work in our laboratory [6], both the on-design and off-design atomizer conditions were used in the TFR to determine the influence of atomization quality on DRE. Fuel flow rate of n-heptane was the independent variable and the air flow rate (17.3 liters/second) was maintained constant. For the "on-design" condition, Delavan WDA 60° series nozzles of various capacities (5.7, 3.8, 2.8, and 1.9 liters/hour) were used to maintain constant atomization quality as fuel flow was charged at constant nozzle pressure (125 psig). (The data of Figure 3-3a show the assumption of constant atomization quality was, in fact, reasonable.) The "off-design" condition was obtained by varying the fuel flow of one nozzle (5.7 liters/hour) at constant air flow rate.

The on-design data are presented in Figure 3-7. In Figure 3-8a, the off-design results are compared directly to the on-design results. As shown, the compound destruction efficiency and combustion performance was substantially degraded over the on-design performance. The atomization characterization of the nozzles used for these tests show clearly the degradation in atomization performance associated with the off-design operation (Figure 3-8b). The Sauter Mean Diameter increases as percent theoretical air departs from the on-design condition of 130 percent TA. More important, the percent mass associated with large droplets (d_p>160 measurement) increases dramatically from near zero percent if the total mass at 130 percent TA to over 40 percent at 320 percent TA.

Under the present program, additional testing was conducted to obtain further evidence of the association of atomization with destruction efficiency. The TFR was operated with No. 2 fuel oil doped to 3.0 weight percent with an equimolar mixture of test compounds used in the previous

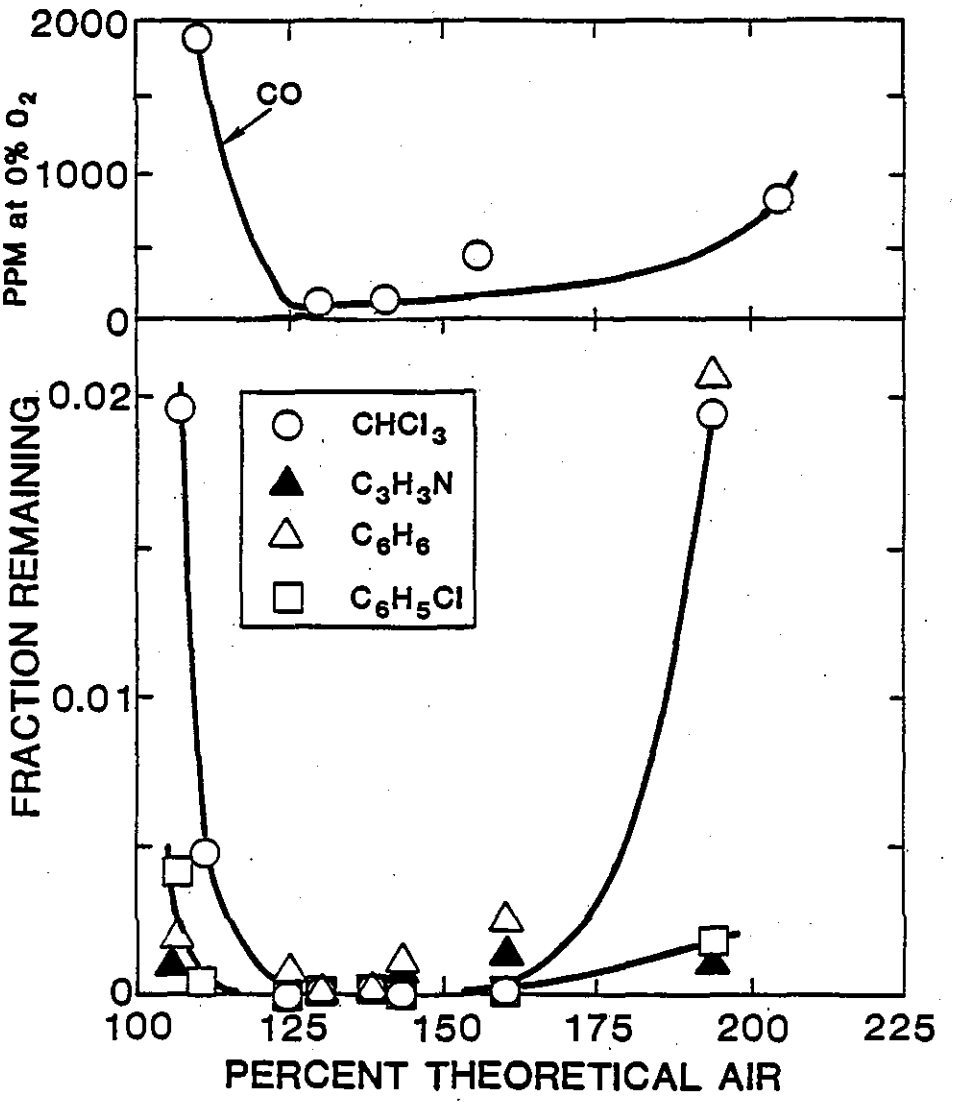

Figure 3-7. Test compound emissions from the TFR as a function of theoretical air n-heptane [6]. © Copyrighted by The Combustion Institute. (Reproduced by permission.)

a) Exhaust CO and Fraction Remaining

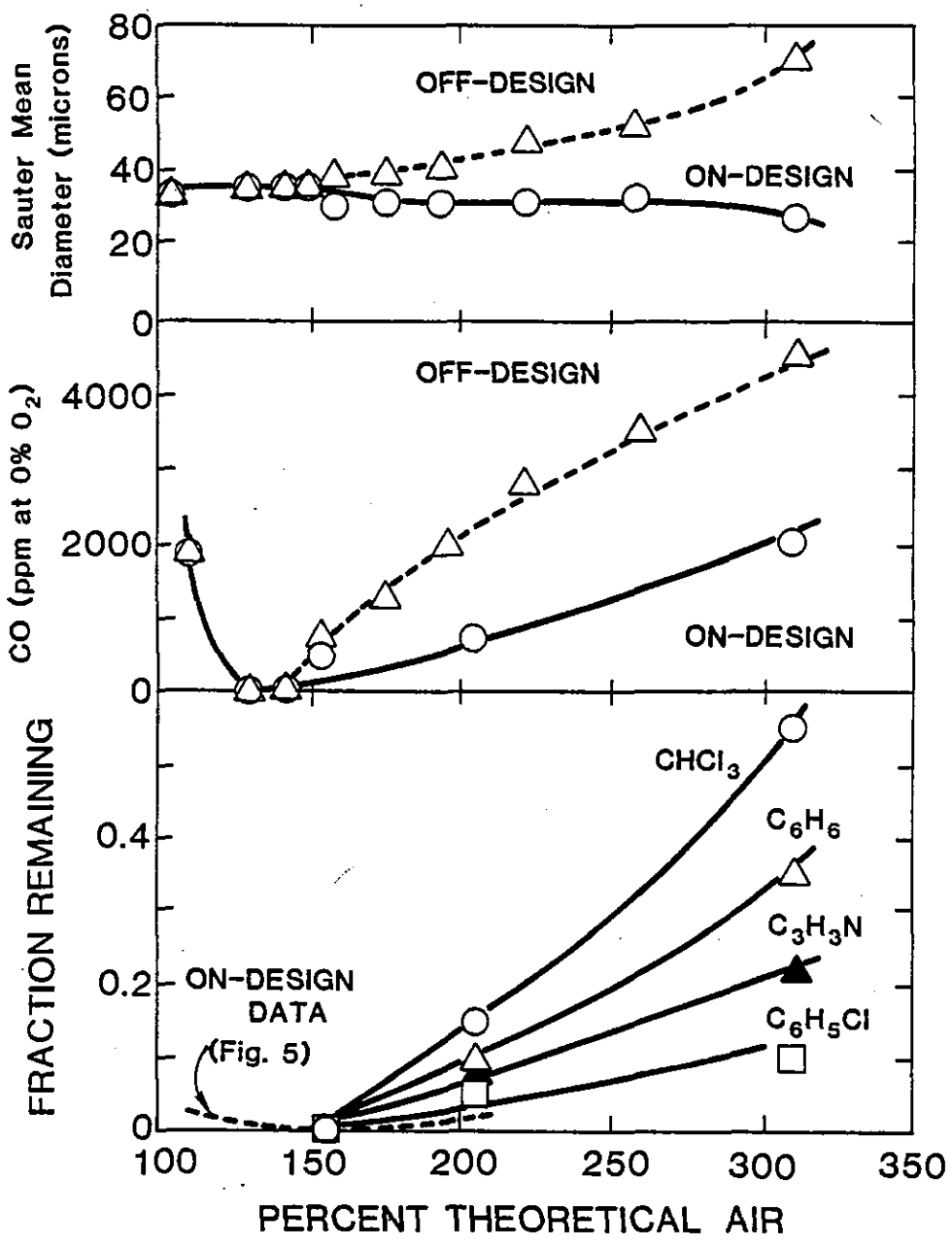

Figure 3-8. Impact of atomizer performance on fraction of test compound and CO in the exhaust, and nozzle SMD n-heptane.

b) Nozzle Performance

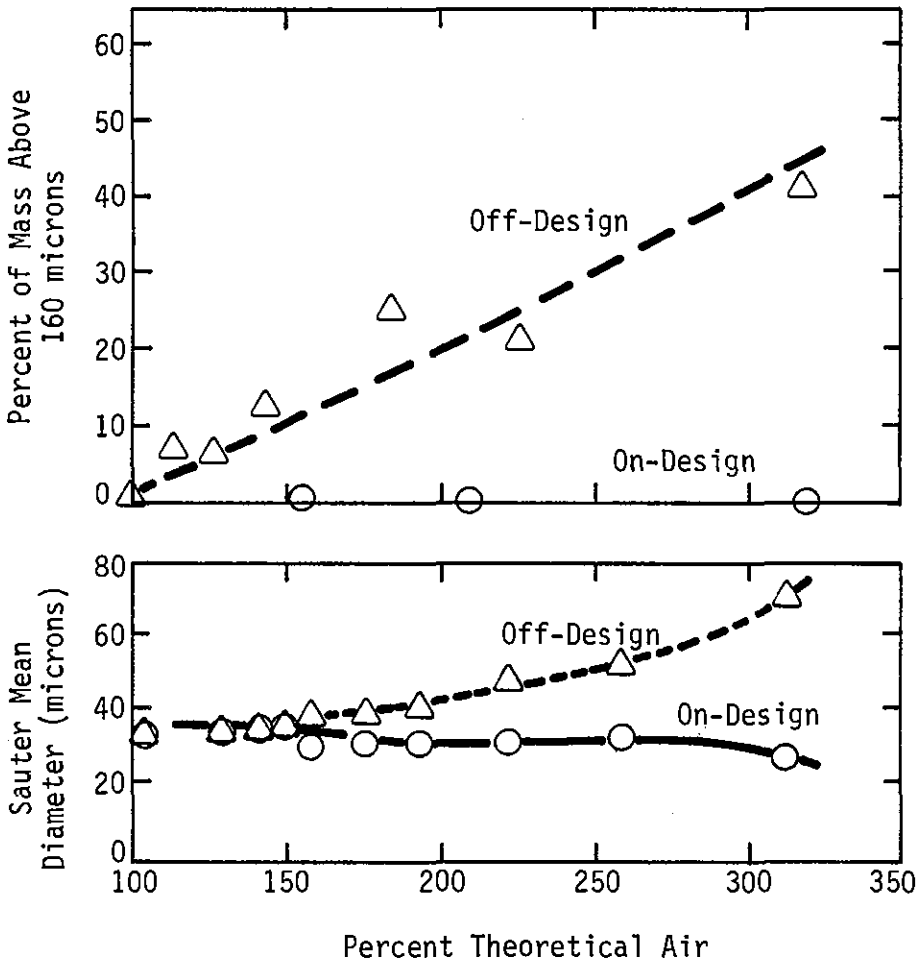

Figure 3-8. Impact of atomizer performance on fraction of test compound and CO in the exhaust, and nozzle SMD n-heptane (concluded).

study. The No. 2 fuel oil was supplied through a 3.8 liters/hour (1.0 gallons/hour) WDA Delavan 60° nozzle at the rated pressure of 200 psig for the "on-design" condition. To achieve "off-design" conditions, an oversized WDA Delavan 60° nozzle (5.7 liters/hour) was used to supply the same fuel flow rate. Theoretical air was the independent variable. Figure 3-9 shows the fraction of each of the compounds that escaped destruction. The on-design nozzle results show results consistent with the previous TFR data, namely:

- A range of high DRE values are indicated at stoichiometries between 100-200 percent theoretical air.

- At low theoretical air the increased waste emissions indicate a failure mode due to fuel-rich pockets breaking through the flame.

- At high theoretical air the increased waste emissions indicates a quenching failure mode in which the high air flow is quenching portions of the flame prior to complete reaction.

Comparison of the on-design and off-design plots shows that the emissions at the rich and lean failure modes are not significantly different. However, the DRE in the region between 100 and 200 percent theoretical air has degraded markedly from the previous high efficiency. An examination of the nozzle characterization data should correlate to these results.

Figure 3-10 illustrates the droplet size distribution obtained for the on-design and off-design nozzles used in the present study. Use of an oversized pressure atomized nozzle for the off-design condition results in low fluid pressure, and low atomization energy. Thus, the off-design results show the dropsize is shifted toward larger values. The key to interpreting the effect of the shift in droplet size is found in the evaporation time plot of Figure 3-10. This plot shows evaporation time as a function of droplet diameter for No. 2 fuel oil, based on the "d^2 law" [26]. The on-design data shows approximately 10 percent of the mass is above 160 microns. According to the evaporation rate plot, this 10 percent will require more than 50 msec

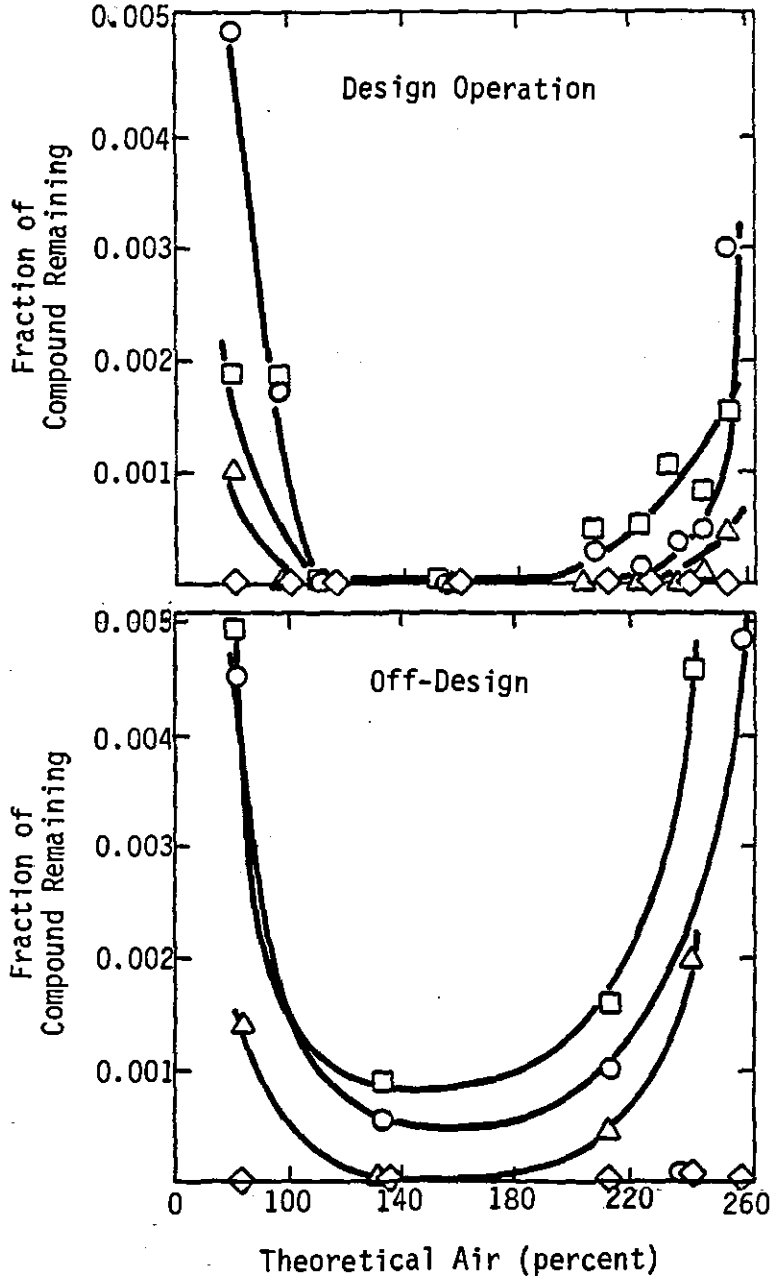

Figure 3-9. Test compound emissions from TFR as a function of theoretical air (No. 2 fuel oil).

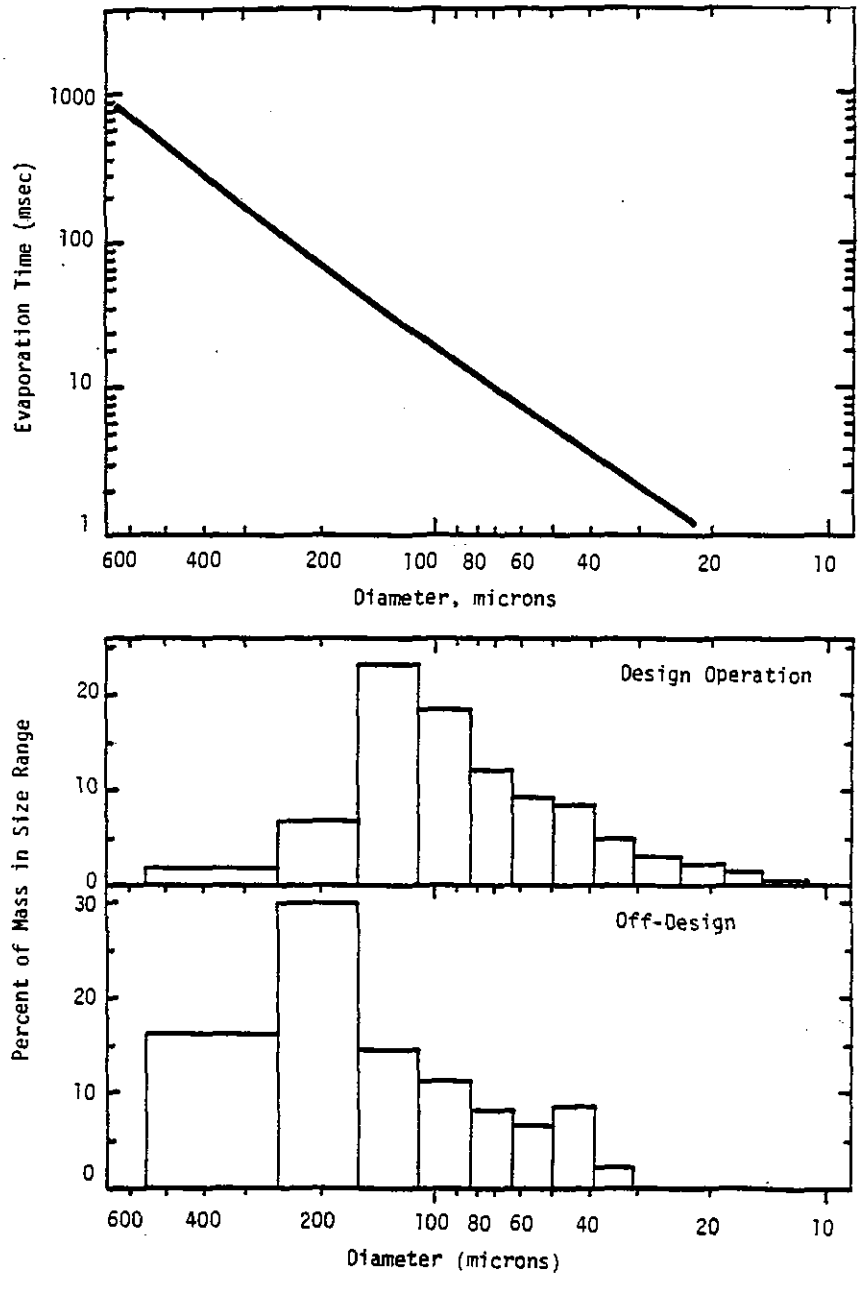

Figure 3-10. Droplet size distributions and estimated evaporation time as a function of diameter.

to evaporate. The off-design data indicate that fully 46 percent of the mass is greater than 160 microns. Also note that the largest size class (250-560 microns) has increased from 2 to 16 percent of the total mass. Since the evaporation times for this category range from 100-700 msec, it is evident that the effect of moving from on- to off-design operation is a substantial increase in the evaporation time of a significant fraction of the fuel. Thus, the change in atomization quality that accompanied the use of the oversized nozzle induced an atomization failure mode; the DRE, which was much greater than 99.99 percent was reduced to the order of 99.9 percent.

3.3.3 Mechanisms of Failure

Two general mechanisms can be identified by which poor atomization can influence DRE. In the first, droplets which are too large to evaporate in the available time penetrate to the reactor wall. The liquid evaporates and exits the reactor along the cold boundary layer at the wall. In the second mode, the droplets penetrate through the flame-zone without fully evaporating until well into the postflame region. Here, mixing or temperature may not be sufficient to ensure complete destruction.

Estimation of the maximum droplet diameter for which the droplets avoid striking the wall involves 1) determination of fraction of the hydrodynamic energy released by the nozzle that is converted into droplet velocity, and 2) determination of the aerodynamic drag on the droplets as they simultaneously evaporate and burn. While such calculations cannot be performed to a great degree of accuracy, the estimation indicates that the threshold diameter for striking the wall is approximately 200-300 microns. This is consistent with the shift in DRE behavior associated with the spray degradation and it indicates the following methodology for evaluating the atomization adequacy of full-scale nozzles:

- Evaluate atomization quality in cold flow on either the actual waste stream or on a surrogate stream of identical properties. If possible, both dropsize and droplet velocity information should be obtained.

- Use the spray information to evaluate the adequacy of the match between the combustion chamber and the spray pattern.

The manner in which the spray data would be used to evaluate the adequacy of the match is not well defined at this juncture, but a general direction is clear. The spray data, in conjunction with the fuel properties, will allow a characteristic evaporation time to be calculated. Second, the nozzle design and incinerator dimensions will then provide the necessary input to establish whether (1) droplets directed toward the walls will contact the walls, and (2) droplets directed away from the walls will evaporate. Required to establish this information is a characteristic time model for representative incinerator designs.

Areas of research evolve from this scenario in order to delineate a realistic and practical evaluation methodology:

1. The need for droplet velocity information in addition to droplet SMD measurements needs to be ascertained. The methodology will benefit if simple Sauter Mean Diameter (SMD) data, coupled perhaps with spray angle, are sufficient.

2. The relationship between droplet size and fuel properties on one hand, and characteristic evaporation times on the other, must be established for fuels representative of incineration feed stock.

3. A major effort is required to apply and test characteristic time modeling to the configuration and conditions representative of practical incinerators.

4. Finally, the methodology established must be tested first at bench scale, and then in scaled units.

4.0 SECONDARY ATOMIZATION

This section describes the experiments which evaluated the effect of secondary atomization on DRE in subscale liquid spray combustion.

4.1 Background and Objectives

One mechanism by which a liquid injection incinerator could fail to achieve acceptable DRE is through poor liquid atomization quality. As discussed in the previous section, poor atomization can cause a significant fraction of the liquid to appear as large droplets. These can penetrate to the wall or pass through the flame without completely evaporating.

Droplets that reach the wall would eventually evaporate at lower temperature than the bulk of the incinerator. Thus, the probability of destruction is reduced. Also, droplets that penetrate the flame-zone would release waste that would experience a lower temperature path than those released in the flame.

Large-scale atomizers generally fail to provide acceptable atomization quality for two reasons:

1. The liquid is unusually viscous or it contains solids (i.e., slurry). This can be a particular problem for waste streams because of the wide variability in liquid properties and solid loadings that occur.

2. Portions of the nozzle have degraded during use such that design operation cannot be obtained. Again, this problem can be aggravated for waste streams through their corrosive nature or because of their solid content.

In either case secondary atomization has been proposed as a means of reducing droplet size after the liquid has left the nozzle.

Secondary atomization is the term used to describe the fragmentation of droplets in hot gas due to internal generation of vapor. The presently accepted mechanism is as follows [27]:

- The process requires at least two miscible components of substantially varying volatility to be present.

- During heating the volatile component is depleted in a thin boundary layer at the droplet surface.

- Since the low volatility compound predominates at the droplet surface, the surface temperature rises to a value approximating the boiling point of the low-volatility compound.

- Heat transfer from the surface to the interior is much more rapid than mass transfer of the light component from the interior to the surface. Thus, the temperature of the droplet interior may reach the point where fractionation occurs at the droplet center.

- As the fractionation process generates gas the droplet expands into a bubble which in due course ruptures. The rupture shatters the droplet into many small fragments.

Thus, the objective of inducing secondary atomization is to cause large droplets to break into small ones in the flame, and thereby to increase the net evaporation rate. If poor atomization or droplet penetration to the wall is the process limiting DRE in a particular application, then secondary atomization may be a tool to improve DRE. The volatile component could be obtained by selective blending of waste streams or by the addition of a pure volatile compound. Note that we do not consider here the use of emulsions, which is an approach that has been investigated elsewhere [28].

The objective of the work reported here was to examine the potential that high concentrations of volatile waste compounds in an auxiliary fuel can promote secondary atomization. A second objective was to demonstrate whether

and compare the DRE in the small-scale reactor for conditions where secondary atomization was present against conditions for which it did not occur. These tests were performed under a previously characterized atomization failure mode.

4.2 Approach

The first objective was addressed by investigating the effect of compound concentration in No. 2 fuel oil auxiliary fuel on secondary atomization. A series of compounds were selected for screening to represent a range of boiling points from very volatile to numbers representative of No. 2 fuel oil (210-260°C). The screening tests were performed in the slip flow reactor (Section 2.1). The following compounds were selected for screening (shown with their normal boiling points):

- Dichloromethane: 39°C
- Acrylonitrile: 77°C
- Benzene: 80°C
- Isopropanol: 82°C
- Benzal Chloride: 205°C

The procedure was to first demonstrate that the compounds were miscible with No. 2 fuel oil up to 40 percent by weight. Second, the degree of secondary atomization was estimated visually and assigned a value in an approach similar to that used at Princeton [29]. Third, the degree of secondary atomization was evaluated as a function of compound concentration. Fourth, a series of tests were performed in the turbulent flame reactor in which DRE for the various compounds was compared under conditions where the degree of secondary atomization was known from the slip-flow screening studies.

4.3 Results and Discussion

Each of the compounds was screened in the slip reactor at 0.5, 2, 5, 10, 20, and 40 weight percent in the No. 2 fuel oil. The results are presented graphically in Figure 4-1 as a plot of secondary atomization intensity vs. concentration for each of the compounds. The results indicate:

- Secondary atomization is active only for compound concentrations above 2 percent, except for isopropanol, which showed some activity at 2 percent but none at 0.5 percent.

- For any secondary atomization to occur there must be some difference between the boiling points of the constituents. For example, benzal chloride, which has a boiling point comparable with that of No. 2 fuel oil, showed no activity at any concentration.

- The results indicate that intensity is not entirely a function of boiling point differential. For example, isopropanol has a boiling point of 82°C, but it induced a substantially more active reaction than dichloromethane (39°C). Thus, other factors than boiling point differential (e.g. compound polarity) are related to intensity.

To ensure that the disruption observed in the reactor was indeed secondary atomization, high-magnification shadow photographs were employed to visualize the process. An example of this process is shown in Figure 4-2. Sequence 1-4 shows the droplet, here a double drop, expanding into a bubble. Between sequences 4 and 5 (approximately 0.2 msec) the bubble has ruptured and the remaining liquid has started to disperse as small droplets.

Based on these results, two compounds were selected for testing in the turbulent flame reactor: isopropanol and benzal chloride.

The objective of the turbulent flame reactor work was to evaluate whether secondary atomization intensity, as determined in the slip flow

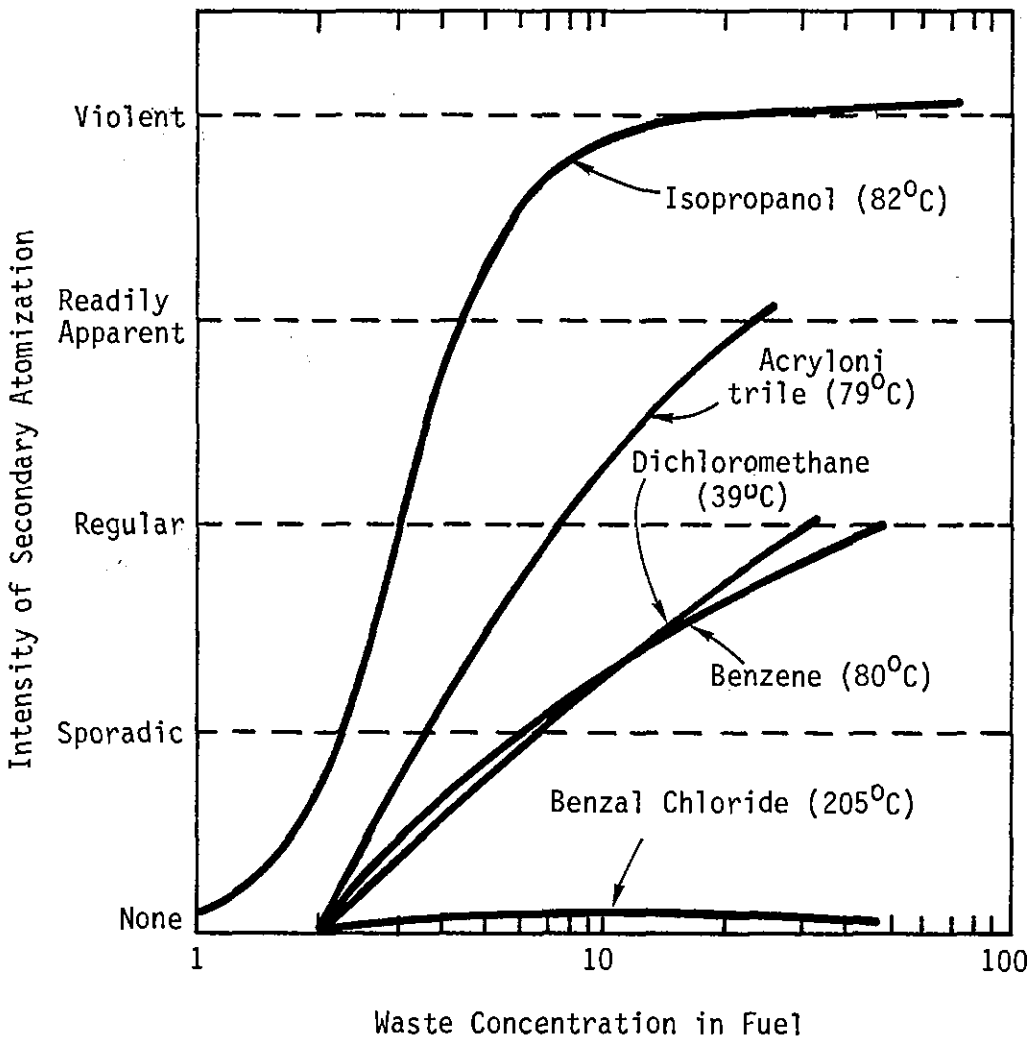

Figure 4-1. Effect of waste concentration on secondary atomization intensity.

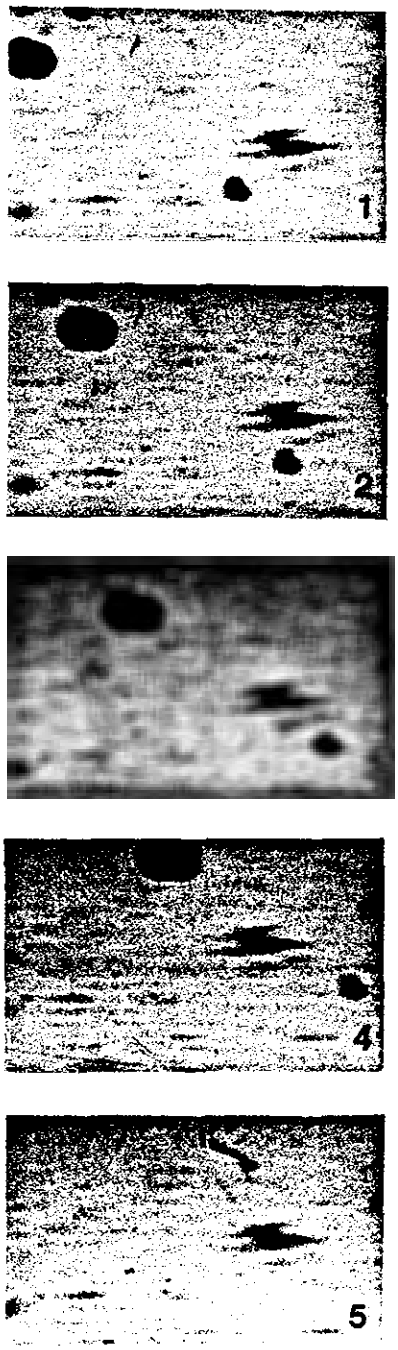

Figure 4-2. Sequence of Hycam pictures showing expansion and rupture of fuel droplet.

screening experiments, could directly affect DRE. The experimental matrix is shown in Table 4-1. The experiments were designed to determine the effect of compound concentration on DRE for 1) a compound for which no secondary atomization occurs across the entire concentration range, and 2) a compound for which no secondary atomization occurs at low concentrations, but a strong response is obtained at high concentrations. Thus, the first compound yields the concentration dependence in the absence of secondary atomization. Any strong additional concentration dependence for the second compound can be attributed to an increase in secondary atomization intensity with concentration.

TABLE 4-1. SECONDARY ATOMIZATION TESTS IN THE TURBULENT FLAME REACTOR[1]

Compound	Concentration		
	0.5	2.0	10.0
Benzal Chloride	None	None	None
Isopropanol	None	Sporadic	Violent

[1]Labels in table are intensity of secondary atomization from slip flow screening.

The test condition corresponded to the off-design atomization condition illustrated in Figure 3-10. In all other respects, the TFR was set for high efficiency operation (120 percent theoretical air, 0.8 swirl number). Thus, the only variables were test compound type and concentration.

The results for DRE of the test compounds are shown in Figure 4-3. Waste penetration (fraction of original waste escaping the reactor) is plotted against the percent waste in the fuel for the two test compounds. Benzal chloride shows an approximately one order of magnitude decrease in penetration between 0.5 and 10 percent waste concentration. Since no

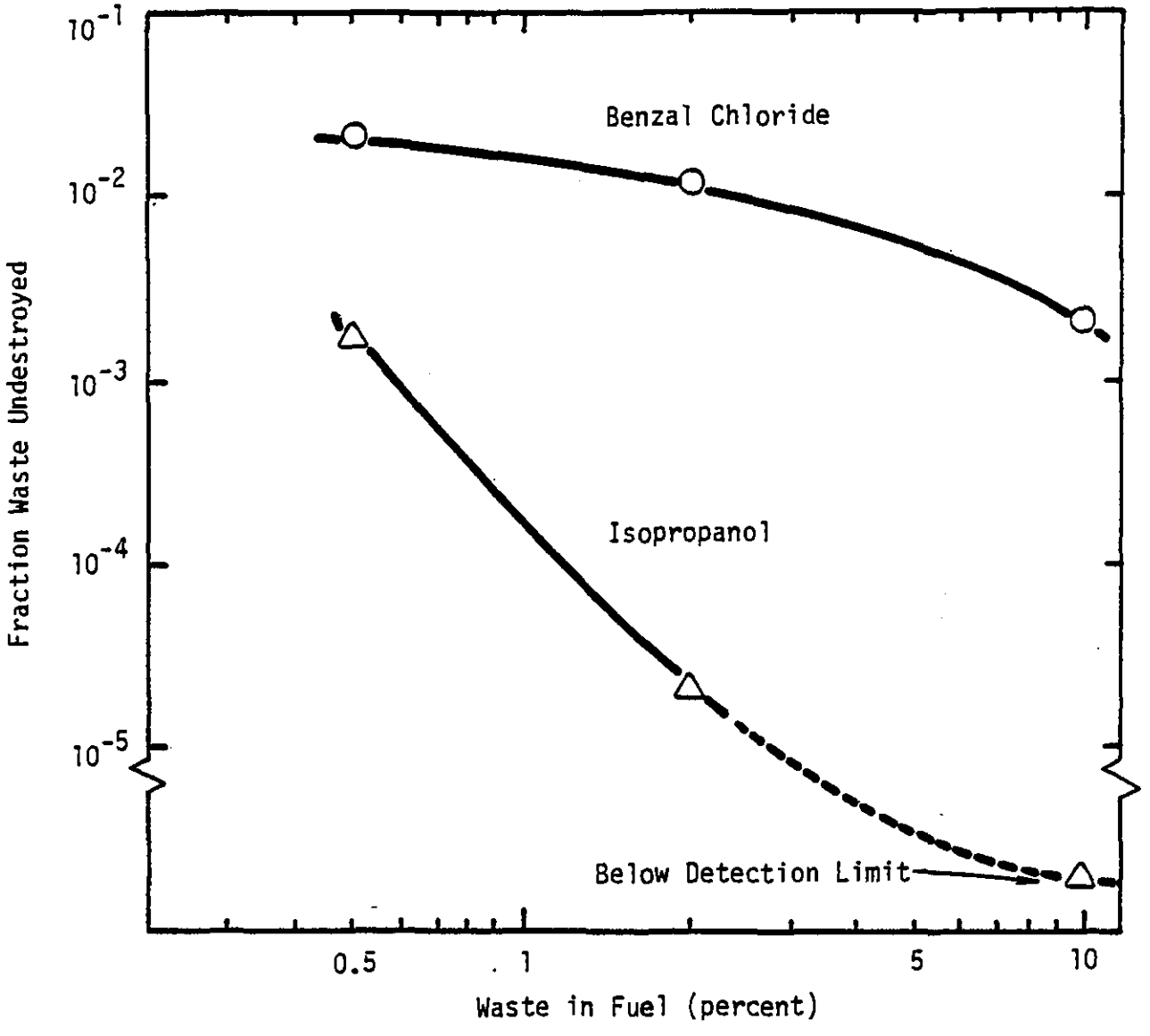

Figure 4-3. Comparison of compound penetration for benzal chloride and isopropanol as a function of compound concentration in the auxiliary fuel. Results are for the turbulent flame reactor operating under an atomization failure condition.

secondary atomization takes place for this compound, the concentration effect on penetration must be due to other factors (see discussion in Section 5). For isopropanol, however, the effect of concentration is much more pronounced. Between 0.5 and 10 percent concentration DRE improves from less than 99.9 percent to greater than 99.9999 percent. Significantly, this increase in DRE occurs concurrently with an increase in secondary atomization intensity from none to violent. Thus, at least a substantial portion of the difference in behavior between benzal chloride and isopropanol can be attributed to the secondary atomization behavior of isopropanol.

In addition to DRE, the overall combustion efficiency was also influenced by the dopants. Figure 4-4 shows CO and hydrocarbon emissions (as measured by a flame ionization detector) as a function of dopant concentrations. Note that dopant type and concentration were the only variables; in all other respects each of the experiments were identical. The data show three key points:

1. Increased isopropanol concentration increased combustion efficiency. This occurred concurrently with increased secondary atomization intensity.

2. Increased benzal chloride concentration decreased combustion efficiency. This occurred in the absence of secondary atomization.

3. At 0.5 percent, where secondary atomization was absent for both compounds, the CO and hydrocarbon emissions for the benzal chloride were lower than those for isopropanol.

This final point shows that other dopant dependent mechanisms than secondary atomization are active.

This work suggests that the DRE of liquid injection incinerators operating under atomizer limited conditions can be improved by the blending of small amounts of high volatility liquids into the waste stream. The blending agent may be a second waste stream of markedly different volatility

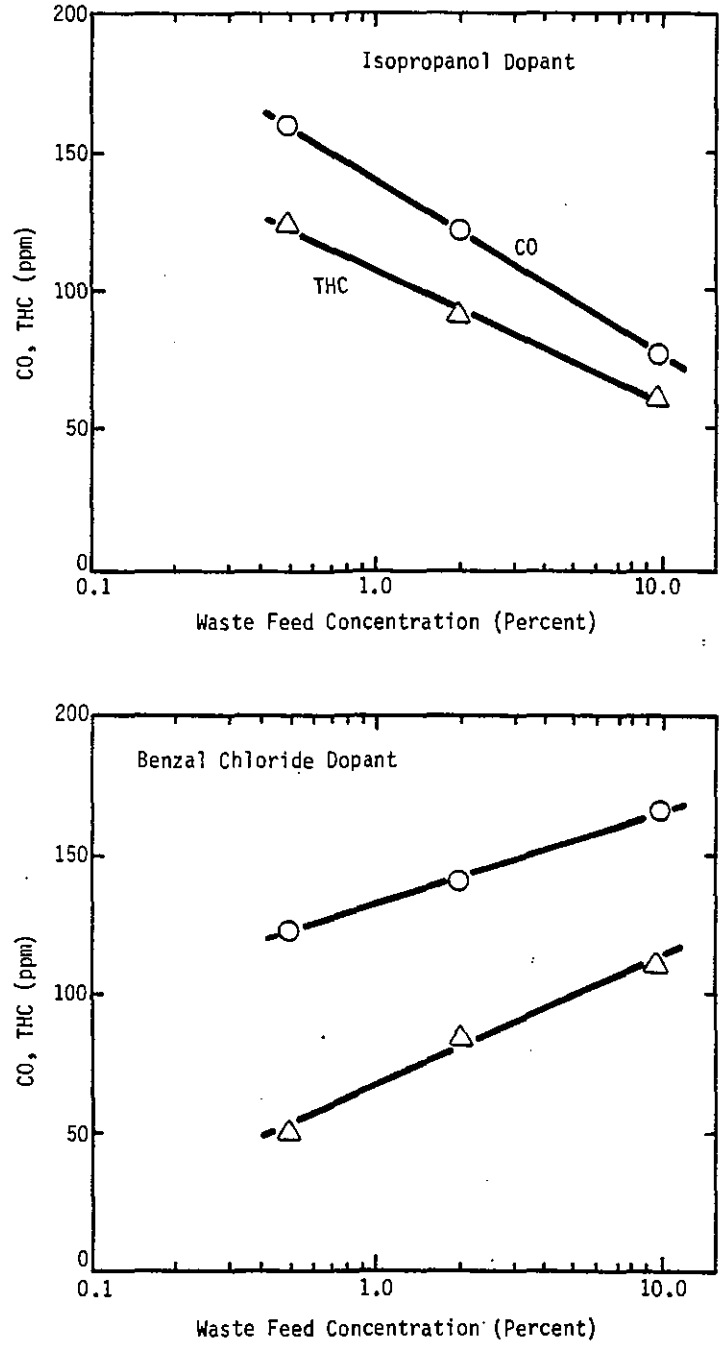

Figure 4-4. Emissions of CO and hydrocarbons from the TFR as a function of dopant concentration.

rather than a pure organic liquid. These blending agents may be particularly appropriate for slurry atomization, whose primary atomization quality is usually limited.

4.4 Implications and Conclusions

Secondary atomization has been demonstrated to be a potential means of improving incineration efficiency in situations where DRE is dominated by atomization quality. For secondary atomization to occur, the following requirements must be met:

- A component of high volatility, relative to the fuel, must be present. The component may be either miscible with the fuel or it may be present as an emulsion.

- The volatile component must be present at a concentration of the order of at least a percent.

- The volatile component may be either a waste compound or a nonhazardous blending agent. In other studies water emulsions have been used in place of a miscible volatile component.

During field testing, researchers at Midwest Research Institute [29] noted that DRE appeared to be correlated with waste concentration in the feed. Figure 4-5 shows a compilation of the field data for a series of units and tests. The plot shows considerable scatter, as might be expected from the large number of test conditions and devices included; however, the trend of increasing DRE with increasing waste concentration in the feed is both readily apparent and statistically significant. One explanation offered for this behavior is that as waste concentration increases, secondary atomization becomes more active and DRE is improved. One problem with this scenario is that below approximately 1.0 percent concentrations volatile additives do not induce secondary atomization. If secondary atomization is not active over the left two-thirds of the plot, then this scenario cannot explain all of the correlation (see further discussion in Section 5).

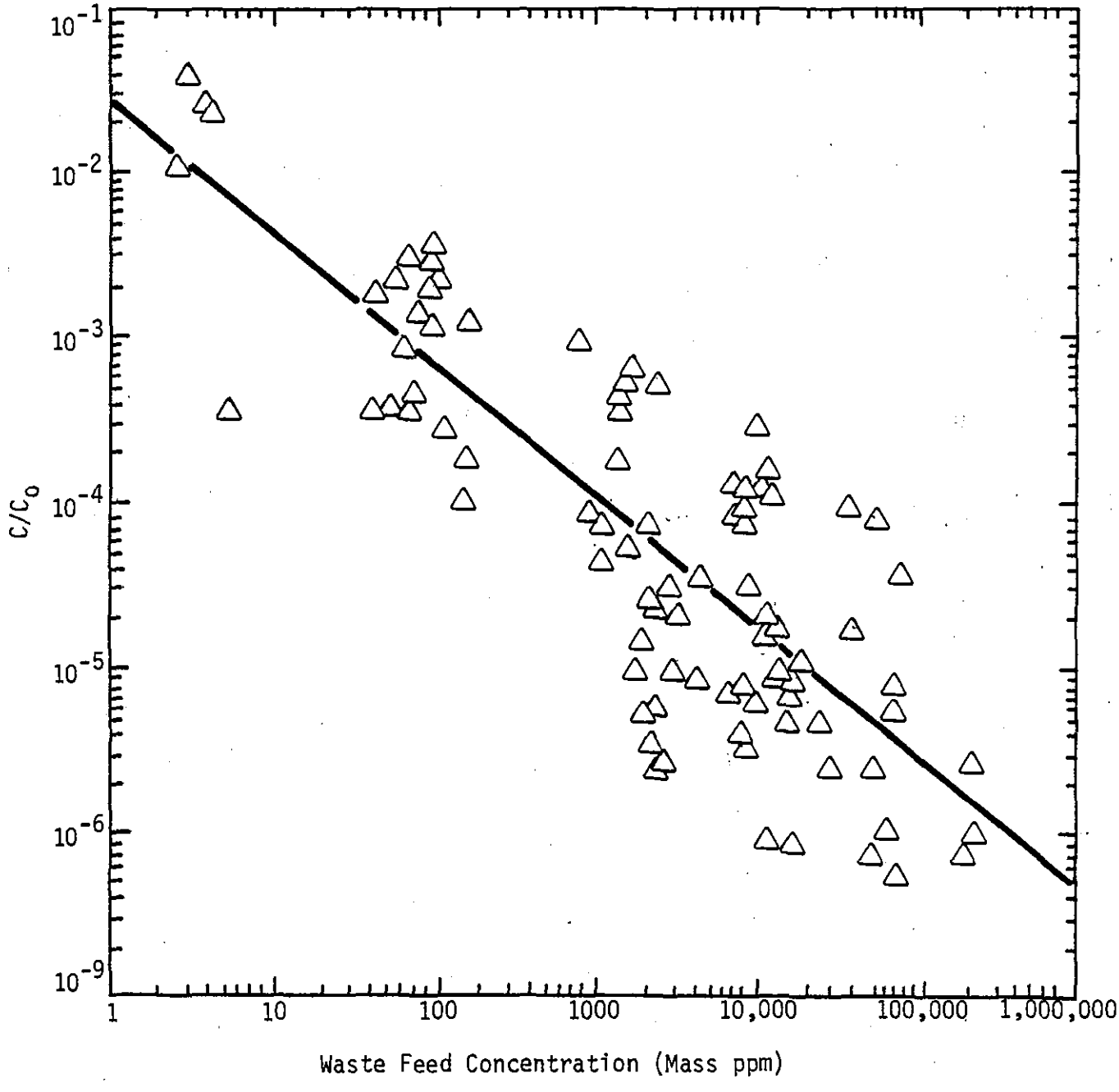

Figure 4-5. Waste penetration as a function of waste concentration in the feed stream. Data compiled for many units and operating conditions [29].

The results presented here have shown the following:

- Secondary atomization is a potential means of improving DRE in situations where DRE is limited by liquid atomization.

- To first order secondary atomization potential can be predicted from boiling point differential between the fuel and the waste.

- A minimum of approximately 1.0 percent of the volatile component is necessary to induce secondary atomization.

- Use of emulsified water as a volatile agent may be feasible for those cases in which streams contain waste concentrations too low to induce secondary atomization.

- Secondary atomization is probably not the phenomena that controls the DRE vs. waste concentration correlation noted from the MRI field data.

5.0 EFFECT OF COMPOUND CONCENTRATION ON DRE

5.1 Background and Objectives

Under EPA contract Midwest Research Institute (MRI) and others have performed extensive field tests on a wide variety of practical incineration devices. The objectives of these tests were to characterize the waste destruction performance of present incineration technology and to determine if any common factors correlate waste destruction among full-scale units. To address the second objective MRI has performed an extensive statistical treatment of their data [29]. The most significant statistical correlation found was the relationship between waste penetration (= 1 - DRE/100) and waste concentration in the original feed stream. This relationship is shown in Figure 5-1. The data show considerable scatter; this is not surprising since the data represent a wide variety of operating conditions, wastes, and incinerator designs. Nonetheless, the correlation (represented by the solid line on the figure) is statistically significant.

One item of significance is that all points above the horizontal dashed line represent noncompliance under the 99.99 percent DRE rule. These results indicate that current technology has difficulty meeting the licensing regulations when the waste represents less than 1000 ppm of the feed stream. This finding has significance with respect to waste streams contaminated by low concentrations of extremely hazardous materials (e.g. dioxin or chlorophenol contaminated pesticides).

A second significant point deals with the mechanisms that give rise to the correlation. In any thermal destruction device a certain amount of the waste feed compounds escape destruction. The understanding of this mechanism or mechanisms is critical to:

- The design and modification of incinerators for improved efficiency.

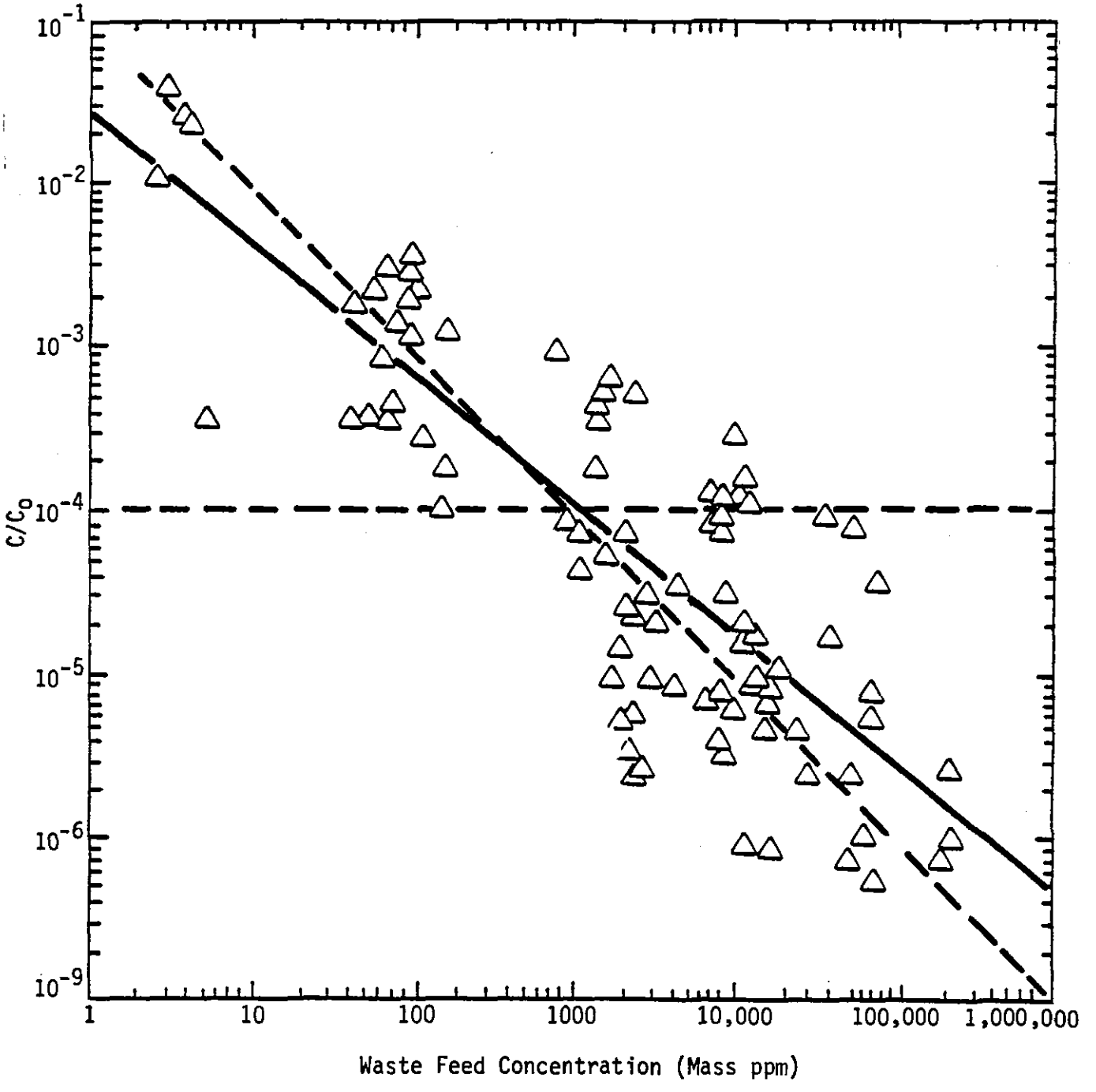

Figure 5-1. Waste penetration as a function of waste concentration in the feed stream. Data compiled for many units and operating conditions [29].

- The understanding of what makes one compound more difficult to destroy than another in identical circumstances.

- The understanding of the portions of the incinerator environment that dominate PIC formation. This is necessary to design appropriate laboratory- or sub-scale experiments to develop waste-PIC chemistry.

The field correlation shown in Figure 5-1 provides insight into the mechanism controlling waste release; whatever model is developed, it must be constant with the behavior of the correlation.

The objective of the work performed in the present study was to determine whether the correlation is representative of flame-zone or post-flame behavior. The specific issues addressed are:

- Does a laboratory scale spray flame reproduce the DRE vs. waste feed concentration behavior noted in the field tests?

- Is the correlation characteristic of high efficiency operation or failure mode operation?

- Do compound rankings change as waste feed concentration changes.

5.2 Approach

The approach was to use the turbulent flame reactor to simulate the processes occurring in incinerator flame zones. As described in Section 2, this unit is a 100,000 Btu/hr liquid spray combustor. The flame zone is surrounded by water-cooled walls to minimize post-flame reactions. In the present application the reactor was fired on No. 2 fuel oil doped with a soup of five test compounds. The soup was an equilimolar mixture of acrylonitrile, benzene, chlorobenzene, chloroform, and 1,1,1-trichloroethane. The soup was added to the No. 2 fuel oil in various concentrations for testing: 30 ppm, 300 ppm, 3000 ppm, 3 percent, and 30 percent by weight.

Two reactor conditions were selected for testing. Both utilized on-design atomization. The two conditions were selected to represent the lean and rich limits of the high efficiency window. These limits were defined by the points where CO started to rise. The stoichiometries selected were 120 and 150 percent theoretical air.

The sampling and analysis system used in these tests is described in detail in Appendix A. The estimated measurement system detection limit corresponds to 99.999 DE ($C/C_0 = 10^{-5}$) with 3 percent soup in the No. 2 fuel oil. Thus, at a 30 ppm soup doping level, the detection limit is $C/C_0 = 10^{-2}$ while $C/C_0 = 10^{-6}$ is detectable with 30 percent soup doping.

5.3 Results and Discussion

The DRE results for four of the compounds at 150 percent theoretical air are shown in Figure 5-2. This stoichiometry represents a point on the fuel-lean side of the high efficiency "window." The results indicate that DRE values generally increase at higher waste concentrations for each of the compounds. No values for chloroform are shown because for several cases chloroform recoveries exceeded the feed stream value; i.e., the reactor was a net chloroform producer. Note that the effect of waste concentration on DRE is less apparent if only the points at 3000 ppm waste concentration and below are considered. Conversely, if only the points at and above 3000 ppm are considered the dependence is amplified. One conceivable explanation is that secondary atomization is the phenomena responsible for the improvement in DRE in the turbulent flame reactor. As discussed in Section 4, secondary atomization would be expected to be active only above ca. 1 percent waste concentration. Thus, if secondary atomization is responsible, the waste concentration parameter would influence DRE much move strongly above 10,000 ppm waste.

Similar results for 120 percent theoretical air are shown in Figure 5-3. These data are for a point on the fuel-rich side of the high efficiency window. The results again indicate an increase in DRE with waste concentration in the feed. The effect is more pronounced at and above 3000 ppm

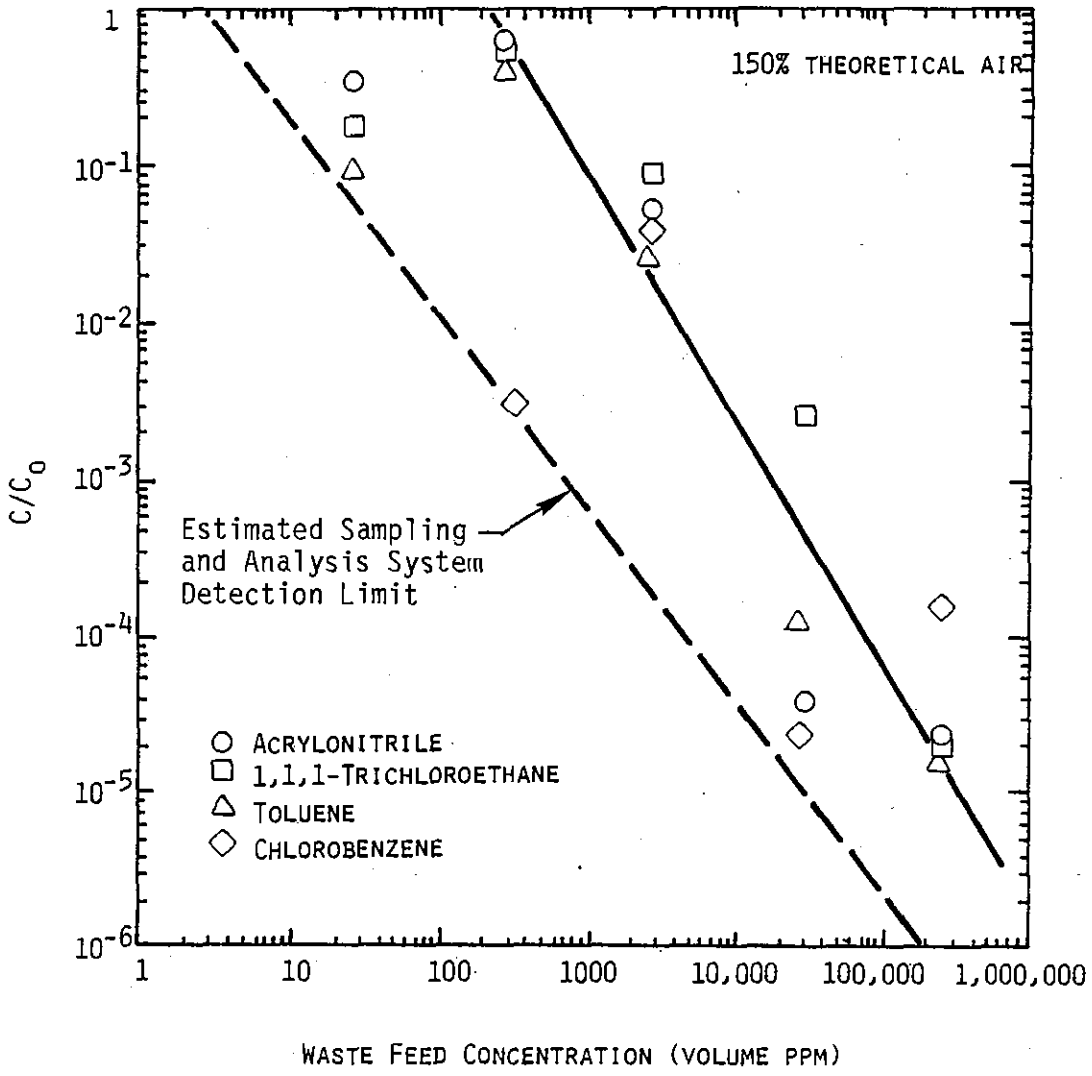

Figure 5-2. Waste penetration as a function of waste concentration in the feed stream for 150 percent theoretical air.

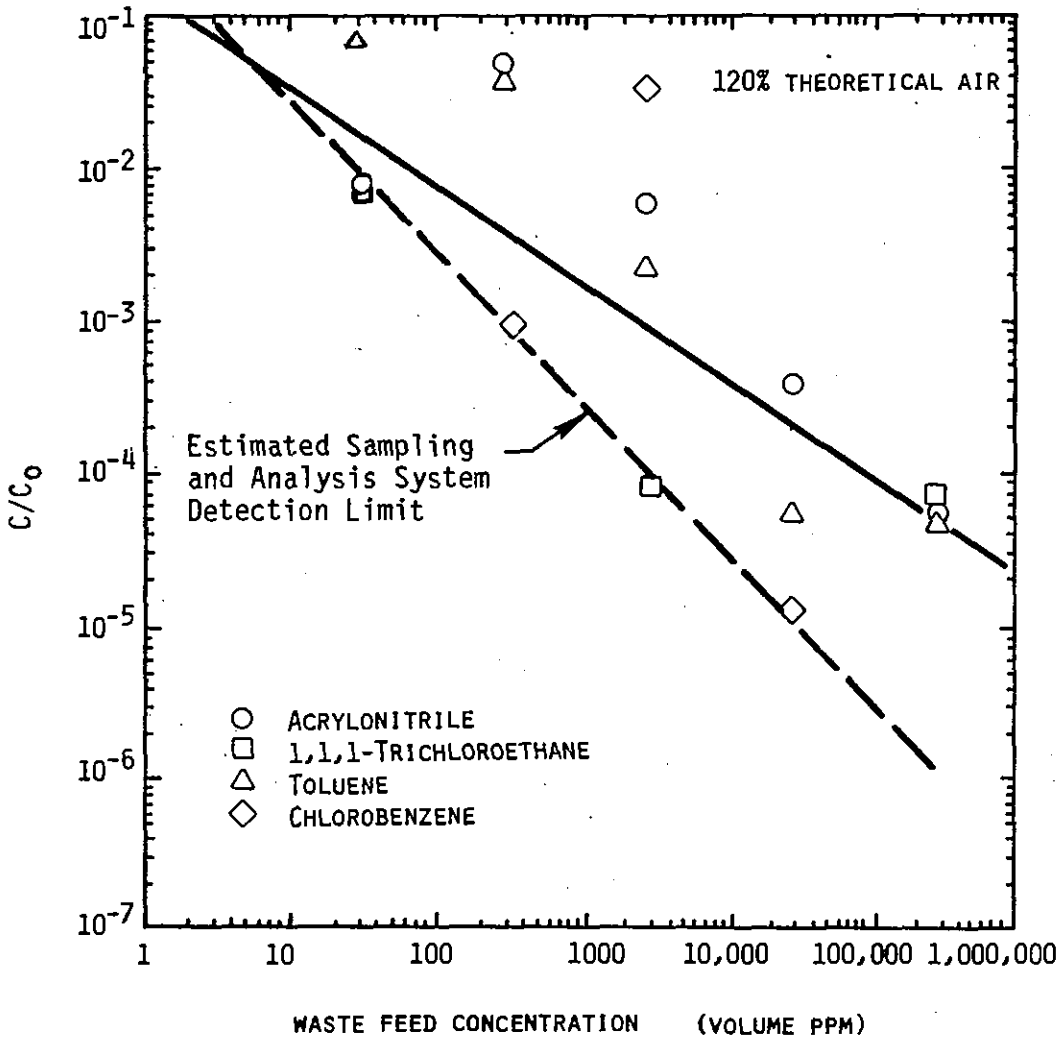

Figure 5-3. Waste penetration as a function of waste concentration in the feed stream for 120 percent theoretical air.

waste than at and below 3000 ppm. The DRE values are generally similar between Figures 5-2 and 5-3, within the scatter associated with this type of measurement. However, below 300 ppm waste feed concentration the 150 percent theoretical air case showed approximately an order of magnitude higher emissions.

The excess chloroform measurements that were noted in both data sets can be attributed to formation of chloroform as a PIC during reaction of the other compounds. Indeed, chloroform has been identified as a common PIC in field testing [26] and in pilot scale waste studies [27]. Its appearance is generally associated with wastes containing chlorine-substituted light hydrocarbons,such as 1,1,1-trichloroethane in the present experiments. To prove that chloroform was a PIC in the current experiment the 150 percent theoretical air case was repeated without the chloroform in the feed. The DRE results for this repeat are shown in Figure 5-4. With a few exceptions the data repeat the general trends noted in Figure 5-2:

- Moderate influence of waste concentrations in the feed on DRE below 3000 ppm.

- Strong influence above 3000 ppm.

Furthermore, chloroform was tentatively identified in the reaction products (based on retention time) at concentrations comparable with those observed in the original (Figure 5-2) test.

The effect of changing the auxiliary fuel is shown in Figure 5-5 where heptane replaced No. 2 fuel oil. The results indicate a less strong effect of waste concentration on DRE. If secondary atomization is accepted as the cause of the DRE variation in the previous data, then it follows that a more volatile auxiliary fuel (heptane) will reduce droplet disruption intensity. Thus, secondary atomization would be minimized and DRE would show less variation with compound concentration.

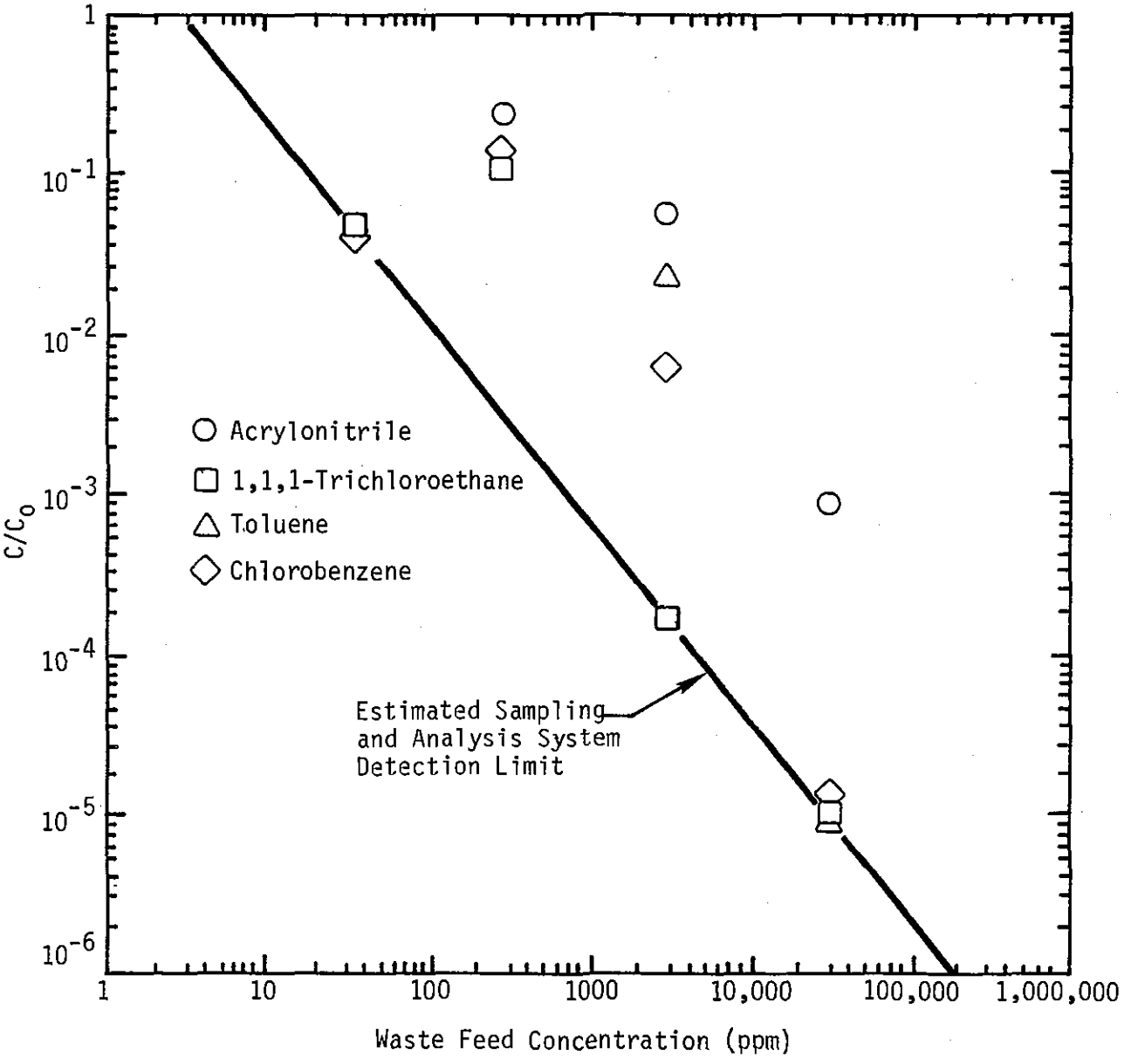

Figure 5-4. Waste penetration as a function of waste concentration in the feed stream for 150 percent theoretical air. Repeat data without chloroform feed.

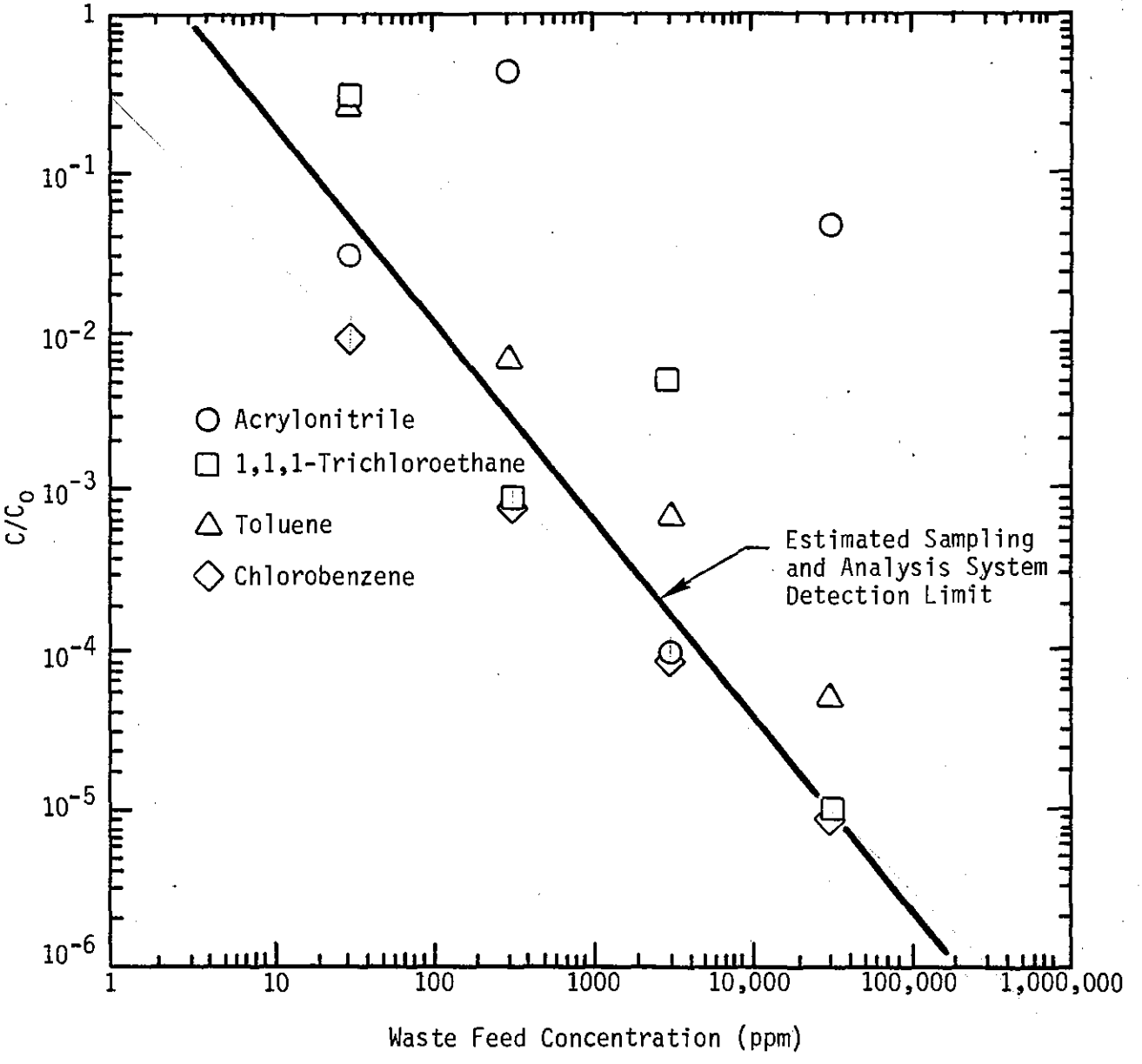

Figure 5-5. Waste penetration as a function of waste concentration in the feed stream for heptane auxiliary fuel at 150 percent theoretical air. Chloroform not in feed stream.

5.4 Implications and Conclusions

These experiments were performed to determine if the flame zone of a liquid injection incinerator (specifically a sub-scale flame zone) would be capable of reproducing the correlation developed from the MRI field data (Figure 5-1). The objective was to provide insight into a phenomena that is directly related to the processes that limit the DRE of field units. The results of this study show that DRE is positively correlated with waste concentration in the feed. The results also suggest that the influence of feed concentration is stronger at waste concentrations above 3000 ppm than below, a trend not noted in the field data.

An examination of Figures 5-2 through 5-5 shows that no single compound order predicts the relative destruction of the test compounds. Table 5-1 shows the number of times each compound appeared in the indicated ranking by emission concentration. Acrylonitrile is generally the most refractory compound and chlorobenzene the easiest compound to destroy. In the previous lab-scale incineration study [7] chloroform was the most refractory compound; here chloroform was shown to be a PIC formed from the other chlorinated compounds.

TABLE 5-1. CONCENTRATION RANKINGS' RANK BY HIGHEST EMISSIONS[1]

	1	2	3	4
Acrylonitrile	10	5	3	0
1,1,1-Trichloroethane	5	3	5	5
Toluene	1	8	6	3
Chlorobenzene	2	2	4	10

[1]Number of times each compound appeared in the indicated ranking.

As briefly mentioned above, one explanation for the observed behavior is that secondary atomization becomes active at high waste concentrations. In Section 4 we described how No. 2 fuel oil, when doped with volatile waste compounds, can undergo in-flame droplet fragmentation due to the vaporization of the more volatile components within the droplet. This fragmentation was shown to result in improved DRE. In the present experiment the improvement in DRE was associated with waste feed concentrations where secondary atomization would become active ($\geq$3000 ppm). Also, because of its higher volatility, heptane auxiliary fuel would not be expected to undergo secondary atomization when doped with the present waste compounds. The corresponding DRE data, Figure 5-5, do not indicate a consistent improvement in DRE with waste concentration at and above 3000 ppm. Thus, the heptane results are not inconsistent with a secondary atomization hypothesis.

The field data correlation, Figure 5-1, cannot be supported in its entirety by a secondary atomization hypothesis. For waste feed concentrations below ca. 0.5 percent no secondary atomization would be expected. Thus, the substantial variation of DRE below this inlet concentration must be explained in another way.

A first step toward investigating the cause of the correlation is to evaluate attributes of the correlation. In Figure 5-1, the diagonal dashed line corresponds to a constant waste emission concentration of about 7 ppt. If this dashed line can be assumed to represent the true correlation, and the scatter to represent nonrelated second-order effects, then the conclusion is that the waste emission concentration of field units is, to first order, constant. Thus, waste emission concentrations are relatively independent of feed concentrations over many orders of magnitude.

One approach is to determine what form of reaction kinetics are consistent with this correlation. If a general reaction rate expression is assumed:

$$dC/dt = -KC^n \qquad (5\text{-}1)$$

where C = waste concentration
K = rate constant
n = order of reaction with respect to C.

Equation 5.1 is integrated to yield

$$C_f/C_o = \exp(-kt) \text{ for } n = 1$$
$$C_f^{1-n} - C_o^{1-n} = (n-1)kt \text{ for } n = 1 \qquad (5\text{-}2)$$

where C_f, C_o = final and initial waste concentrations
t = total time

Under no circumstances are C_f and C_o independent for fixed k and t. Thus, simple kinetics do not reproduce the correlation behavior.

A situation in which C_f would be independent of C_o is under thermochemical equilibrium. As long as the overall elemental input (e.g. C, H, Cl, O, etc.) is relatively invarient the final concentrations will be independent of the initial feed concentrations. However, for an overall fuel-lean incinerator, equilibrium predicts essentially zero emissions of waste type compounds. However, a real incinerator is not at a single uniform stoichiometry but rather a range of stoichiometries that varies from fuel-lean to fuel-rich. A hypothetical distribution is plotted in Figure 5-6A, which shows that even though the overall stoichiometry is fuel-lean, a certain local fraction of the gas is fuel-rich due to mixing limitations in large scale equipment. Figure 5-6b shows equilibrium benzene concentration as a function of stoichiometry. (Here benzene is used as a simple example of how most waste compounds would be expected to behave). Thus, extremely fuel-rich pockets would have high benzene concentrations independent of residence time or initial feed composition. Figure 5-6c is a conceptual product of Figures 5-6a and 5-6b which shows the mass of benzene emitted as a function of equivalence ratio. It represents a "window" in which benzene concentrations are high and, simultaneously, a significant amount of gas exists with its stoichiometry in the window. The total emissions of benzene would be obtained by integrating Figure 5-6c over stoichiometry. The

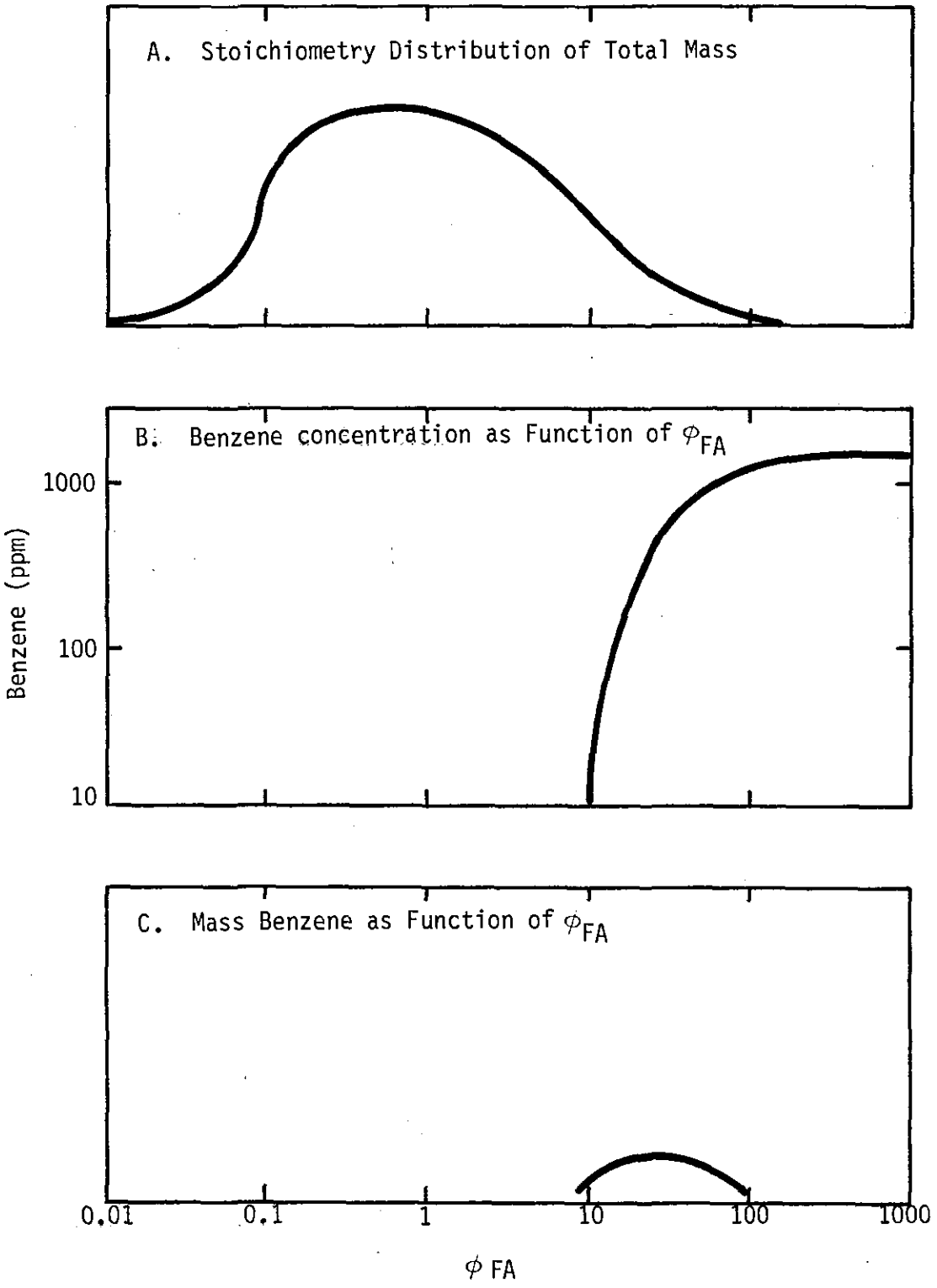

Figure 5-6. Distribution of mass equilibrium, benzene concentration, and mass benzene with stoichiometry.

concentration obtained by this procedure has the required property that it is invarient with feed concentration.

The results of the work reported in this section lead to the following conclusions:

- Waste DRE in subscale flame zones is increased as waste concentration in the feed fuel is increased.

- Waste DRE shows the most dramatic increase at high waste concentrations. This suggests that secondary atomization may be the cause of the correlation in the turbulent flame reactor.

- Secondary atomization is probably not the phenomena responsible for all of the DRE variation with waste concentration in the field tests. This is because the tests show that the variation continues at waste concentrations where secondary atomization should not occur.

- Application of thermochemical equilibrium to a mixing limited incinerator yields a model that reproduces the first order aspects of the field data; i.e., emission concentrations independent of feed concentrations.

6.0 PIC FORMATION

This task was directed towards determination of the identify and source of hazardous PIC's observed in the exhaust of the turbulent flame reactor.

6.1 Background and Objectives

One present concern for application of incineration technology is that the hazard associated with a waste stream may not be removed even though the original waste compounds are destroyed. Transformation of the waste into hazardous products of incomplete combustion (PICs) can potentially aggravate the hazard associated with the waste stream. For example, a hazardous but nontoxic waste can be partially transformed into chlorinated dibenzo-p-dioxins or dibenzofurans upon incineration.

Field testing on practical incinerators burning multicomponent wastes have shown that a broad distribution of Appendix VIII compounds appear in the exhaust [30]. The key question is defining the source of these emissions. Potential sources are [30]:

- Chemical transformation of waste to PIC.
- Low DRE of Appendix VIII compounds present in trace amounts in the auxiliary fuel.
- Transformation of nonhazardous auxiliary fuel constituents into Appendix VIII compounds.
- Trace Appendix VIII compounds in the combustion air that experience a low DRE in the flame.
- Trace Appendix VIII compounds that are stripped from the scrubber water.

Midwest Research [30] examined each of these but was unable to conclude which mechanism was dominant. Limited characterization of feed and waste streams indicated that certain PICs could be accounted for by each of the mechanisms.

The turbulent flame reactor (TFR) testing described in the preceding sections offers an opportunity to examine certain of the mechanisms. The advantages of the TFR for these tests include:

- The waste stream is well characterized because it is made up of mixtures of reagent grade chemicals. Field testing rarely involves pure or well characterized waste streams.

- The auxiliary fuel stream is also a well characterized light hydrocarbon liquid (No. 2 fuel oil).

- The TFR does not use a scrubber before the sample point. Thus, PICs observed in the sample stream cannot arise from the scrubber water.

The TFR affords the opportunity to examine trace organic product distributions from a turbulent spray flame whose feed streams are better characterized than field incinerators.

The objective of this task was to complement the data generated in the previous sections by examining, for a limited number of conditions, the full organic product distribution in addition to the DRE data. The key questions were:

- Are waste-PIC relationships readily identifiable.
- Can PICs be attributed to the fuel oil.

6.2 Approach

For these tests the TFR was operated on No. 2 fuel oil doped with 2-chlorophenol. Only a single doping compound was used to avoid ambiguity in

determining waste-PIC relationships. The TFR was operated over a range of stoichiometries for what was otherwise a high-efficiency condition. Samples were obtained in the usual manner using the VOST train. Those samples were analyzed by GC-MS by S-CUBED. Each Tenax trap was connected and desorbed at 175°C for 10 min. onto a liquid nitrogen cooled cryo trap. 1.2 g of gaseous external standard perfluorotholuene (PFT) was then injected onto the trap. The cryo trap temperature was raised to 220°C and the data acquisition started. A GC program of 40° (10 min) -285°C at 8°/min was used with a 30 m, DB-5, narrow bore, then film fused silica capillary column. The mass spectrometer was repetitively scanned from 35-400 AMU in 1 sec.

This provides an identification and a semiquantitative analysis of all of the volatile organic compounds present on the traps. Low volatility compounds (generally polycyclic hydrocarbons) cannot be recovered by this procedure.

6.3 Results and Discussion

The conditions under which samples were obtained for GC-MS analysis are detailed in Figure 6-1. The CO and total hydrocarbon traces indicate the presence of the high efficiency window. Sample A was obtained under an apparent fuel-rich failure condition. Sample B and C were obtained at the fuel-rich and fuel-lean extremes of the high temperature window, respectively.

A total of 57 organic species were identified in the three pairs of traps. Thus, a large number of product species were identified in the combustion products of a simple hydrocarbon fuel and a single Appendix VIII compound. However, examination of the concentrations of the various products showed that only a small number of compounds were present under all conditions at relatively high concentrations. These are listed in Table 6-1. (For reference, note that zero DRE of the chlorophenol would result in 163 micrograms/gm and 99.99 percent DRE would result in 0.0163 micrograms/gm). Thus, each of these compound concentrations is substantially above what would be the legal limit for chlorophenol release if it had been a POHC. The

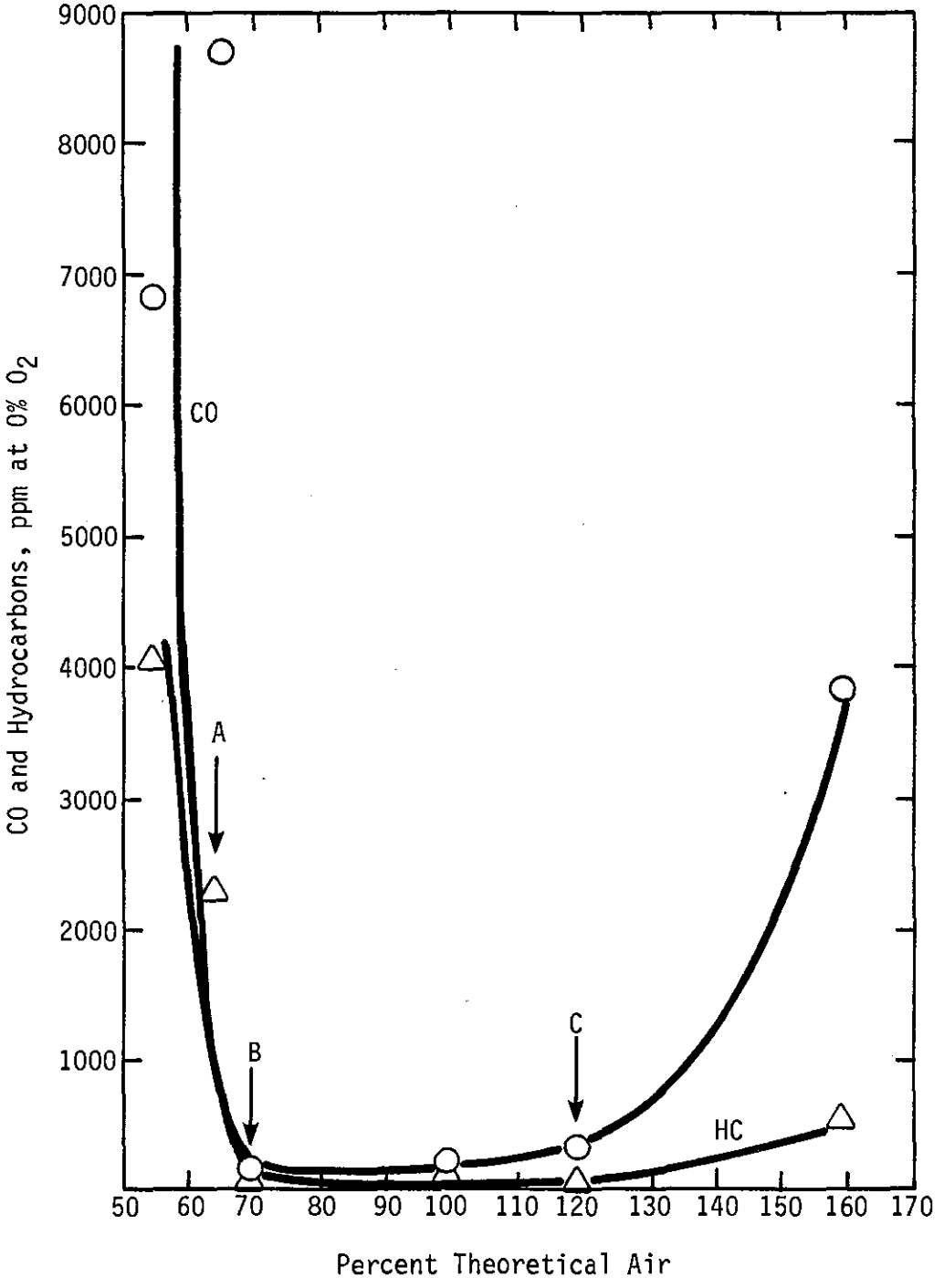

Figure 6-1. Variation of CO and total hydrocarbons with stoichiometry. Points A, B, and C indicate the conditions under which GC-MS analysis was obtained.

appearance of thiophene is key to understanding the source of these hydrocarbon compounds. Since the doped waste compound is sulfur free, the thiophene must have appeared from the sulfur in the fuel oil. Since No. 2 fuel oil can, by code, contain up to 1 percent sulfur, the thiophene would be the result of unreacted organic sulfur escaping destruction or reformed sulfur that avoids oxidation to SO_2. By inference, the other compounds shown in Table 6-1 can be assigned as unreacted No. 2 fuel oil constituents or products of partial decomposition of the fuel oil.

TABLE 6-1. MAJOR COMPONENTS IDENTIFIED

	Sample		
	A	B	C
Methyl Ethyl Ketone	.75	1.7	2.9
Toluene	0.10	0.39	0.93
Benzene	0.13	*	*
Thiophene	0.020	0.027	0.019
Methylene Chloride	0.053	*	*
Dimethyl Benzene	0.0042	0.024	0.24

*Interference with MEK, cannot be quantified.
Values are micrograms/gram flue gas.

Table 6-2 shows the remaining compounds identified on the cartridges. In general these compounds are present in very small concentrations (see Appendix C). The series of fluorenated hydrocarbons cannot be attributed to the doped waste compound and thus must originate from the fuel or the combustion air. Thus, at least a large fraction of these trace organic compounds arise from the combustion of the light fuel oil rather than the partial reaction of any Appendix VIII compounds.

TABLE 6-2. TRACE ORGANIC COMPOUNDS FOUND ON THE CARTRIDGES

methane, dichlorodifluoro	benzene, ethylmethyl***
methane, trichlorofluoro	2-methylundecane
ethane, 1,1,2-trichloro	benzene, ethyldimethyl***
1,2,2-trifluoro	2-methylnaphthalene
1-butanol	naphthalene
ethene, trichloro	trimethyl benzene***
2-pentene-3,4-dimethyl	cyclohexane, ethylmethyl***
cyclohexane, methyl	2-propyl-1-heptanol
cyclopentane, 1,2,3-trimethyl	4-propylheptane
1-hexene, 3,5,5-trimethyl	3-methyl-1-hexene
2-pentanone, 4-methyl	nonane
acetic acid, propylester	pentalene, octahydro- 2-methyl
cyclopentane 1,1,3,4-tetramethyl	isooctanol
3-methyl heptane	3-methylhexane
cyclohexane, dimethyl***	cyclohexane, butyl
benzene, chloropentafluoro	1-hexene- 3,5,5-trimethyl
acetic acid, butylester	cyclohexane, diethyl***
octane	decene
ethene, tetrachloro	decane
cyclohexane, trimethyl***	decane, 4-methyl
chlorobenzene	benzene, 1,2,3-trichloro
ethylbenzene	cyclopentane, 1-methyl- 2-(2-propenyl)
2-methylnonane	decahydro naphthalene
	undecane
	3-ethylheptane
	cyclohexane, propyl
	diethyl phthalate

These results indicate that organic products of incomplete combustion can arise from any organic compound present in the feed stream. This is independent of whether it is associated with the hazardous waste compound, the non-Appendix VIII compounds in the waste, the auxiliary fuel, or the burner air. Thus, conditions which maximize the combustion efficiency (of all organic compounds into CO_2) will be expected to minimize the formation of hazardous compounds, independent of source. The field tests [30] generally indicated that waste and PIC emissions were of similar magnitude for each facility. The PIC concentrations measured in this study were also generally comparable with the waste compound emissions found in the previously described tests. Thus, it appears that combustion efficiency, DRE, and PIC destruction are coupled problems, and that design and operating criteria that address one aspect will address each.

7.0 CONCLUSIONS

This study was directed toward a series of related fundamental issues in the hazardous waste area. The principal conclusions are summarized as follows:

1. Waste Atomization: For degraded atomizers, the principal cause of poor waste destruction efficiency is the increase in the fraction of very large droplets. The extreme delay in evaporation associated with these large droplets can lead to unreacted material reaching the wall or penetrating through the flame zone. Design to avoid this behavior is more difficult for hazardous waste incineration than for conventional combustors because:

- A large amount of empirical experience has been obtained on liquid fuel combustion.
- The atomization properties of waste streams (viscosity, surface tension, presence of solids) can vary considerably.

The results suggest a design methodology in which atomization quality is directly measured in cold flow. The size and trajectory of the largest droplets are compared to the combustion chamber geometry to determine the initial suitability of the design.

2. Secondary Atomization: Some materials may have sufficiently poor atomization properties to prevent acceptable spray fineness at any conditions. The use of a volatile waste dopant was shown to induce in-flame droplet fragmentation and to improve DRE. This suggests that use of volatile dopants, or the blending of different waste streams can be used to avoid poor DRE due to penetration of large droplets through the flame.

3. Compound Concentration: Field test data show a remarkable correlation between compound concentration in the feed and DRE. Testing in the turbulent flame reactor also showed this correlation. However, the pattern for the subscale flame indicated that secondary atomization was a

potential cause of the behavior at higher concentrations. This does not explain the subscale variation of DRE with waste concentration at low waste concentrations, nor does it fully explain the field data. A mechanism involving mixing limited equilibrium chemistry was proposed for the field data.

4. PIC Formation: The yield of trace organic compounds was measured from the turbulent flame reactor. The results indicated that:

- PIC concentrations were comparable with waste emissions.

- Incomplete combustion of the auxiliary fuel rather than true PICs from the doped waste dominated the apparent PIC emissions.

Thus, Appendix VIII PICs can arise from any of the hazardous or nonhazardous constituents of the waste stream or the auxiliary fuel. The implication is that conditions that promote high combustion efficiency will favor reduced PIC emission.

8.0 REFERENCES

1. Resources Conservation and Recovery Act, Public Law 94-580, 1976.

2. Environmental Protection Agency: "Hazardous Waste and Consolidated Permit Regulations." Federal Register 45:138, July 16, 1980.

3. Environmental Protection Agency: "Incineration Standards for Owners and Operators of Hazardous Waste Management Facilities." Federal Register 46:138, July 16, 1980.

4. Environmental Protection Agency: "Incineration Standards for Owners and Operators of Hazardous Waste Management Facilities." Federal Register 46:264, January 2, 1981.

5. Trenholm, A. P., P. Gorman, B. Smith, and D. Oberacker: "Emissions Test Results for a Hazardous Waste Incinerator RIA." Ninth Annual Research Symposium on Hazardous Waste, EPA-600/9-84-015, NTIS PB84-234525, U.S. EPA, 1984, p. 160.

6. Kramlich, J. C., M. P. Heap, W. R. Seeker, and G. S. Samuelsen: "Flame-Mode Destruction of Hazardous Waste Compounds," 20th Int. Symp. Combust., The Combustion Institute, Pittsburgh, PA, 1985, p. 593.

7. Kramlich, J. C., M. P. Heap, J. H. Pohl, E. M. Poncelet, G. S. Samuelsen, and W. R. Seeker: Laboratory Scale Flame-Mode Hazardous Waste Thermal Destruction Research, EPA-600/2-84-086, NTIS PB84-184902, U.S. EPA, 1984.

8. Duvall, D. S., and W. A. Rubey: Laboratory Evaluation of the High Temperature Destruction of Kepone and Related Pesticides" EPA-600/2-79-299, NTIS PB 264892, U.S. EPA, 1979.

9. Duvall, D. S., and W. A. Rubey: Laboratory Evaluation of High Temperature Destruction of Poly-chlorinated Biphenyls and Related Compounds, EPA-600/2-77-228, NTIS PB 279139, U.S. EPA, 1977.

10. Dellinger, B., D. S. Duvall, D. L. Hall, and W. A. Rubey: "Laboratory Determinations of High Temperature Decomposition Behavior of Industrial Organic Materials," Presented at the 75th Annual Meeting of the APCA, New Orleans, LA, 1982.

11. Dellinger, B., J. L. Torres, W. A. Rubey, D. L. Hall, J. L. Graham, and R. A. Carnes: "Determination of Thermal Stability of Selected Hazardous Organic Compounds," Hazardous Waste 1:137, 1984.

12. Lee, K. C., J. L. Hansen, and D. C. Macauley: "Predictive Model of the Time-Temperature Requirements for Thermal Destruction of Dilute Organic Vapors," Presented at the 72nd Annual Meeting of the APCA, Cincinnati, OH, 1979.

13. Lee, K. C., N. Morgan, J. L. Hansen, and G. M. Whipple. "Revised Model for the Prediction of the Time-Temperature Requirements for Thermal Destruction of Dilute Organic Vapors and its Usage for Predicting Compound Destructibility," Presented at the 75th Annual Meeting of the APCA, New Orleans, LA, 1982.

14. Tsang, W. and W. Shaub: "Chemical Processes in the Incineration of Hazardous Waste," Presented at the ACS Symposium on Detoxification of Hazardous Waste, New York, NY, 1981.

15. Cudahy, J. J. and W. Troxler: "Incineration Characteristics of RCRA Listed Hazardous Wastes," Journal of Hazardous Materials 8:59, 1983.

16. Nihart, R. K., J. C. Kramlich, G. S. Samuelsen, and W. R. Seeker: "Continuous Performance Monitoring Techniques for Hazardous Waste Incinerators," EPA-600/2-89-021, U.S. EPA, May 1989.

17. Kramlich, J. C., W. D. Clark, W. R. Seeker, G. S. Samuelsen, and C. C. Lee: "Engineering Analysis of Hazardous Waste Incineration - Continuous Monitoring of Incinerators," ASME/AIChE National Heat Transfer Conference, Denver, CO, 1985.

18. Clark, W. D., M. P. Heap, W. Richter, and W. R. Seeker: "The Prediction of Liquid Injection Hazardous Waste Incinerator Performance," 22nd National Heat Transfer Conference, Niagara Falls, NY, 1984.

19. Bridle, T. R., B. K. Afghan, H. W. Campbell, R. J. Wilsinson, J. Carron, and A. Sachdev: "The Formation and Fate of PCDD's and PCDF's During Chlorophenol Combustion," Presented at the 77th Annual Meeting of the APCA, San Francisco, CA, 1984.

20. Berglund, R. N. and B. Y. H. Liu. "Generation of Monodisperse Aerosol Standards." Environ. Sci. Technol. 147, 1973.

21. Baker, R. J., P. Hutchinson, E. E. Khalil, and J. H. Whitelaw: "Measurements of Three Velocity Components in a Model Furnace With and Without Combustion," 15th Symposium (International) on Combustion, The Combustion Institute, Pittsburgh, PA, 1975, p. 553.

22. Jungclaus, G. A., P. G. Gorman, G. Vaughn, G. W. Scheil, F. J. Bergman, L. D. Johnson, and D. Friedman: "Development of a Volatile Organic Sampling Train (VOST)," 9th Research Symposium on Hazardous Waste, EPA-600/9-84-015, NTIS PB84-234525, U.S. EPA, 1984. p. 1.

23. Edwards, J. B. Combustion: Formation and Emission of Trace Species, Ann Arbor Science, Ann Arbor, MI, 1974.

24 Dietrich, V. E.: "Dropsize Distribution for Various Types of Nozzles." Proceedings of the 1st International Conference on Liquid Atomization and Spray Systems, The Fuel Society of Japan, Tokyo, Japan, 1982, p.69.

25. Jones, A. R.: "Factors Affecting the Performance of Large Swirl Pressure Jet Atomizers." Report R/M/N1054, Central Electricity Generating Board, Marchwood, England, 1978.

26. Glassman, I.: Combustion. Academic Press, New York, 1977.

27. Wang, C. H., X. Q. Liu, and C. K. Law: "Combustion and Microexplosion of Freely Falling Multicomponent Droplets," Combust. Flame 56:175, 1984.

28. Lasheras, J. C., A. C. Fernandez-Pello, and F. L. Dryer. "On the Disruptive Burning of Free Droplets of Alcohol/n-Paraffin Solutions and Emulsions," 18th Symposium (International) on Combustion, The Combustion Institute, Pittsburgh, PA, 1981. p. 293.

29. Trenholm, A., P. Gorman, and G. Jungclaus: Performance Evaluation of Full Scale Hazardous Waste Incinerators, Volume 2, EPA-600/2-84-181b, NTIS PB85-129518, 1984.

30. Trenholm, A., R. Hathaway, and D. Oberacker: "Products of Incomplete Combustion from Hazardous Waste Incinerators," 10th Symp. Inciner. Treatment Hazard. Waste, EPA-600/9-84-022, NTIS PB85-116291, U.S. EPA, 1984.

APPENDIX A

VOLATILE ORGANIC ANALYSIS

The following discussion covers the volatile organic analytical equipments, the operating techniques, and the quality assurance procedures.

A.1 Analytical Equipment

Sampling and Adsorption: The equipment is illustrated in Figure A-1. Exhaust gas samples were collected from the stack by an uncooled 6.35 mm OD (0.25 in.) stainless steel probe. After leaving the stack, the sample passed through a glass valve and into the Volatile Organic Sampling Train (VOST). The sample first passed through a glass coil condenser being cooled by circulating ice-water before entering the first Tenax cartridge. The cartridge consists of an 8.5 mm long by 16 mm OD Pyrex trap with 6.35 mm OD (0.25 in.) ends packed with 2.0 grams of Tenax-GC (40-80 mesh). The adsorbent was held in place with small plugs of silianized glass wool. The sample line was connected to the cartridge by Ultra-Torr fittings. Next, the sample passed through a water trap, a straight water-cooled condenser, the Tenax/charcoal cartridge, and a second water trap. The Tenax/charcoal cartridge was packed with Tenax-GC (40-80 mesh) and activated charcoal (60-80 mesh) at a 1:1 weight ratio. The sample subsequently passed through a gas dryer, a rotameter, and a dry test meter. All connections upstream of the cartridge were either 316 stainless steel or 6.35 mm OD (0.25 in.) Teflon.

Desorption and Analysis: This system is based on a Perkin-Elmer Sigma-2 gas chromatograph with a Sigma-10 integrator/data station. The column is a 0.5-long, 3.18 mm OD (1/8 in.) Teflon tube packed with Porapak-Q. The 30 cc/min. carrier gas flow is maintained through the Tenax cartridges, the column, and the analytical trap, as shown in Figure A-2, 320 Thermal Desorption System.

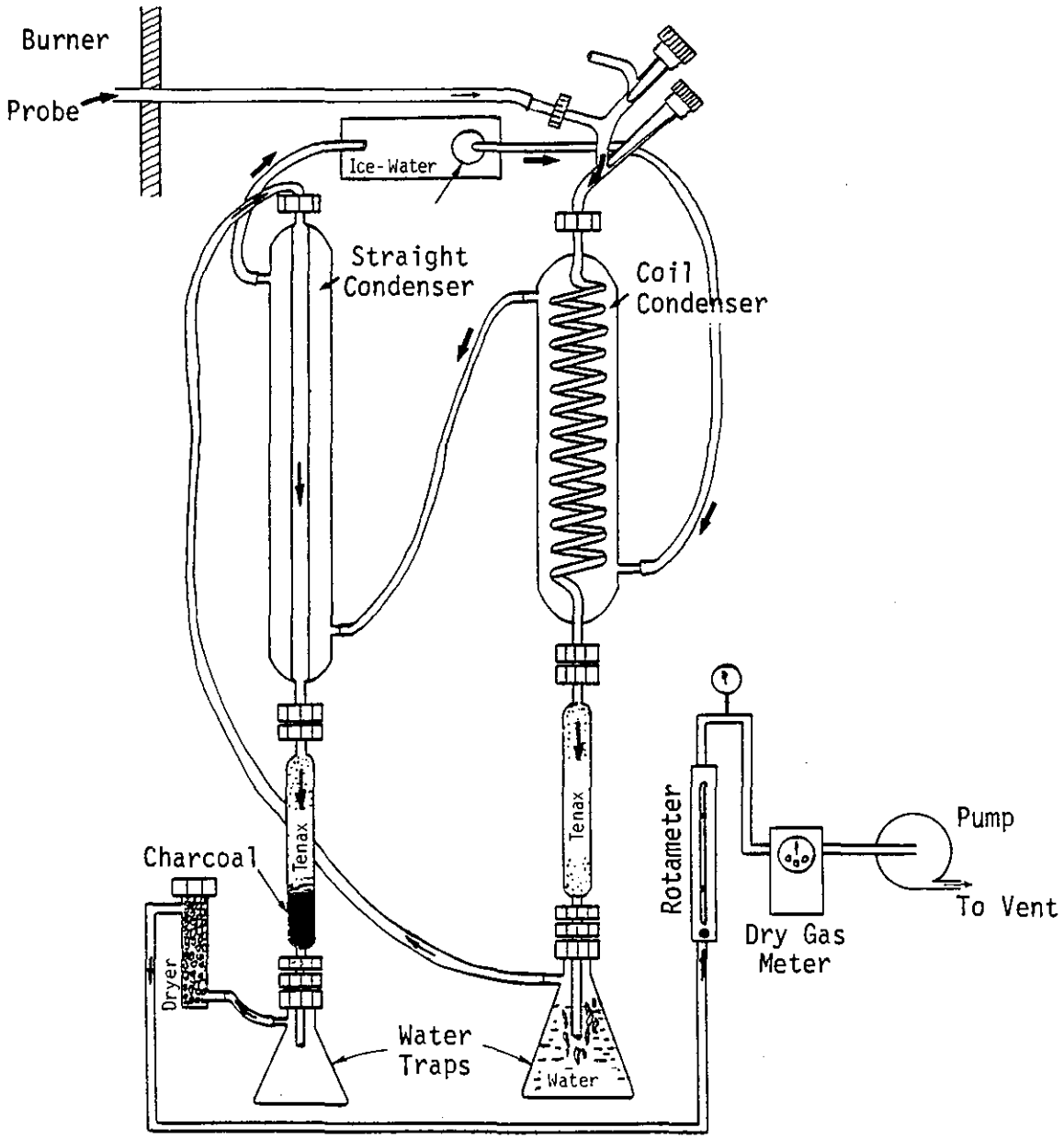

Figure A-1. Sampling and VOST adsorption system.

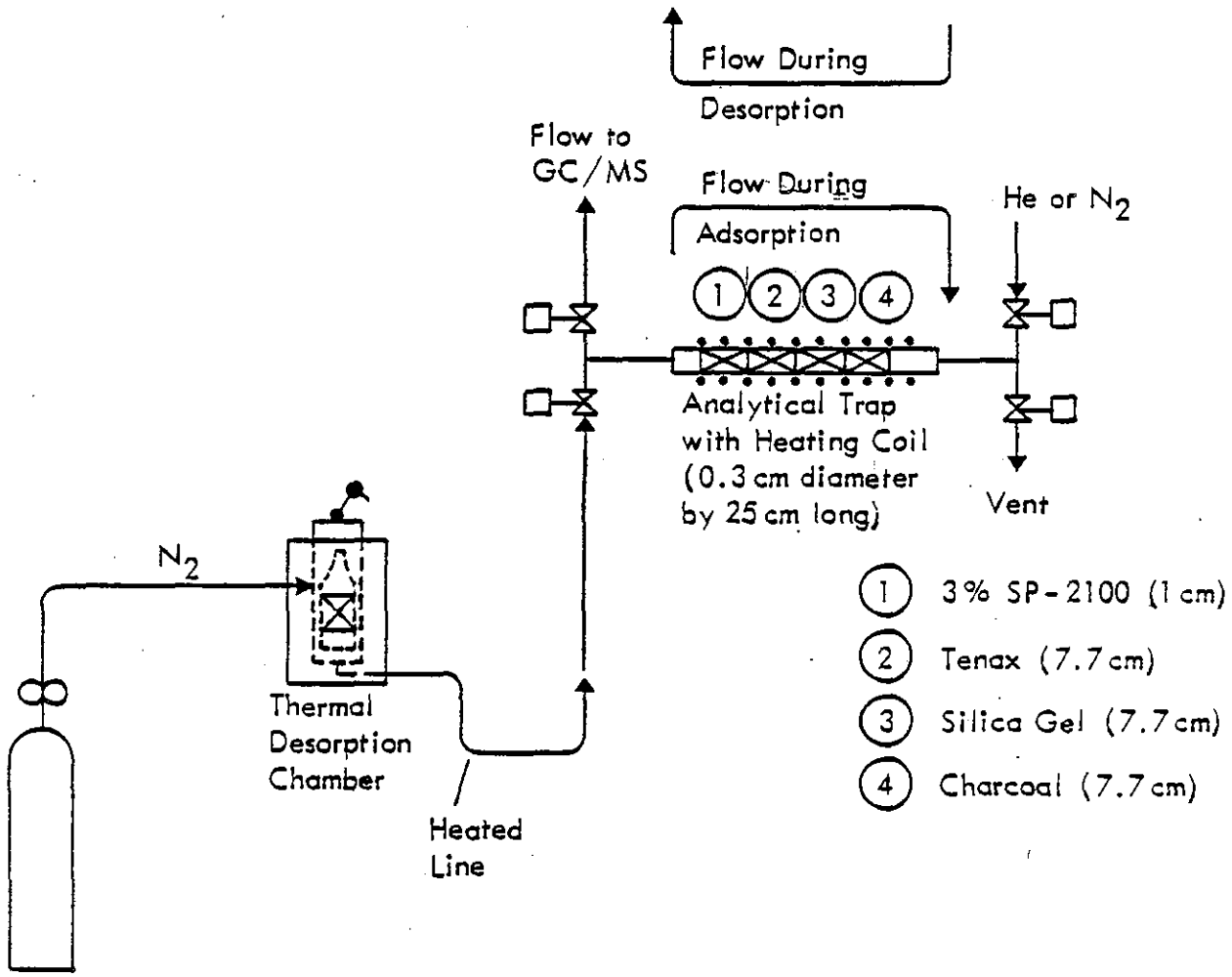

Figure A-2. Schematic diagram of trap desorption/analysis system.

A.2 Operating Procedures

Prior to use, the Tenax and Tenax/charcoal cartridges are conditioned under a 20 cc/min. helium flow at 200 C for 45 min. Both before and after sampling the tube ends are covered with celophane and refrigerated.

After the reactor condition has been set, the cartridges are placed in the adsorption train, the cooling water started, and the sample flow opened. A sample flow rate of 0.23 liters/min. has been found satisfactory as discussed below. At the conclusion of sampling (2.3 liters or 10 min.) the cartridges are removed and refrigerated.

For analysis, the cartridges are connected into the GC carrier gas line and placed in the desorption block. The block is raised to 120°C and held at this temperature for 5 min. This time and temperature have been found sufficient to quantitatively desorb all of the test compounds. During desorption the GC oven is maintained at room temperature. As the compounds desorb, they are collected at the inlet of the GC column. The compounds do not start to separate at room temperature. If this was not the case, peaks would be broadened by the deposition of newly desorbed compound at the column inlet after separation had started. At the conclusion of the 5-min. desorption time the column was heated to 120°C, held at this temperature for 25 min., and programmed at 5 C/min. to 150°C when samples containing heptane or No. 2 fuel oil were analyzed; or to 180°C for all other cases. Under the present analytical conditions, benzene and 1,2-dichloroethane have nearly identical retention times; because of this, these two compounds were never used in the same experiment. The FID gas flows were 71 cc/min. hydrogen and 442 cc/min. air.

The integrator output record consists of a chromatogram detector signal trace and a table of integrated peak areas. The trace is compared with the tabulated output to insure that the compound peaks are free of interferences, that the baseline boundary conditions were correctly constructed by the integrator, and that the presence of unanticipated peaks could be noted. Integrated peak area values were converted into ppm by use of the calibration

curves and destruction efficiencies were calculated using the ppm anticipated from zero destruction operation.

A.3 Calibration Techniques

Test compound calibration was performed by three independent procedures. This was necessary to determine the inherent scatter and reproducibility of the measurement technique, and to locate any of the calibration tests. The three techniques were 1) direct syringe injection of test compound onto the GC column; 2) syringe injection of liquid test compound into a Tenax cartridge, followed by routine desorption and analysis; and 3) preparation of known standards in a dilution tank, followed by routine Tenax sampling and analysis of the tank contents.

Direct Column Injection: Liquid samples were withdrawn with a calibrated microliter syringe and directly injected onto the column through the injection septa. Chromatograph conditions were identical to the nominal operating procedure except:

1. The Tenax cartridge desorber was not a part of the system.

2. Rather than follow the prescribed oven temperature programming, an isothermal temperature of 120°C was used (except for chlorobenzene where 180°C was used (except for chlorobenzene where 180°C was used). The isothermal temperatures increased the speed at which calibrations were performed. The programming is necessary during normal sampling to separate light hydrocarbons from the earliest test compound peaks. Because of the linearity of the FID amplifier, the change in temperature programming does not affect the calibration.

Table A-1 lists the FID mass sensitivity for the various compounds tested, relative to methane.

TABLE A-1. MASS SENSITIVITY RELATIVE TO METHANE FOR THE FID

Compound	Relative Sensitivity	Compound	Relative Sensitivity
Acrolein	0.54	Ethyl Acrylate	0.59
Phenol	1.22	Hexachlorobenzene	0.0
Benzene	1.23	Toluene	1.09
Carbon Disulfide	0.0	Vinyl Chloride	0.69
Acrylonitrile	0.59	Methyl Ethyl Ketone	0.68
1,1,1-Trichloroethane	1.64	Chlorobenzene	0.77
Chloroform	0.09		

Syringe Injection Onto Tenax: Liquid test compound samples were directly injected onto packed Tenax cartridges. These were subsequently desorbed and analyzed. The results in the present study were used as an initial, qualitative test for breakthrough volume. After injection, helium was drawn through the cartridge. For some tests a second cartridge was placed behind the first. Breakthrough was detected by the appearance of test compound on the second cartridge and, simultaneously, by the loss of response from the analysis of the first cartridge.

Dilution Tank: Dilute samples were prepared by evacuating an 11-liter glass tank and injecting a known amount of sample into the tank as the tank was rapidly repressurized. After repressurization the tank was allowed to equilibrate and the tank pressure and temperature were noted for calculation of the correct dilution factor. A portion of the tank contents are pumped through the Tenax sampling system. The remainder of the calibration test is identical to the normal sampling and analytical procedure.

A.4 Calibrations

Figures A-3 through A-6 show sample calibration plots for benzene, chlorobenzene, chloroform, and acrylonitrile. These are plotted as microliters liquid vs. integrator peak area. The two plots shown on each graph correspond to the direct injection calibration and the Tenax calibration. The close agreement between the two curves for all compounds indicates that breakthrough volume was not exceeded for these compounds.

Sample Storage: Each GC analysis required about 1.5 hours. Thus, a backlog of unanalyzed samples occasionally accumulated. In no case was a sample held longer than 24 hours before analysis. However, a series of tests were performed to determine if 24 hours was a safe period for storage. A standard gas was prepared and adsorbed onto two cartridges in parallel. The first was analyzed immediately and the second was stored under nominal storage conditions for 24 hours and analyzed. The results, shown in Table A-2, indicate that no significant loss of test compound occurred. The scatter between the two analyses is typical of the measurement technique.

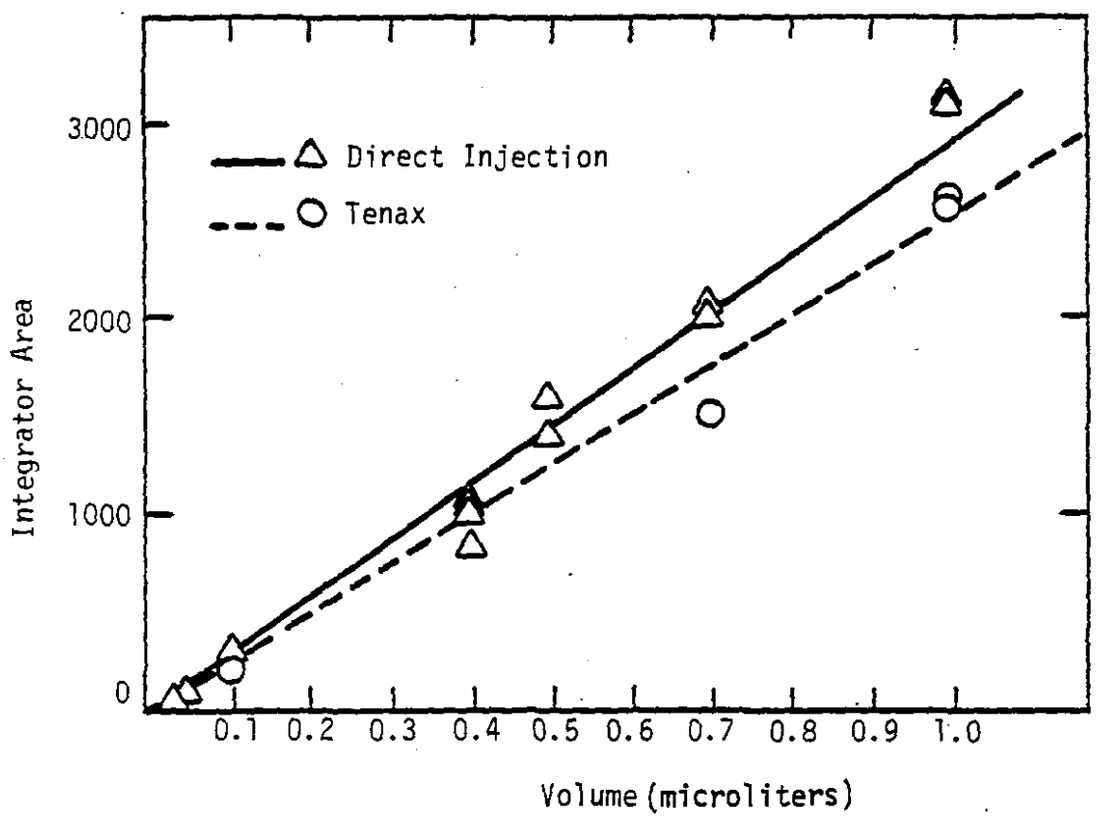

Figure A-3. Calibration curves for benzene.

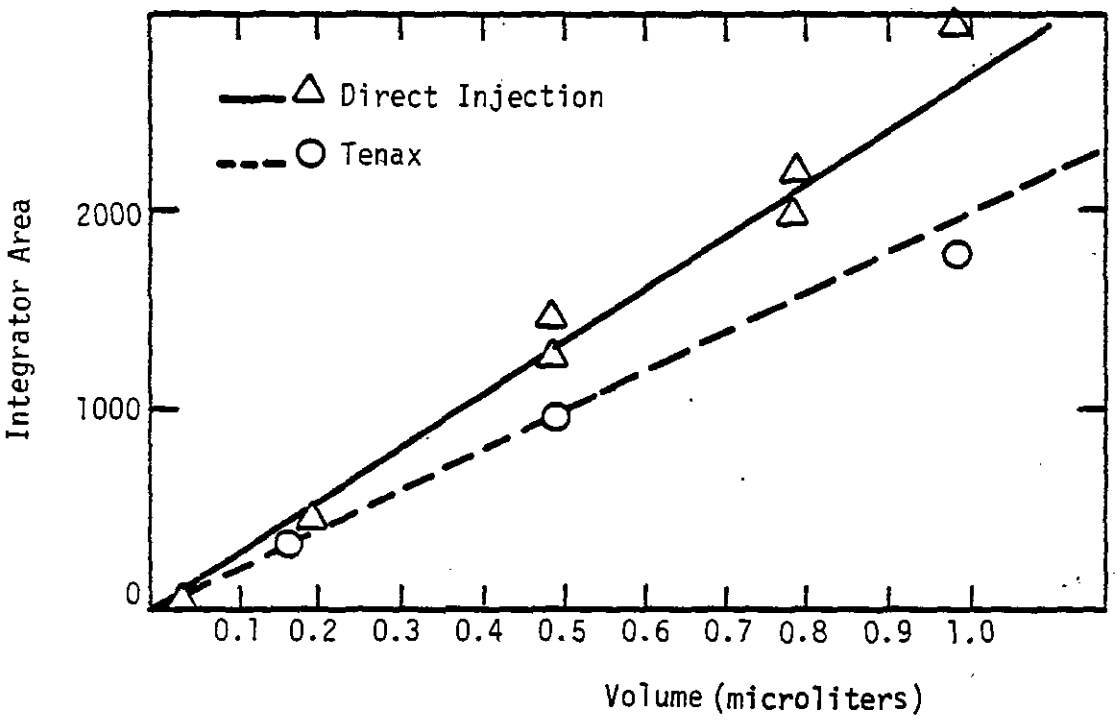

Figure A-4. Calibration curves for chlorobenzene.

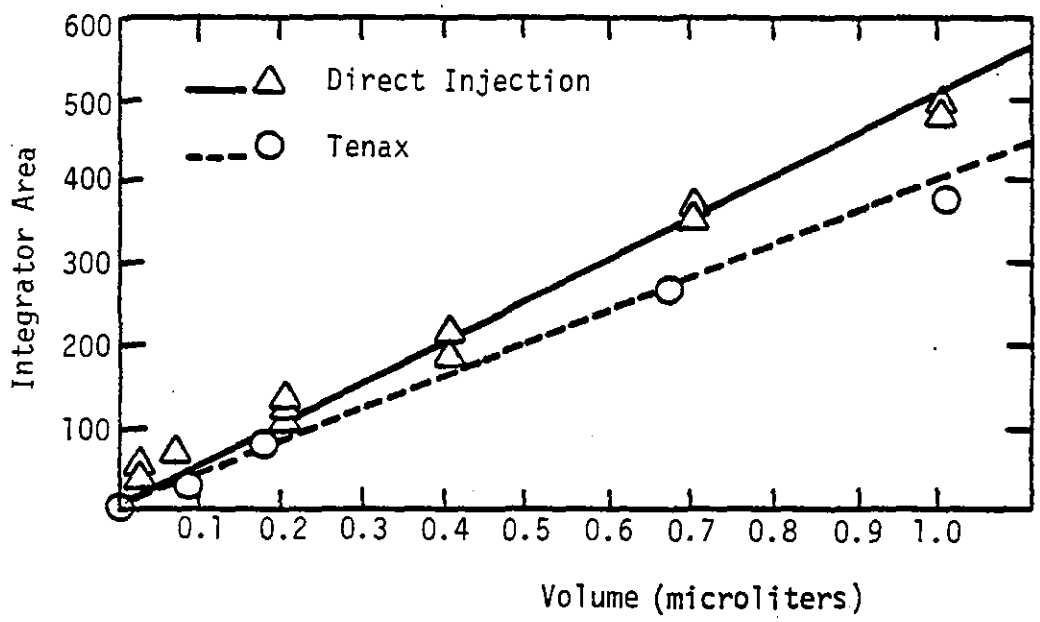

Figure A-5. Calibration curves for chloroform.

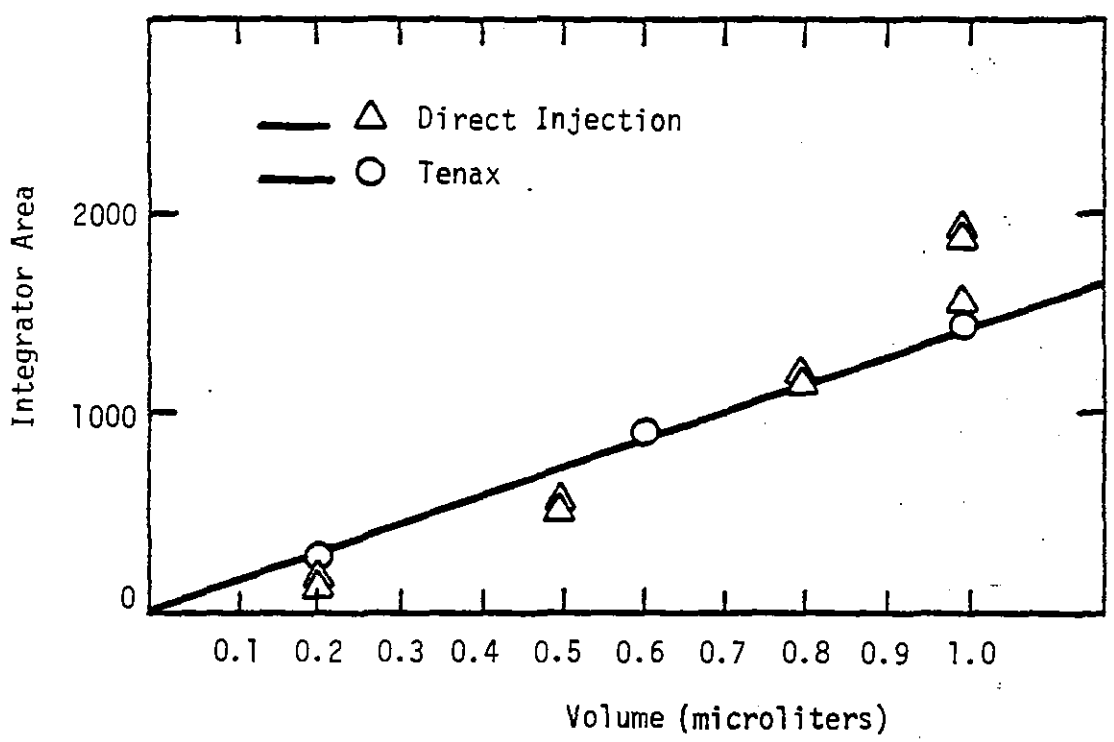

Figure A-6. Calibration curves for acrylonitrile.

TABLE A-2. SAMPLE STORAGE STABILITY

Compound	Analysis	
	Immediate (ppm)	After 24 Hours (ppm)
Acrylonitrile	16.7	18.2
Chloroform	16.2	14.5
1,2-Dichloroethane	16.2	16.9
Chlorobenzene	8.77	9.5

A.5 Uncertainty, Accuracy, and Precision

The problem of sample repeatability and precision really involves two questions:

- What is the repeatability of the analytical technique given a time-steady, known concentration to measure?

- What is the time-steadiness of the experiment, assuming a perfect measurement technique?

The first of these questions were addressed by the repeated analysis of known calibration standards. An example of such a series is shown in Table A-3 for benzene. The resulting standard deviation of the relative error is 2.1 percent. Thus, for the measurements to be accepted at the 90 percent confidence interval, the relative error is approximately $\pm$ 4.2 percent. The error for all calibration data as a group indicated an approximate $\pm$ percent at the 90 percent confidence interval for the Tenax procedure.

The data indicate that the inherent time unsteadiness of the experimental DE measurements was small under nonoptimum conditions and substantial under optimum conditions. For the optimum conditions the observed time unsteadiness exceeded the $\pm$ 5.0 percent uncertainty associated with the analytical system and, thus, led to the conclusion that optimum DE measurements and rankings were random, time unsteady, and were probably related to the statistical nature of a turbulent flame. However, none of these optimum data were used to establish the ranking presented in this study.

Quality Assurance/Quality Control requirements are applicable to this project. The data contained in this report are NOT supported by QA/QC documentation as required by the United States Environmental Protection Agency's Quality Control Policy.

TABLE A-3. CALIBRATION REPEATABILITY DATA FOR BENZENE

Response (peak area)		Relative Error
Expected	Obtained	
1141	1101	.0350
1141	1126	.0131
1470	1399	.0483
1470	1451	.0129
2129	2090	.0183
2129	2138	-.0042
3118	3146	-.00898
3118	3153	-.0112
3118	3136	-.0058

APPENDIX B

RAW DATA

This section presents the raw test compound data and describes the procedure for converting the raw data into destruction efficiencies.

B.1 Sample Chromatograms

A selection of chromatograms typical of various turbulent flow reactor conditions are presented below. The numbers printed next to each peak are the retention times in minutes. A chromatogram typical of high-efficiency turbulent flow reactor operation is shown in Figure B-1. Few peaks are present and only one peak, associated with a fuel fragment at 45.18 min. is measurable. Figure B-2 shows a chromatogram for moderate DE turbulent flow reactor data. A low-DE turbulent flow chromatogram is shown in Figure B-3. At very low efficiency operating conditions significant quantities of fuel and fuel fragments are released by the flame in addition to the test compounds. These conditions can result in an uninterpretable chromatogram, as shown in Figure B-4.

B.2 Calculation Procedures

Chromatogram peak areas were related to moles for each compound by use of the calibration figures in Appendix A. This number is converted into mole fraction based on dry gas by:

$$\text{Mole Fraction (Dry)} = \frac{(\text{moles compound})\ (24.63\ \text{liters/mole})}{(\text{sample volume - liters})} \qquad \text{(B.1)}$$

The mole fraction water in the wet combustion gas is estimated from a complete combustion model and the dry mole fractions are corrected to burner (wet) mole fractions by:

$$\text{Burner Mole Fraction} = (\text{Dry Mole Fraction}) - (1 - \text{Water Mole Fraction}) \qquad \text{(B.2)}$$

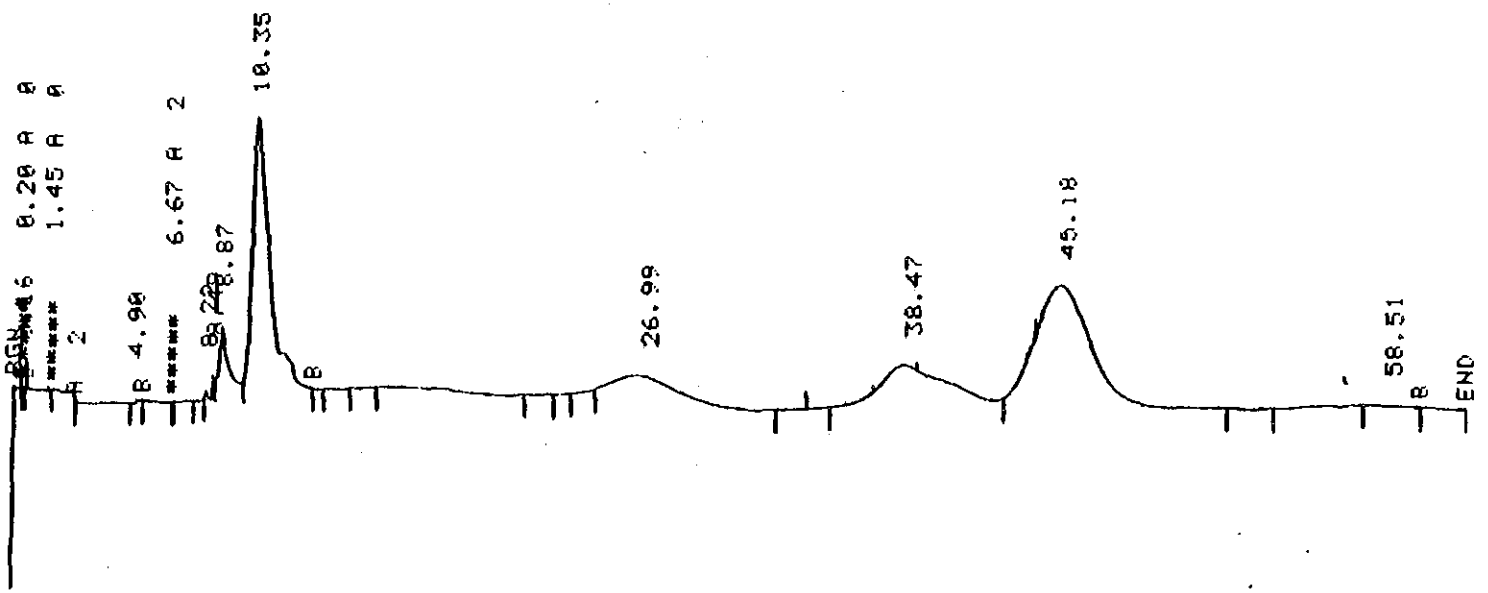

Figure B-1. Chromatogram for a high-DE turbulent flow reactor condition.

Figure B-2. Chromatogram for moderate-DE heptane-fueled turbulent flow reactor condition.

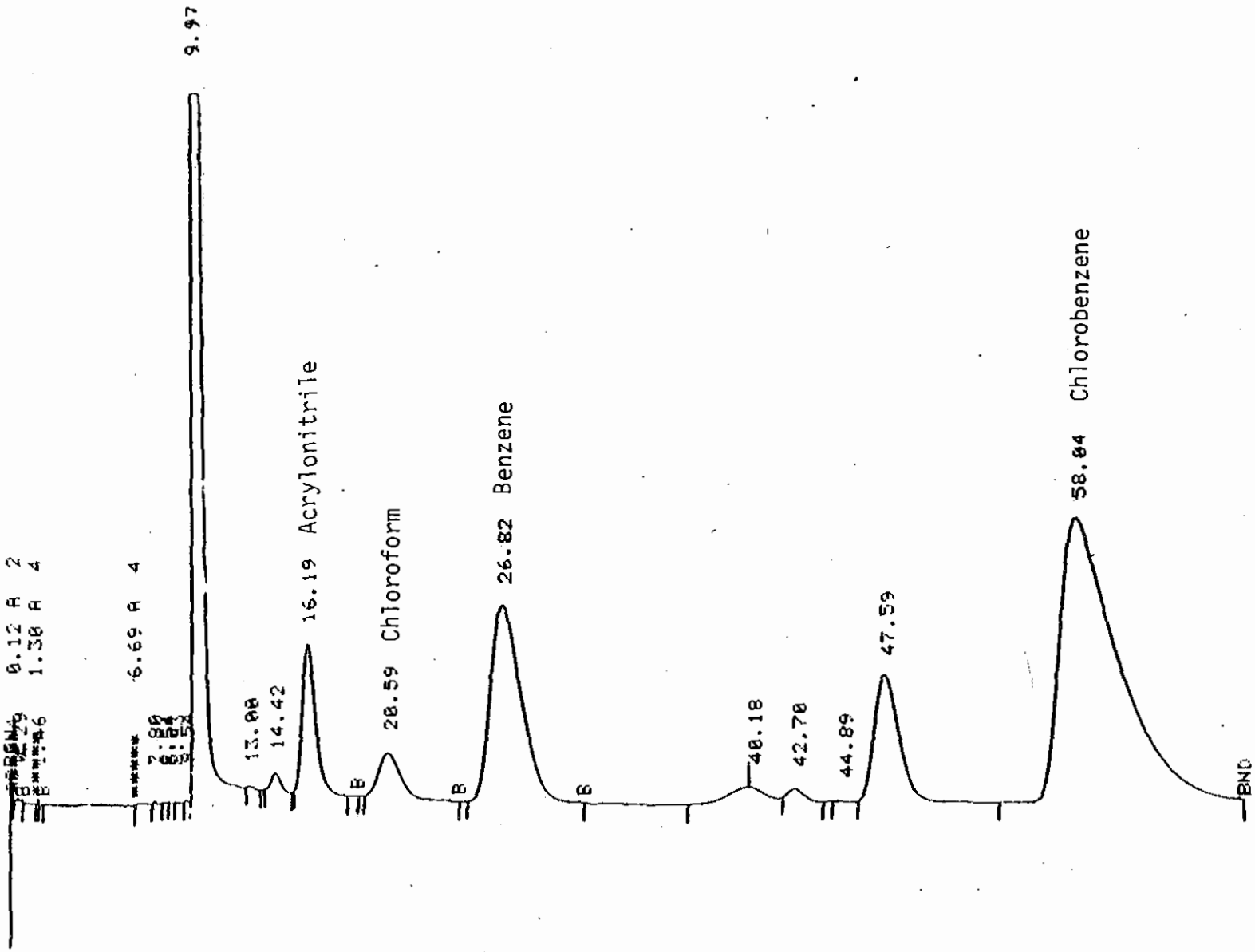

Figure B-3. Chromatogram showing a poor-DE turbulent flow reactor condition.

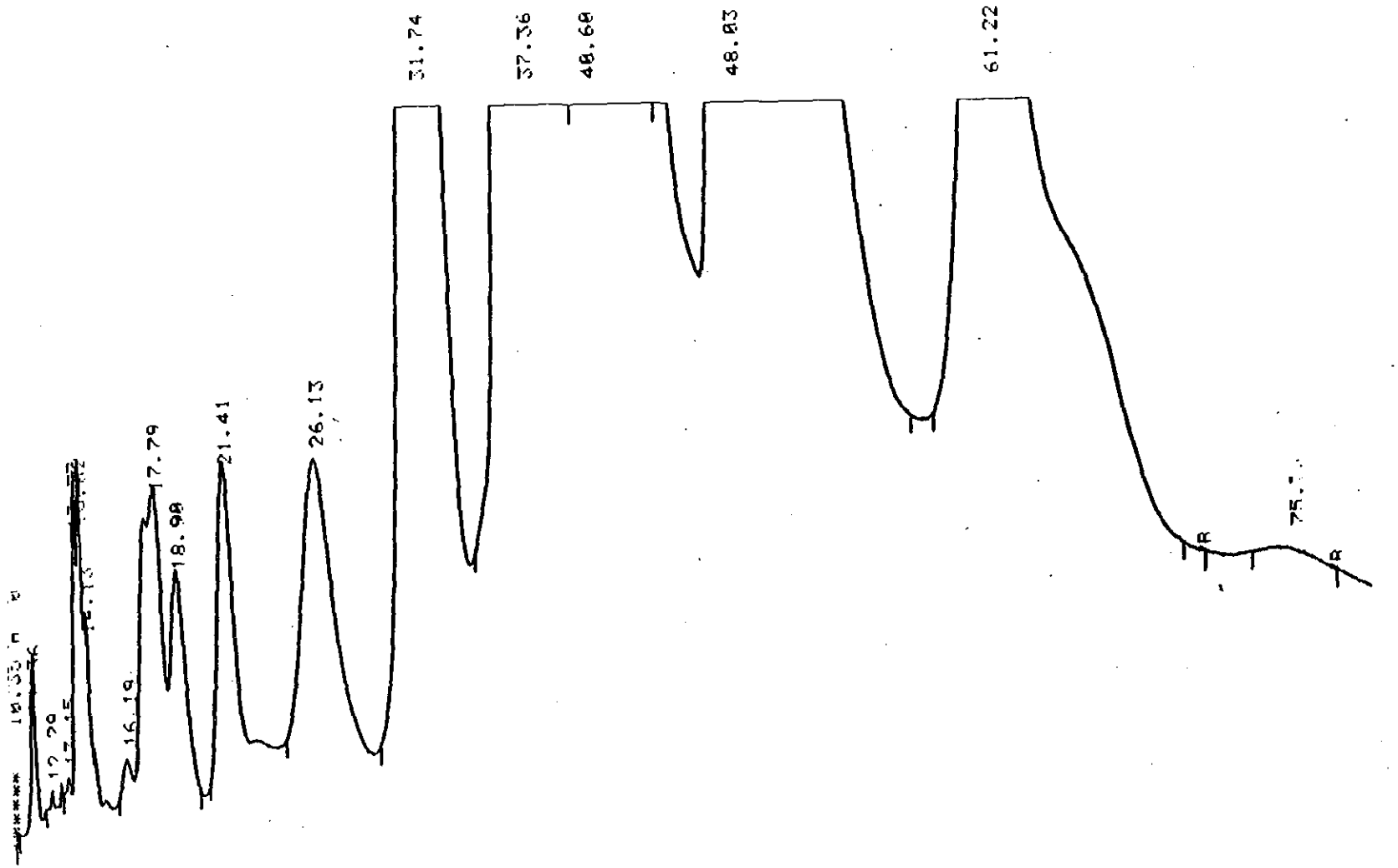

Figure B-4. Chromatogram showing very low efficiency turbulent flow reactor operation with significant fuel fragments present.

The mole fraction of compound that would be present at the burner exit if efficiency were zero is calculated by:

$$\text{Zero Efficiency Mole Fraction} = \frac{(\text{Fuel Flow})\ (\text{Moles Compound/Mass Fuel})}{\text{Total Reactor Molar Flow}} \qquad \text{(B.3)}$$

The (Moles Compound/Mass Fuel) is calculated from the fuel mixture composition and the (Total Reactor Molar Flow) is calculated from the fuel flow, the air flow, and the complete combustion model. The fraction unreacted compound is the ratio of Equation B-2 and B-3.

B.3 Raw Data Tables

Tables B-1 through B-4 summarize the data from the volatile organic analysis.

TABLE B-1. PIC FORMATION--TEST CONDITIONS

Sample No.	Compound	SR	CO (ppm)	CO_2 (%)	O_2 (%)	HC (ppm Propane)
92802	No. 2 Fuel Oil	0.55	19,000	7.1	7.1	3,750
92705		0.6	4,060	13.7	2.8	60
92704		0.7	120	131	3.9	50
92701		1.0	110	9.0	8.5	20
92702		1.2	1,970	7.6	10.3	200
92801		1.6	5,350	5.8	12.2	2,000
100102	No. 2 Fuel Oil +0.1% Chlorophenol	0.55	12,420	5.8	12.8	7,400
100101*		0.65	13,400	11.4	4.4	3,500
92804*		0.7	254	11.6	4.9	82.5
92803		1.0	224	8.5	8.9	100
92805*		1.2	302	7.4	10.8	55
92806		1.6	2,400	7.9	10.6	350

*GC-MS Data resolved for those conditions.

TABLE B-2. SECONDARY ATOMIZATION

Sample No.	Compound	Compound Concentration	CO (ppm)	CO_2 (%)	O_2 (%)	HC (ppm Propane)	Destruction Removal Efficiency (%)
92102	Isopropanol	0.5%	160	11.0	5.8	125	99.821
92103		2.0%	124	12.0	4.7	32	99.998
92104		10.0%	77	12.1	4.8	62.5	100
92502	Benzal Chloride	0.5%	124	10.9	6.2	50	97.636
92503		2.0%	140	11.2	5.8	85	98.766
92602		10.0%	165	10.5	6.2	110	99.781

TABLE B-3. COMPOUND CONCENTRATION DATA (CHLOROFORM FREE)

Sample No.	Compound Concentraion	Fuel	CO (ppm)	CO_2 (%)	O_2 (%)	HC (ppm Propane	Destruction Removal Efficiency (%)			
							Acrylon-itrile	Trichlo-roethane	Toluene	Chloro-benzene
100401	30 ppm	No. 2 Fuel Oil	240	9.1	9.2	100	94.62	99.999	100.00	99.999
100402	300 ppm		-	-	-	-	75.77	89.694	88.90	86.89
100403	3000 ppm		1333	7.2	11.4	500	94.52	99.995	97.75	99.39
100501	3%		338	9.1	9.1	200	99.912	99.999	99.999	99.999
100502	30 ppm	Heptane	157	7.2	10.7	48	97.07	68.04	71.79	99.999
100503	300 ppm		106	9.0	7.8	70	58.56	99.999	99.29	99.999
100504	3000 ppm		90	9.0	8.0	40	99.999	99.46	99.93	99.999
100506	3%		-	-	-	-	95.39	99.999	99.995	99.999

TABLE B-4. COMPOUND CONCENTRATION DATA (WITH CHLOROFORM)

Sample No.	Compound Concentration	SR	CO (ppm)	CO_2 (%)	O_2 (%)	HC (ppm Propane	Destruction Removal Efficiency (%)				
							Acrylon-itrile	Chlor-oform	Trichlo-ethane	Toluene	Chloro-benzene
91902	30 ppm	1.2	120	11.2	5.0	90	99.236	0.00	99.629	92.710	99.999
91903	30 ppm	1.5	150	9.5	7.6	30	78.62	0.00	81.159	89.764	99.999
91803	300 ppm	1.2	112	9.5	7.5	34	94.081	65.284	99.999	77.84	95.516
91804	300 ppm	1.5	650	8.6	8.9	85	91.595	0.00	47.13	54.309	99.999
91805	3000 ppm	1.2	73	10.4	6.2	28	99.677	88.578	99.993	99.897	99.999
91806	3000 ppm	1.5	1465	7.9	9.5	150	94.597	0.00	91.830	89.457	97.208
91807	3%	1.2	450	11.1	5.0	52	98.954	99.146	99.565	99.007	98.668
91904	3%	1.2	108	12.0	3.9	35	98.984	99.869	99.999	99.996	99.999
91905	3%	1.5	69	9.8	7.2	25	99.996	90.295	99.750	99.990	99.999
92001	30%	1.2	191	11.4	5.8	24	99.9999	99.925	99.995	99.998	99.998
92002	30%	1.5	300	13.3	3.5	40	99.998	99.712	99.998	99.999	99.999

APPENDIX C

GC-MS RAW DATA

The following section is a transcript of the analysis obtained from the GC-MS analysis of the three cartridge traps used in the present study.

TABLE 1

TENAX TRAP DATA

COMPOUND	SAMPLE AMOUNT (ug)						
	92804A	92804B	92805A	92805B	100101A	100101B	4VBLK
CO_2	5.7	0.75	11	1.1	6.6	0.50	0.03
methane, dichlorodifluoro	*	0.09			*		*
methane, trichlorofluoro		1.15		0.10		0.76	
ethane, 1,1,2-trichloro 1,2,2-trifluoro		0.04		0.06			
methane, dichloro	*	**			*	0.62	
benezene		**				1.5	
methylethylketone (MEK)		21	2.5	32		8.8	
thiophene		0.32		0.23		0.24	
1-butanol		1.0					
ethene, trichloro		0.15					
2-pentene-3,4-dimethyl						0.05	
cyclohexane, methyl			0.71			0.20	
cyclopentane, 1,2,3-trimethyl		0.02	0.41				
1-hexene, 3,5,5-trimethyl		0.02					
2-pentanone, 4-methyl		0.15					
toluene		4.6	9.1	1.9	0.51	1.6	
acetic acid, propylester						0.07	
cyclopentane 1,1,3,4-tetramethyl						0.006	
3-methyl heptane			0.09				
cyclohexane, dimethyl***			0.07		0.02		
benzene, chloropentafluoro		0.04		0.003			0.005
acetic acid, butylester		0.04		0.03			
octane		0.02	0.23				
ethene, tetrachloro		0.03	0.08	0.01		0.003	
cyclohexane, trimethyl***		0.16	0.25	0.16	0.03	0.04	
chlorobenzene		0.02		0.009			
ethylbenzene		0.09	0.44	0.07	0.05	0.005	
2-methylnonane			0.13				

TABLE 1 - TENAX TRAP DATA (Continued)

COMPOUND	SAMPLE AMOUNT (ug)						
	92804A	92804B	92805A	92805B	100101A	100101B	4VBLK
benzene, ethylmethyl***			0.21		0.002		
2-methylundecane			0.10				
benzene, ethyldimethyl***			0.02				
2-methylnaphthalene			0.009				
naphthalene			0.002	0.005			
trimethyl benzene***		0.03	0.14	0.02			
cyclohexane, ethylmethyl***		0.20	0.54	0.15	0.01	0.01	
2-propyl-1-heptanol				0.01			
4-propylheptane					0.009		
3-methyl-1-hexene					0.004		
benzene, dimethyl***		0.28	2.6	0.28	0.03	0.02	
nonane		0.14	0.65				
pentalene, octahydro-2-methyl		0.06					
isooctanol					0.008		
3-methylhexane					0.004		
cyclohexane, butyl					0.003		
1-hexene-3,5,5-trimethyl					0.005		
cyclohexane, diethyl***		0.10	0.17		0.006	0.006	
decene		0.16					
decane		0.07					
decane, 4-methyl			0.07	0.01			
benzene, 1,2,3-trichloro		0.004	0.004				
cyclopentane, 1-methyl-2-(2-propenyl)		0.02					
decahydro naphthalene		0.04		0.03			
undecane		0.01	0.04				
3-ethylheptane			0.13				
cyclohexane, propyl					0.009		
diethyl phthalate							0.004

* Co-elutes with CO_2, unquantitatable.
** Co-elutes with MEK, unquantitatable.
*** Isomers present, reported as a single entry.

(1595V-7)

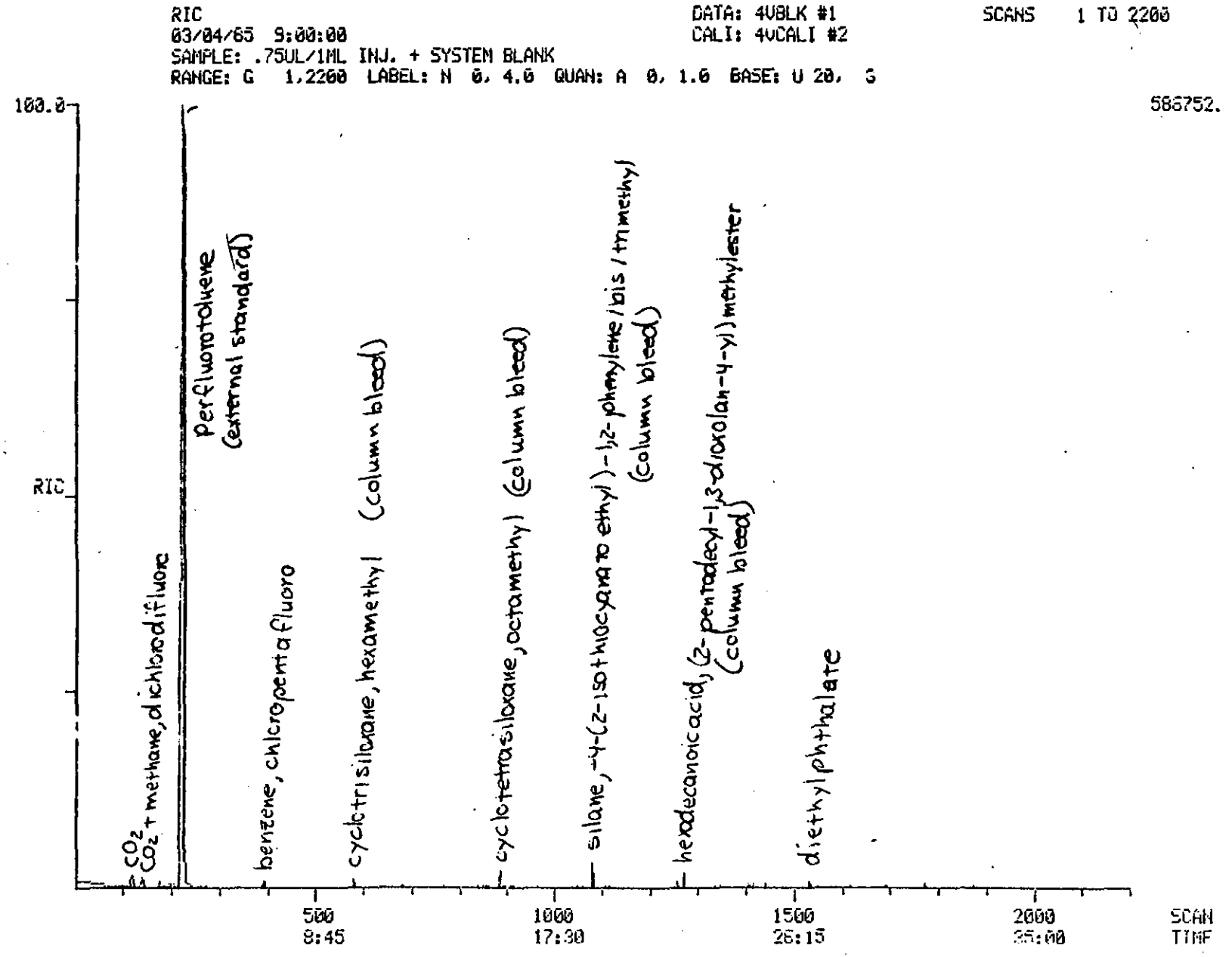
RIC
03/04/65 9:00:00
SAMPLE: .75UL/1ML INJ. + SYSTEM BLANK
RANGE: G 1,2200 LABEL: N 0, 4.0 QUAN: A 0, 1.0 BASE: U 20, 5
DATA: 4UBLK #1
CALI: 4UCALI #2
SCANS 1 TO 2200
100.0
586752.
RIC
CO2
CO2 + methane, dichlorodifluoro
perfluorotoluene (external standard)
benzene, chloropentafluoro
cyclotrisiloxane, hexamethyl (Column bleed)
cyclotetrasiloxane, octamethyl (Column bleed)
silane, -4-(2-isothiocyanato ethyl)-1,2-phenylene bis / trimethyl (Column bleed)
hexadecanoic acid, (2-pentadecyl-1,3-dioxolan-4-yl) methylester (Column bleed)
diethylphthalate
500 8:45
1000 17:30
1500 26:15
2000 35:00
SCAN TIME

C-4

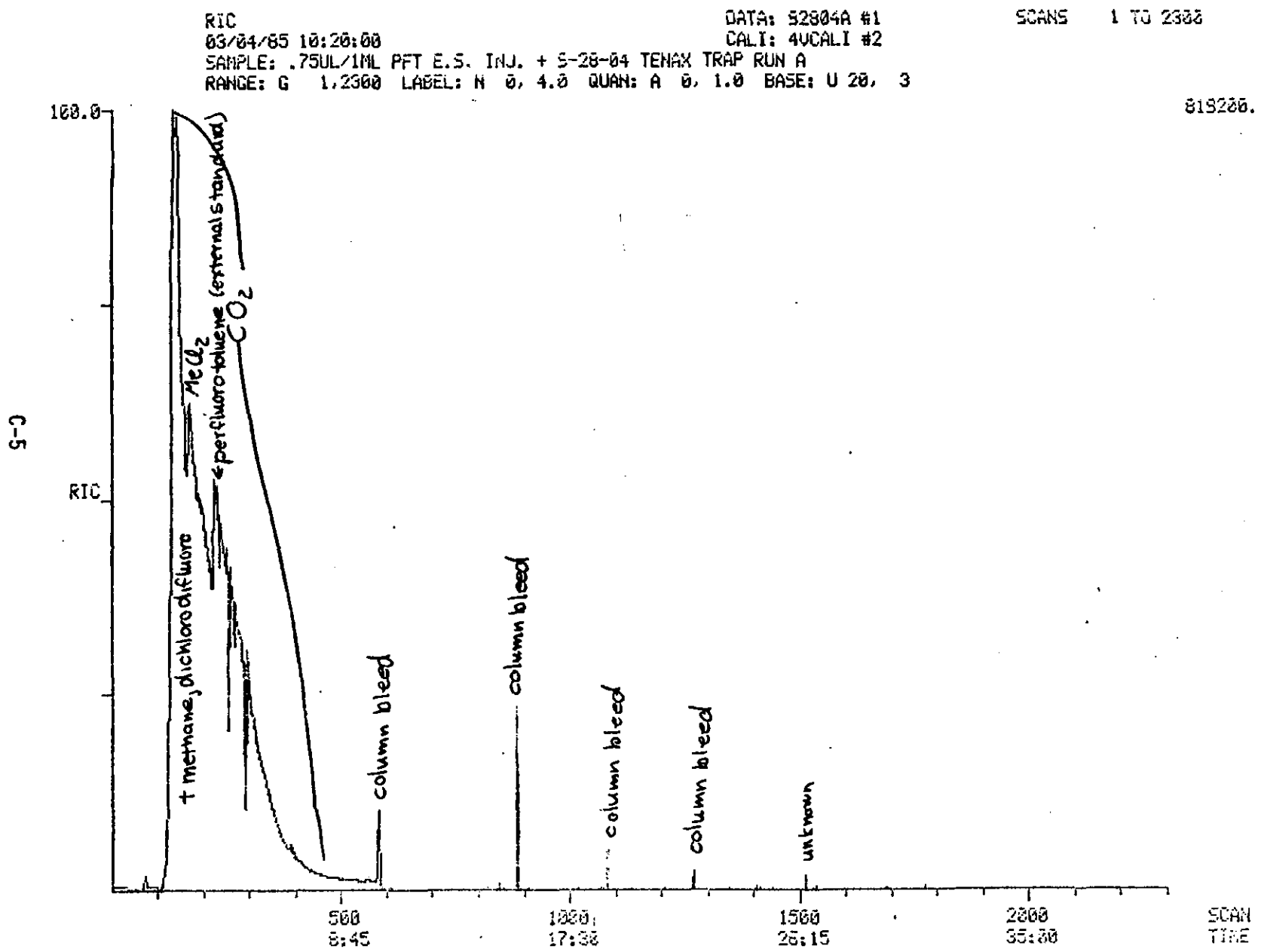
RIC
03/04/85 10:20:00
SAMPLE: .75UL/1ML PFT E.S. INJ. + S-28-04 TENAX TRAP RUN A
RANGE: G 1,2300 LABEL: N 0, 4.0 QUAN: A 0, 1.0 BASE: U 20, 3
DATA: S2804A #1
CALI: 4UCALI #2
SCANS 1 TO 2300
818200.
100.0
RIC
+ methane, dichlorodifluoro
MeCl2
<perfluorotoluene (external standard)
CO2
column bleed
column bleed
column bleed
column bleed
unknown
500
8:45
1000
17:30
1500
26:15
2000
35:00
SCAN
TIME

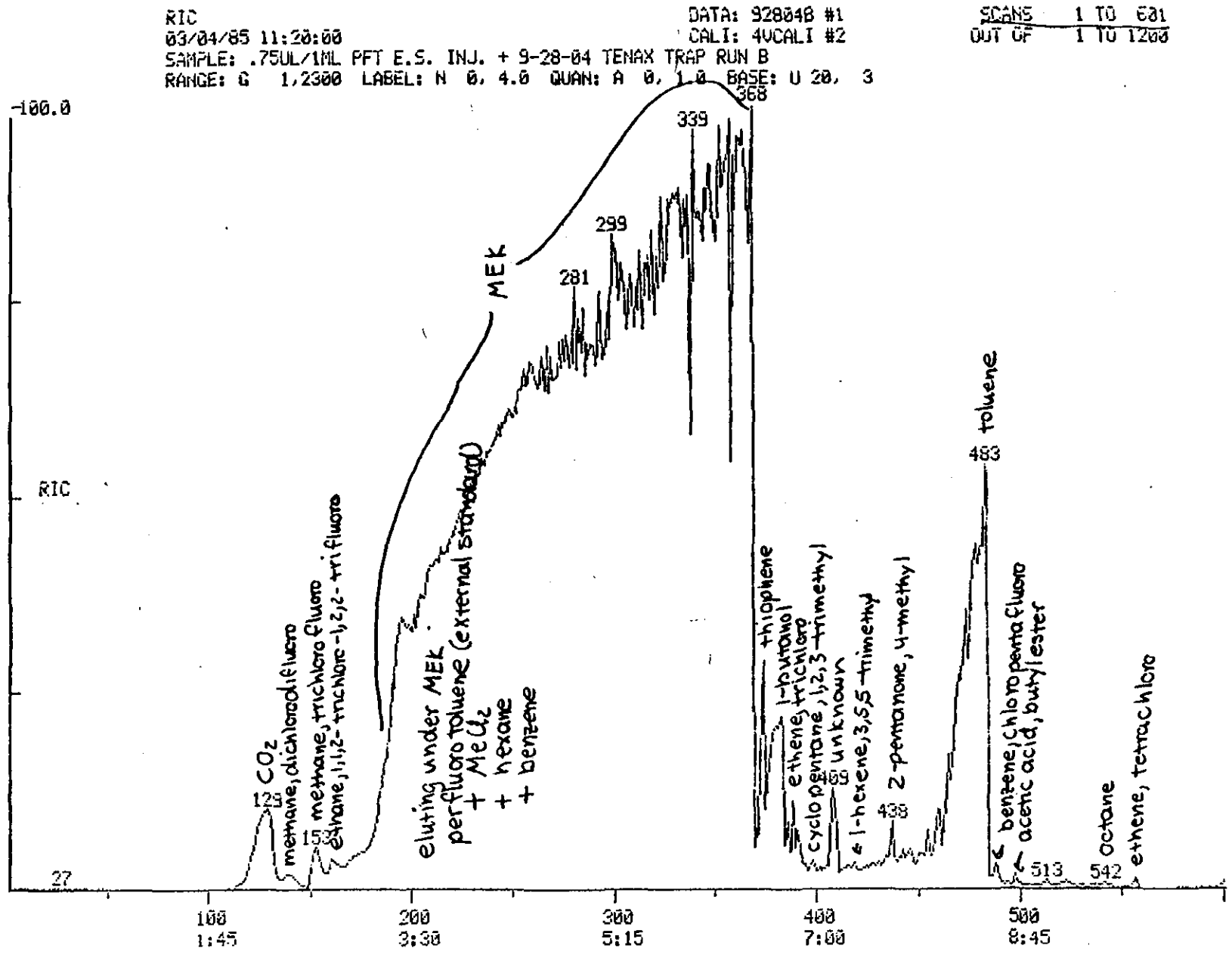
RIC
03/04/85 11:20:00
SAMPLE: .75UL/1ML PFT E.S. INJ. + 9-28-04 TENAX TRAP RUN B
RANGE: G 1,2300 LABEL: N 0, 4.0 QUAN: A 0, 1.0 BASE: U 20, 3
DATA: 928048 #1
CALI: 4VCALI #2
SCANS 1 TO 631
OUT OF 1 TO 1200
100.0
RIC
27
CO2
methane, dichlorodifluoro
methane, trichloro fluoro
ethane, 1,1,2-trichloro-1,2,2-trifluoro
eluting under MEK
perfluoro toluene (external standard)
+ MeCl2
+ hexane
+ benzene
MEK
thiophene
1-butanol
ethene, trichloro
cyclopentane, 1,2,3-trimethyl
unknown
1-hexene, 3,5,5-trimethyl
2-pentanone, 4-methyl
toluene
benzene, chloropentafluoro
acetic acid, butylester
octane
ethene, tetrachloro
128
153
281
299
339
368
409
438
483
513
542
100
1:45
200
3:30
300
5:15
400
7:00
500
8:45

RIC
03/04/85 11:20:00
SAMPLE: .75UL/1ML PFT E.S. INJ. + 9-28-84 TENAX TRAP RUN B
RANGE: G 1,2300 LABEL: N 0, 4.0 QUAN: A 0, 1.0 BASE: U 20, 3

DATA: 928048 #1
CALI: 4UCALI #2

SCANS 601 TO 1203
OUT OF 1 TO 1200

2613240.

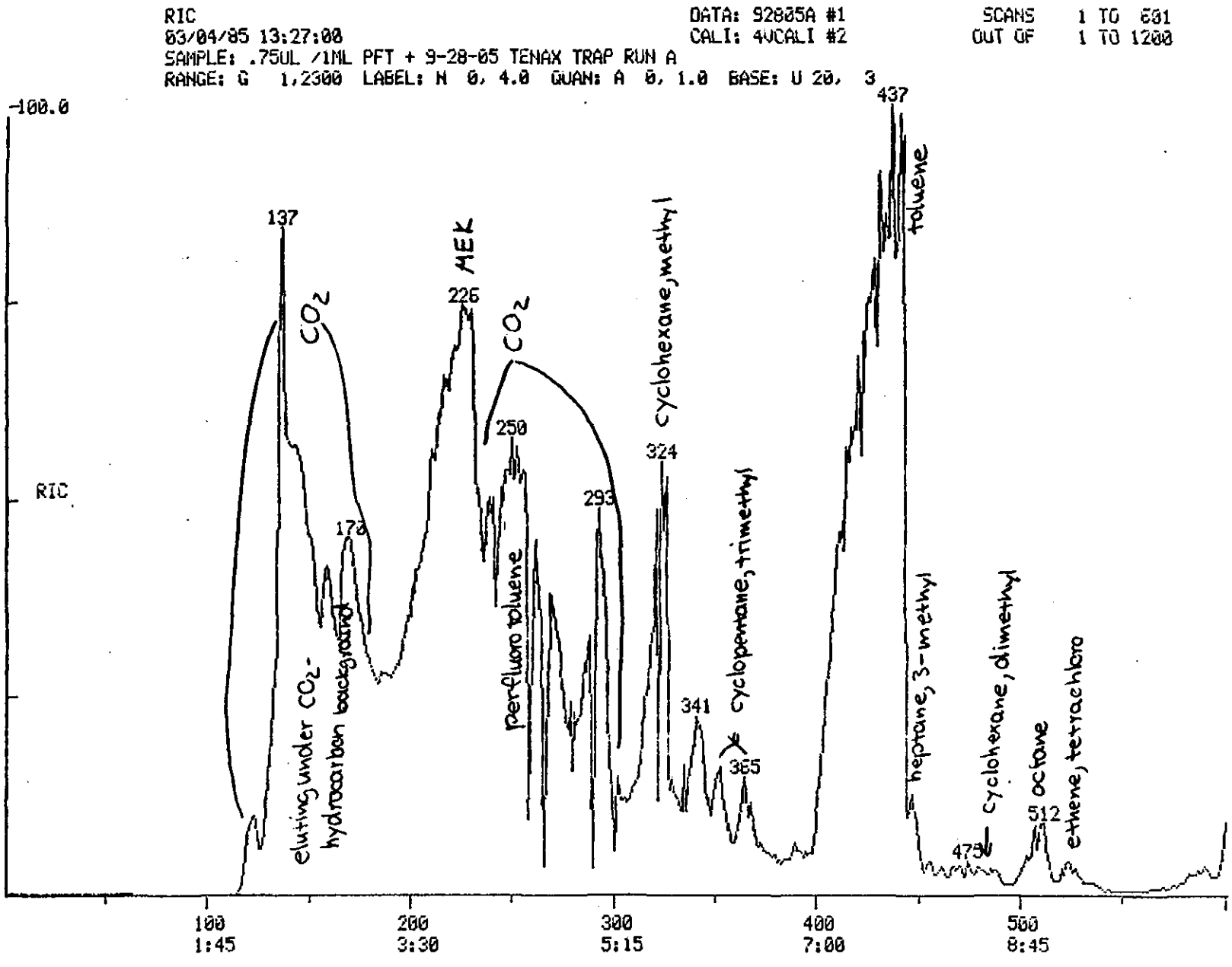
RIC
03/04/85 13:27:00
SAMPLE: .75UL /1ML PFT + 9-28-05 TENAX TRAP RUN A
RANGE: G 1,2300 LABEL: N 0, 4.0 QUAN: A 0, 1.0 BASE: U 20, 3
DATA: 92805A #1
CALI: 4UCALI #2
SCANS 1 TO 631
OUT OF 1 TO 1200
-100.0
RIC
137
CO2
226
MEK
CO2
250
293
324
cyclohexane, methyl
341
cyclopentane, trimethyl
365
437
toluene
heptane, 3-methyl
Cyclohexane, dimethyl
512
octane
ethene, tetrachloro
eluting under CO2 - hydrocarbon background
perfluoro toluene
100
1:45
200
3:30
300
5:15
400
7:00
500
8:45

RIC
03/04/85 13:27:00
SAMPLE: .75UL /1ML PFT + 9-28-05 TENAX TRAP RUN A
RANGE: G 1,2300 LABEL: N 0, 4.0 QUAN: A 0, 1.0 BASE: U 20, 3

DATA: 92805A #1
CALI: 4VCALI #2

SCANS 601 TO 1200
OUT OF 1 TO 1200

1443830.

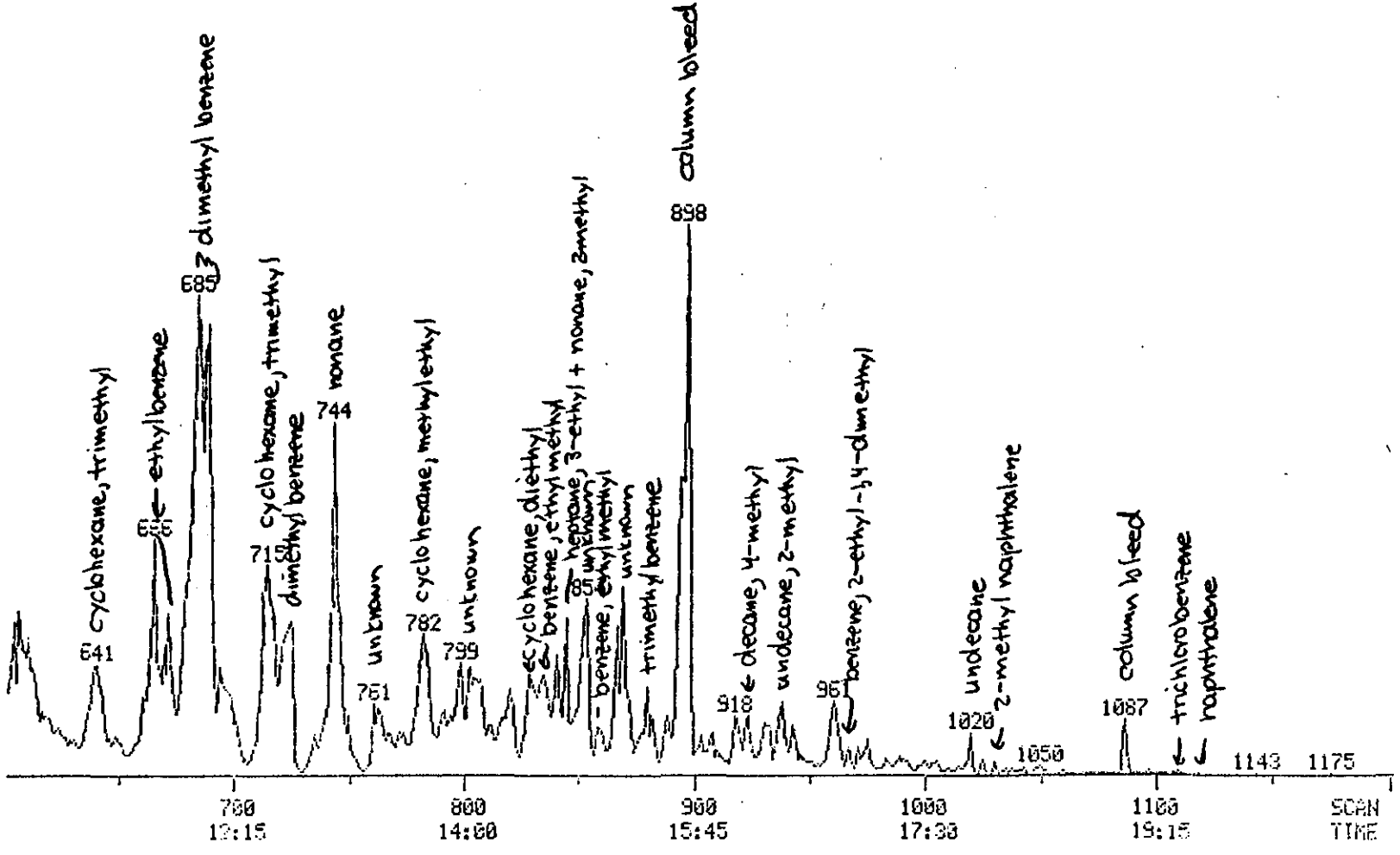

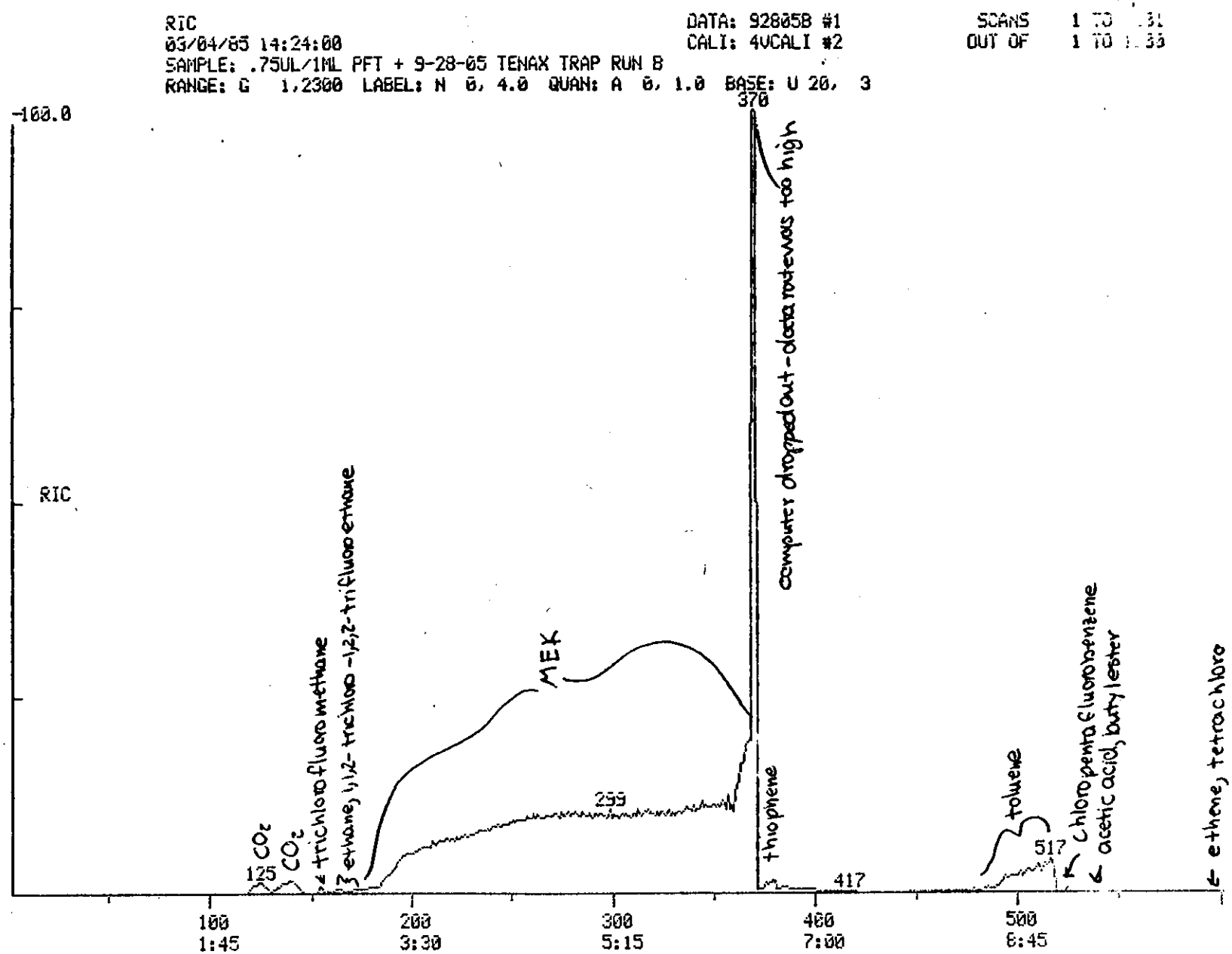
RIC
03/04/85 14:24:00
SAMPLE: .75UL/1ML PFT + 9-28-05 TENAX TRAP RUN B
RANGE: G 1.2300 LABEL: N 0, 4.0 QUAN: A 0, 1.0 BASE: U 20, 3
DATA: 92805B #1
CALI: 4VCALI #2
SCANS 1 TO
OUT OF 1 TO
100.0
RIC
370
computer dropped out - data not even was too high
MEK
255
125
CO2
CO2
trichlorofluoromethane
ethane, 1,1,2-trichloro-1,2,2-trifluoroethane
thiophene
toluene
417
517
chloropentafluorobenzene
acetic acid, butyl ester
ethene, tetrachloro
100
1:45
200
3:30
300
5:15
400
7:00
500
8:45

RIC DATA: 92805B #1 SCANS 601 TO 1200
03/04/85 14:24:00 CALI: 4VCALI #2 OUT OF 1 TO 1200
SAMPLE: .75UL/1ML PFT + 9-28-05 TENAX TRAP RUN B
RANGE: G 1,2300 LABEL: N 0, 4.0 QUAN: A 0, 1.0 BASE: U 20, 3

16760800.

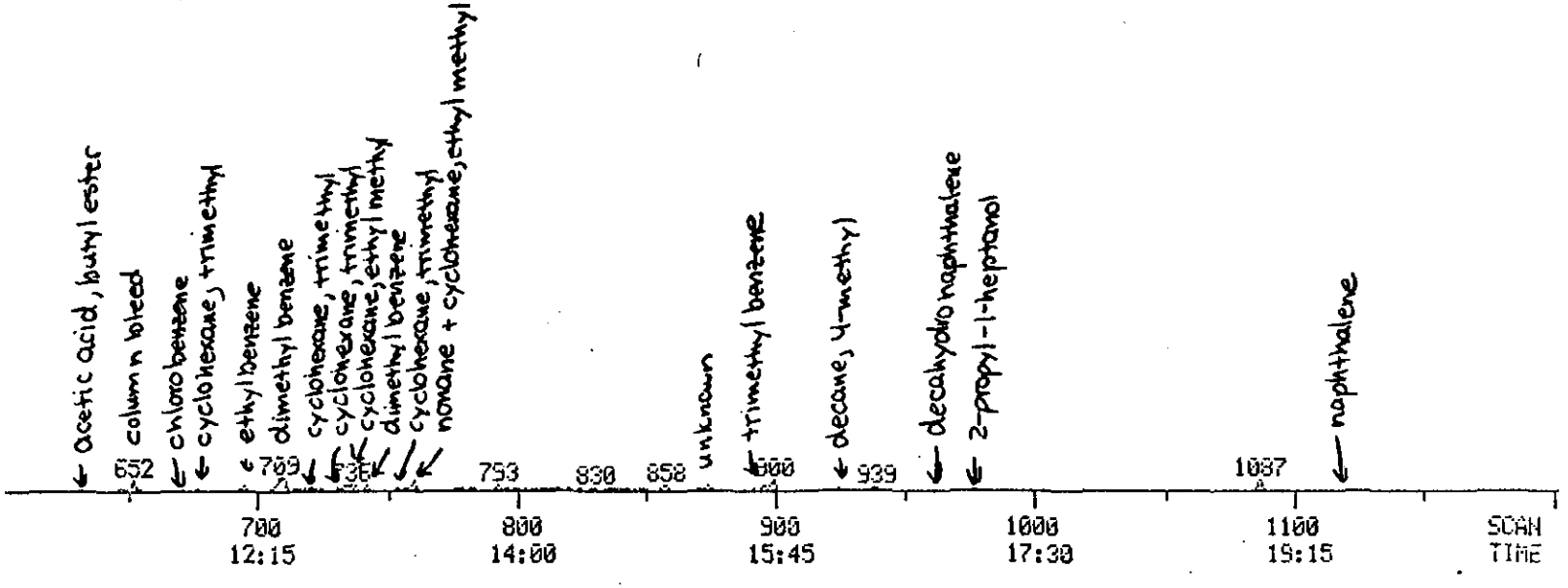

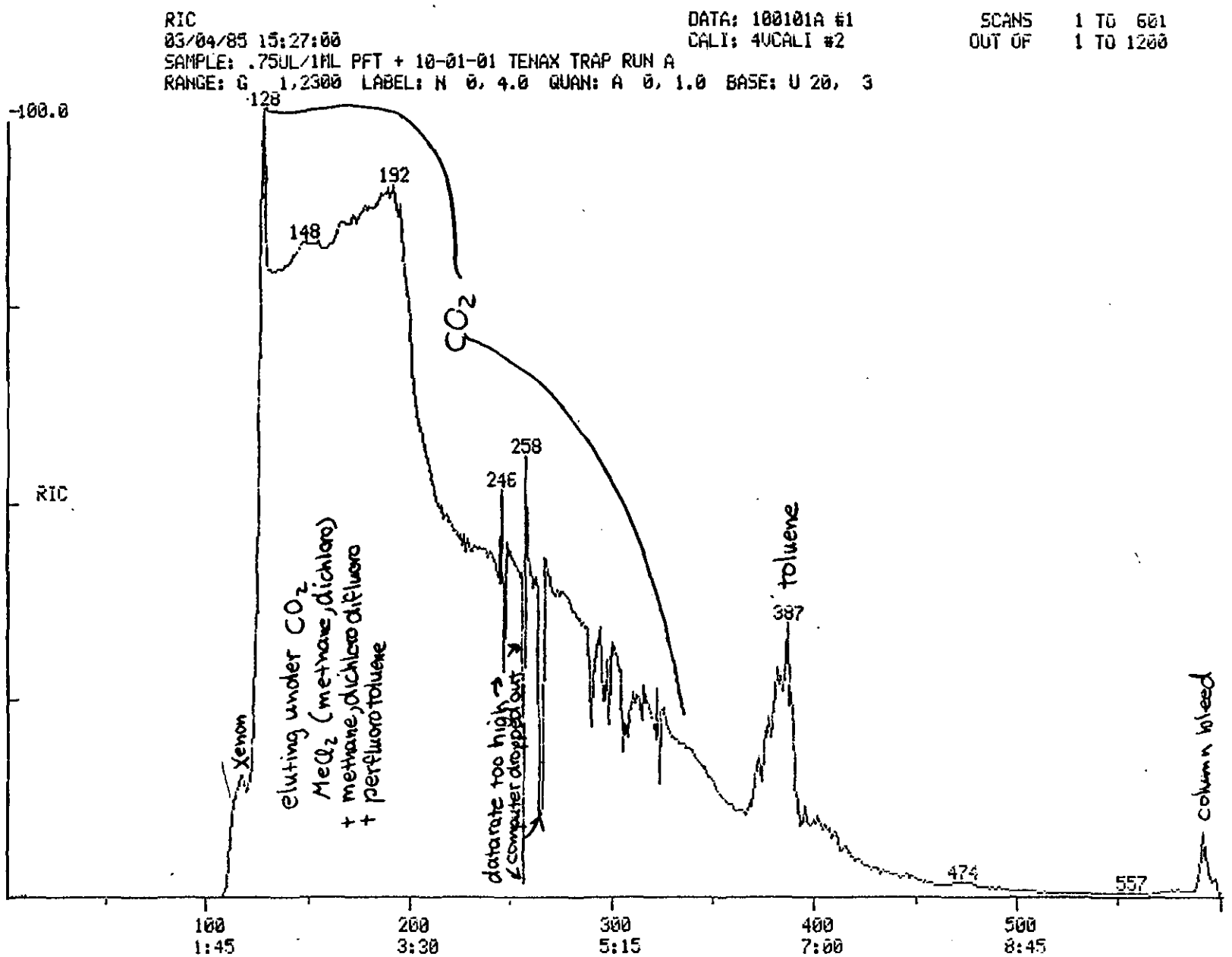
RIC
03/04/85 15:27:00
SAMPLE: .75UL/1ML PFT + 10-01-01 TENAX TRAP RUN A
RANGE: G 1,2300 LABEL: N 0, 4.0 QUAN: A 0, 1.0 BASE: U 20, 3
DATA: 100101A #1
CALI: 4UCALI #2
SCANS 1 TO 601
OUT OF 1 TO 1200
-100.0
RIC
128
192
148
CO2
258
246
toluene
387
474
557
Xenon
eluting under CO2
MeCl2 (methane, dichloro)
+ methane, dichloro difluoro
+ perfluorotoluene
data rate too high →
← computer dropped out
column bleed
100
1:45
200
3:30
300
5:15
400
7:00
500
8:45

RIC
03/04/85 15:27:00
SAMPLE: .75UL/1ML PFT + 10-01-01 TENAX TRAP RUN A
RANGE: G 1,2300 LABEL: N 0, 4.0 QUAN: A 0, 1.0 BASE: U 20, 3

DATA: 100101A #1
CALI: 4VCALI #2

SCANS 601 TO 1200
OUT OF 1 TO 1200

6S6320.

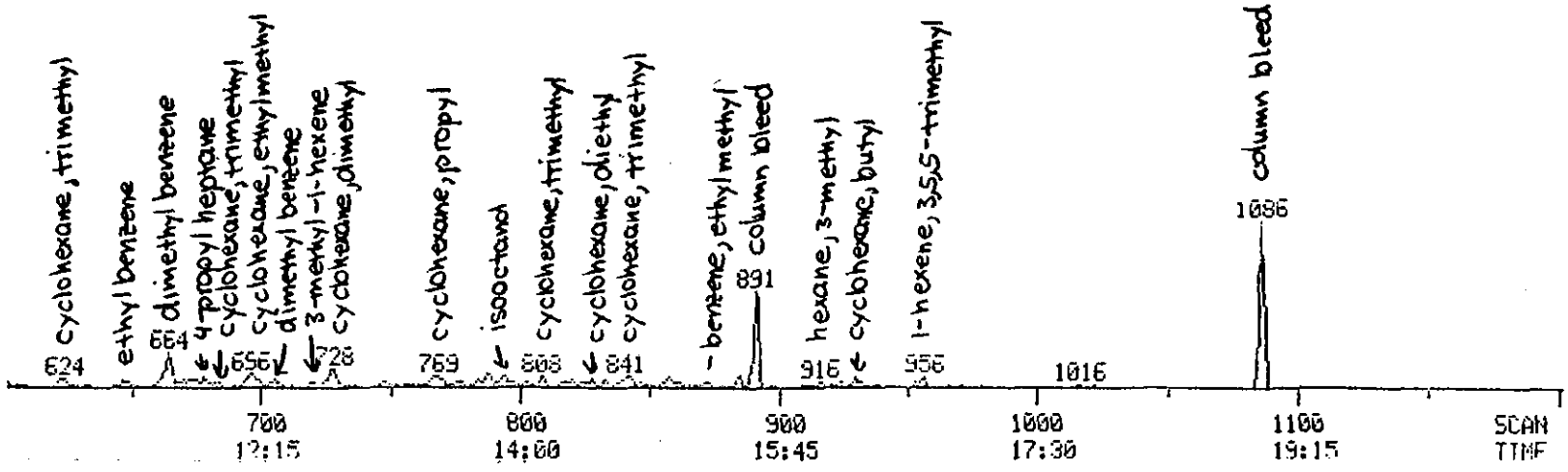

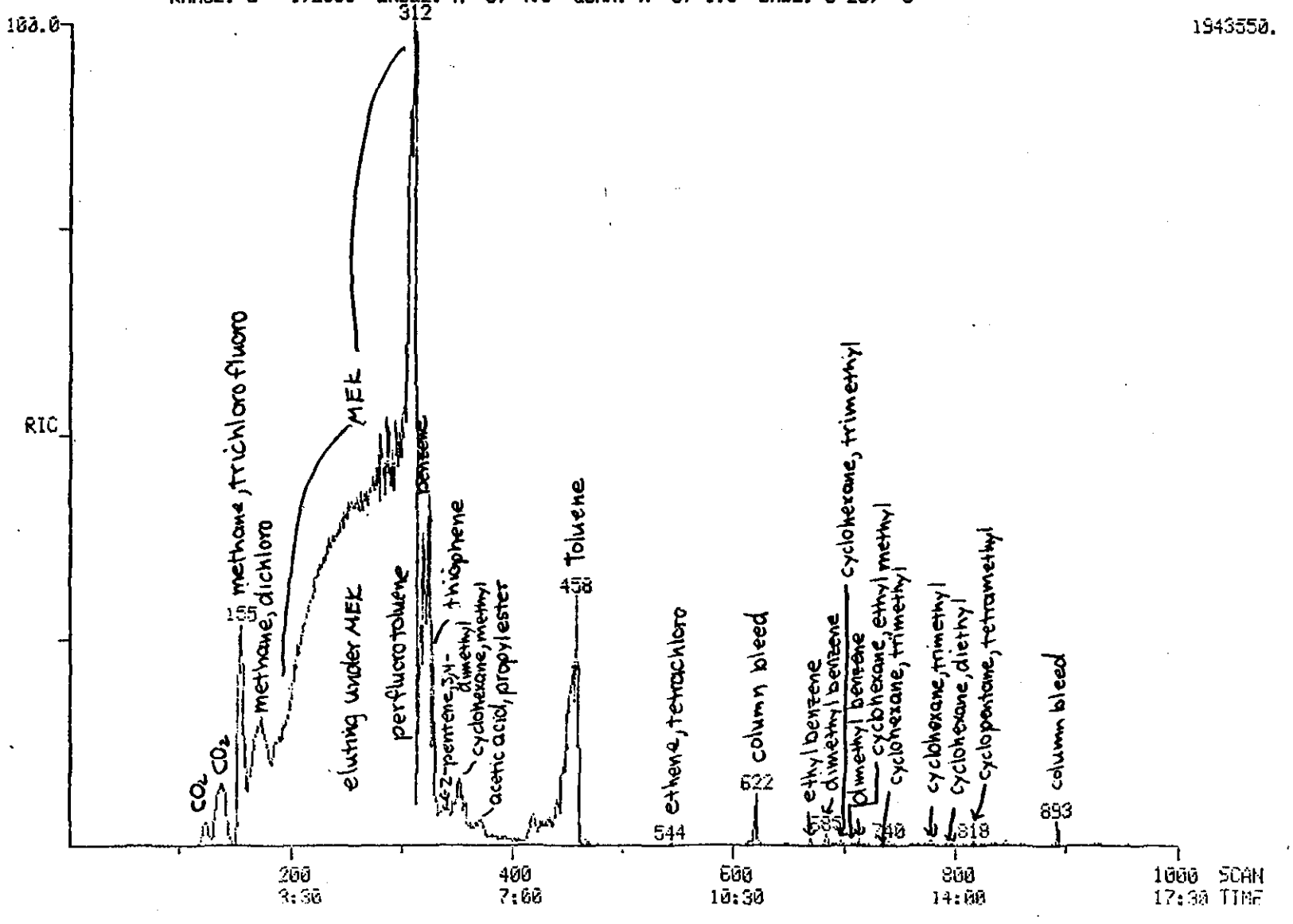
RIC
03/04/85 16:24:00
SAMPLE: .75UL/1ML PFT + 10-01-01 TENAX TRAP RUN B
RANGE: G 1.2300 LABEL: N 0, 4.0 QUAN: A 0, 1.0 BASE: U 20, 3
DATA: 100101B #1
CALI: 4UCALI #2
SCANS 1 TO 1000
100.0
RIC
1943550.
312
MEK
eluting under MEK
perfluorotoluene
benzene
thiophene
2,4-dimethyl pentene
cyclohexane, methyl
acetic acid, propyl ester
Toluene
458
ethene, tetrachloro
544
622
column bleed
ethyl benzene
dimethyl benzene
cyclohexane, trimethyl
dimethyl benzene
cyclohexane, ethyl methyl
cyclohexane, trimethyl
cyclohexane, trimethyl
cyclohexane, diethyl
cyclopentane, tetramethyl
818
893
column bleed
methane, trichloro fluoro
methane, dichloro
CO2
CO2
200
3:30
400
7:00
600
10:30
800
14:00
1000 SCAN
17:30 TIME